INTEGRATED HYDROLOGICAL MODELING OF SURFACE-GROUNDWATER INTERCATIONS

The case of Jembrana region, Western Bali, Indonesia

MAMAN SUPRATMAN

February, 2018

SUPERVISORS:

Dr. Maciek W. Lubczynski
Dr. Zoltan Vekerdy

ADVISOR :

Novi Rahmawati

INTEGRATED HYDROLOGICAL MODELING OF SURFACE-GROUNDWATER INTERACTIONS

The case of Jembrana region, Western Bali, Indonesia

MAMAN SUPRATMAN

Enschede, The Netherlands, February, 2018

Thesis submitted to the Faculty of Geo-Information Science and Earth Observation of the University of Twente in partial fulfilment of the requirements for the degree of Master of Science in Geo-information Science and Earth Observation.
Specialization: Water resources and Environmental Management

SUPERVISORS:
Dr. Maciek W. Lubczynski
Dr. Zoltan Vekerdy

ADVISOR:
Novi Rahmawati

THESIS ASSESSMENT BOARD:
Dr. Ir. C. Van der Tol (Chairman)
Dr. P. Gurwin (External Examiner, University of Wroclaw, Poland)

TABLE OF CONTENTS

ABSTRACT

The Jembrana Region (J.R) is located in the Western part of Bali Island, Indonesia. It has large spatial variability of rainfall. The eastern part has higher rainfall than the western part. Because of this conditions, the J.R was classified to wet and dry zone. It composed of volcanic rocks which store groundwater in unconfined aquifer. In addition, Groundwater is considered as the main source of water supply in this region. Therefore, it is important to understand the dynamics interactions of surface water (SW) and groundwater (GW) in this area for improving water resources management to guarantee its sustainability.

The dynamic of SW-GW interactions was assessed in single hydrologic year (2009) using rational method and baseflow separation Web-based Hydrograph Analysis Tool [WHAT] method. The method was also used to select the catchment and sub catchment for simulation and calibration in MODFLOW-NWT. The unsaturated zone flow (UZF1) and stream flow routing (SFR2) were selected as the active packages in MODFLOW-NWT. All data such as time-series of rainfall, stream discharge and potential evapotranspiration were simulated in three hydrologic years (1st October 2009 to 30th September 2012) on a daily basis. Eventually, the results of [WHAT] was compared to the results MODFLOW-NWT to see the agreements between them.

The percentages of gross recharge (R_g) in Sebual and Jogading were 76.54 % and 87.50 % of the total groundwater inflow. In Sebual, stream to groundwater [q_{sg}] and storage [ΔS_{gin}] contributed 15.70% and 7.75%, while in Jogading 5.85% and 6.65% respectively. The groundwater to stream [q_{gs}], groundwater evapotranspiration [ET_g], surface leakage [Exf_{gw}] and storage [ΔS_{gout}] were 89.85%, 3.12%, 0.31% and 6.71 % of the total outflow in Sebual, while in Jogading 94.60%, 0.70% , 0.05 %, and 4.66 % of the total outflow respectively. It can be observed that streams gain a lot of groundwater from aquifers which means high groundwater potential.

The comparison of WHAT and MODFLOW-NWT was performed in one hydrologic year (2009). In WHAT method, the proportion of groundwater runoff [q_g] to total estimated flow [q_t] were 49.78% for Sebual and 78.12% for Jogading similar proportions for surface runoff [q_s] were 50.22% for Sebual and 21.88% for Jogading of total estimated flow. Then, in MODFLOW-NWT the proportion of q_g was 42.11% for Sebual and 88.85% for Jogading and q_s was 57.89% for Sebual and 11.12% for Jogading. In that case, WHAT has a good agreements with MODFLOW-NWT.

Key Words : Surface-Groundwater interactions, Bali, Volcanic aquifer, rational method and WHAT, Water balance, MODFLOW-NWT

ACKNOWLEDGEMENTS

The thesis would not accomplished without supports and contributions from a lots of people and institutions around me. First, all praises is to my God, Allah SWT, for giving me the opportunity to reach this level of science. Many thanks to Ministry of Finance of Indonesia Republic (LPDP) for giving the funding to study in ITC, University of Twente. Also, Government of Jakarta city which also support me to study in ITC, University of Twente.

I am really would like to thankful to my supervisor Dr. Maciek Lubczynski for guidance, giving knowledge and understanding of this subject, supports and motivated me from the beginning till the end of this thesis. Also, to my second supervisor Dr. Zoltan Vekerdy, thanks you very much for sharing knowledges and discussions, and make me more confident to develop this thesis.

The special thanks to my advisor, Novi Rahmawati, for sharing data and time, discussions and also sharing knowledge about this subjects. Also, thanks to Mr Moiteela Lekula for sharing knowledge and discussions about this subject.

I am grateful to Mr Arno Van Lieshout , the Course Director of Water Resources and Environmental Management Department (ITC), Dr. Chris Mannaerts as the chairman of proposal and midterm and also to all members of academic and non- academic staff for their collaboration during the period of the course.

Thanks to all my classmates in WREM department for sharing knowledge and collaboration. Also, my colleagues from Indonesia, Faried Rahmany, Hariady Mantong, Andri R, Chaidir Adlan, Aldino Rizaldy, Imam Purwadi, Arya Lahasa Putra, Dwi Rini Hartati, Gina Leonita, Oktaniza N, Vidya N Fikriyah, Mbak Dewi, Mas Aji Putra Perdana and Mas Aulia Akbar for being new big family during my study.

Finally, last but not least, this thesis dedicated to half of my hearth, my wife and my children who struggling to keep full patient and survive during my absence in the home for period of 18 months. My blessing to my parents and my mother in-law for giving advices and moral support during the period of my study.

LIST OF FIGURES

LIST OF TABLES

1. INTRODUCTION

1.1. Background

Groundwater is of crucial position in water resources planning, development, and management (Kumar and Singh 2015). It is a key component of environmental flows that support many aquatic, hyporheic, and riparian ecosystem especially during dry periods (Rassam et al. 2008). Therefore, to keep it sustainable in the future, a systematic study is required to analyse the flows, interactions and its behaviour of groundwater. In addition, quantification of exchange fluxes between surface and groundwater is necessity for understanding and preserving of water resources (Anibas et al. 2009). One of the recent approaches in groundwater problems is by creating a model which is a simplified representation of the complexity of nature. It is considered as essential part to overcome groundwater problems by building a conceptual and numerical model then simulated either in a steady state or transient model (Anderson et al. 2015).

Recently, incorporating surface water into groundwater model became a trend because it is considered as one unit resource (Ala-aho et al. 2015). Integrated Hydrological Model (IHM) is a one of modelling technique that simulate simultaneously surface water (SW) and groundwater (GW), and the results of this modelling technique has demonstrated good performance in many studies (Guay et al. 2013; Ely and Kahle 2012). Surface and groundwater systems are linked with different stream/aquifer structures and processes controlling the magnitude and direction of the exchange flux between the two systems. Integrated hydrological model (IHM) of surface water and groundwater interactions are considered as a very important tool for water resources management (Rassam et al. 2013). It has been used to solve several crucial issues such as land use and climate change (Gilfedder et al. 2012). To develop IHM, It needs input parameters such as climate data, digital elevation model, land use and land cover maps, soil and aquifer maps and their parameters, streamflow and groundwater level data are needed (Hassan et al. 2014). Moreover, IHM is the best tool for estimating surface water and groundwater interactions (Lubczynski and Gurwin 2005).

Hydrologic interactions between surface and groundwater arise by vertical flow through the unsaturated soil and by infiltration into or exfiltration from the saturated zones (Sophocleous 2002). The prediction ability of IHM SW-GW model can be developed by improving the representation of aquifer properties such as hydraulic conductivity, storativity and the model-specific fluxes such as river interactions, recharge, and evapotranspiration (Doble and Crosbie 2017). The interchange between groundwater and streams is a crucial constituent which significantly affects not only stream discharge but also water quality, geomorphic development, riparian zone quality and structure, and ecosystem composition (Sophocleous 2010). Surface and groundwater interaction can influence groundwater recharge dynamics and compensate the impact of vertical percolation and root water uptake (Krause et al. 2007).

Bali Island is part of the country of Indonesia. Geographically, it is located at coordinates 8° 24' S and 115° 13' E for latitude and longitude respectively. The total area of the island is ~5380 km² while the study area is located in western part of the island. The island is composed of a variety of volcanic morphologic units such as eroded early Quaternary volcanoes, active stratovolcanoes, thick tephra deposit, pyroclastic flow slopes and closed caldera lakes (Kayane et al. 1993;Purnomo and Pichler 2015). The main factors governing water resources in this island are climate, aquifer characteristics and heterogeneity of rainfall distribution (Rai et al. 2015). Cole (2012) wrote that groundwater is commonly used for daily main consumptions in Bali because aquifers are identified as highly permeable. According to Teketel (2017) who investigated daily surface-groundwater interactions in Southern Bali stated that groundwater outflow contributed to surface water either in steady-state (47.8%) model or transient (30.4%) model simulation.

This study was focus on evaluating of surface water and groundwater interactions and estimate the groundwater budget of Western Bali. Moreover, three years data from 1st October 2009 to 30th September 2012 was used for simulation period to calculate the exchange flux between surface, unsaturated and saturated zones. The model was generated using computer software which is MODFLOW-NWT. This model was chosen because it can integrate surface, unsaturated and saturated zone in trustworthy approach. The model is developed under ModelMuse Graphical User Interface (GUI) and combine with unsaturated zone flow package [UZF1] and stream flow routing package [SFR2] (Niswonger et al. 2011;Hassan et al. 2014). ModelMuse can simulate steady-state or transient model in an irregularly formed flow system in which aquifer layer can be unconfined, confined or combination of unconfined and confined (Winston 2009). The Jembrana region is selected for groundwater study because: (i) no one groundwater modelling in this site either stand-alone or IHM model was performed; (ii) this region has variability distribution of rainfall and stream discharge; (iii) there are available of three years hydrological data ; (iv) it is representative of unconsolidated aquifer with variability of rainfall in the world. Eventually, this MSc research was expected to fill the gaps in understanding of surface and groundwater interactions which is a very important tool for water resources management.

1.2. Problem statement

In the western part of the island, groundwater is the major demand for domestics consumptions whereas surface waters are used for agriculture activities. Based on in situ data, the Jembrana region has varying distribution of rainfall which has an impact indirectly on the groundwater. In general, this area can be defined as consisting of two parts: a drier area and a wet area. The dryer area is located from middle to western side, and the rest part of the catchment is the wet area. However, there are no available tools or models yet that can help in managing and controlling the usage of water resources in this area. This condition might occur due to the lack of knowledge and skills of integrating surface and groundwater resources interactions. Therefore, the models or tools are required to preserve water resources in a sustainable manner, both the quality and quantity aspects with focus on the groundwater resources.

1.3. Research objectives

The general objectives of this study is to improve water resources sustainability and management in western Bali, Indonesia through developing an integrated hydrological model (IHM) that simulate the surface water and groundwater interactions.

The specific objectives of this study are :

1. To set up a transient model based on three hydrologic years from 1st October 2009 to 30st September 2012 for Sebual and Jogading, Jembrana Region, Western Bali, Indonesia
2. To calibrate a transient IHM of Sebual and Jogading, Jembrana Region, Western Bali, Indonesia
3. To estimate the water balance of Sebual and Jogading, Jembrana Region, Western Bali, Indonesia
4. To characterize the dynamics of SW-GW interactions of Sebual and Jogading, Jembrana Region, Western Bali, Indonesia

1.4. Research questions

1. What are the key components of spatiotemporal variability of the water balance in Sebual and Jogading sub catchment, Pergung catchment Jembrana region, Western Bali?
2. How does the water balance differ on the daily and yearly basis in Sebual and Jogading sub catchment Jembrana region, Western Bali?
3. What are the interactions of SW and GW in Sebual and Jogading sub catchment Pergung, Jembrana region, Western Bali?

1.5. Novelty of the study

This study will fill gaps of knowledge on the groundwater resources Western Bali. It is essential because no research has been done to study about groundwater resources in this area, neither by stand-alone groundwater modelling nor by an integrated hydrological model (IHM) that describes surface and groundwater interactions. Therefore, this study will be a very important part for improving sustainability and controlling water resources, particularly groundwater resources.

1.6. Research hypothesis

Research hypothesis in this study is that there are interactions between the surface and groundwater resources and this interaction can be calibrated in transient models. Therefore, models provide a reliable estimation of SW- GW exchange flux and groundwater storage for the Jembrana region.

1.7. Assumptions

The models were calibrated without abstractions data for transient IHM SW-GW interactions because of insufficient availability of those data. Then, the interception and infiltration rate were assumed as spatiotemporally variables based on a land use and land cover map, defined separately for the wet and dry seasons. It was spatially variable during wet season (October - March) and dry season (April-September) then temporally variable based on daily rainfall data. Potential evapotranspiration [PET] date was taken from literature [MODIS] 100 m resolutions (resampling products). It was assumed that PET was constant in the period of eight days since it has been given as cumulative values over eight days.

2. STUDY AREA

2.1. Location

The Jembrana region (J.R) is located in the western of Bali Island, Indonesia. it covers ~789 km². Geographically, it is located at 8º 18' 0" S and 114º 41' 30" E latitude and longitude respectively. It is part of Bali Island with estimated area coverage ~789 km², while the entire of Bali Island covers ~ 5,620 km². The Jembrana region varies in elevation from 0 to 1400 m a. s. l. The highest elevation ranges located in northern part of the region and the lowest in southern part of the catchment, adjacent to the sea.

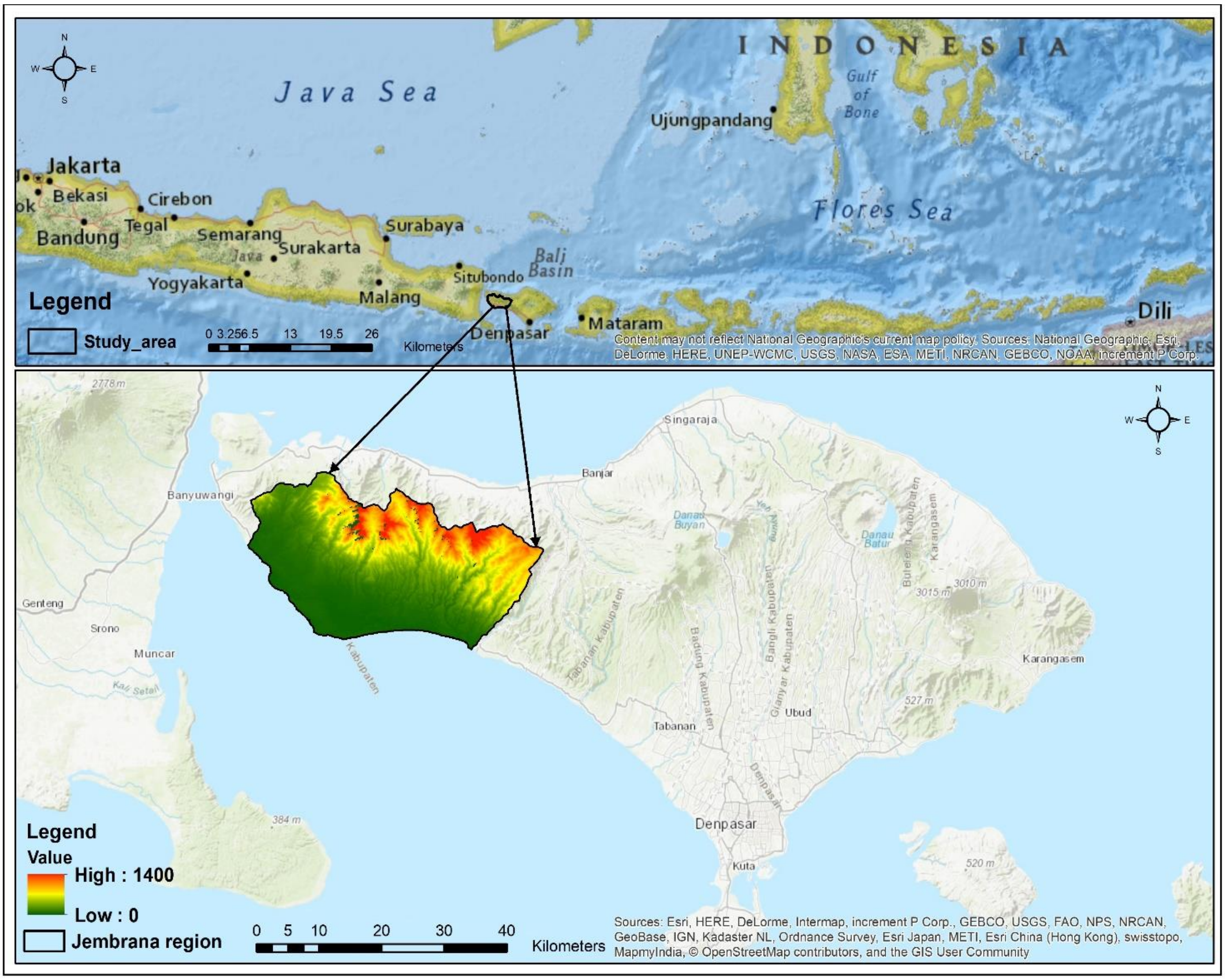

Figure 1. Elevation map of the Jembrana region (J.R). Data source: SRTM 90m resolution

2.2. Monitoring stations

The J.R has eight rain gauge stations for monitoring rainfall, 14 stream discharge gauges for monitoring river discharges and two of temperature measurements (Figure 2). The rain gauges are located sparsely inside the region. Then, stream discharge gauges mostly are located in the outflow of the region which is adjacent directly to the sea. And then the temperature measurements are located around in the middle of the region nearby to downstream and close to each other. All data are available from 1st January 2009 to 31st December 2013 with daily frequency. However, groundwater measurements data such as piezometers and wells are not available in this region.

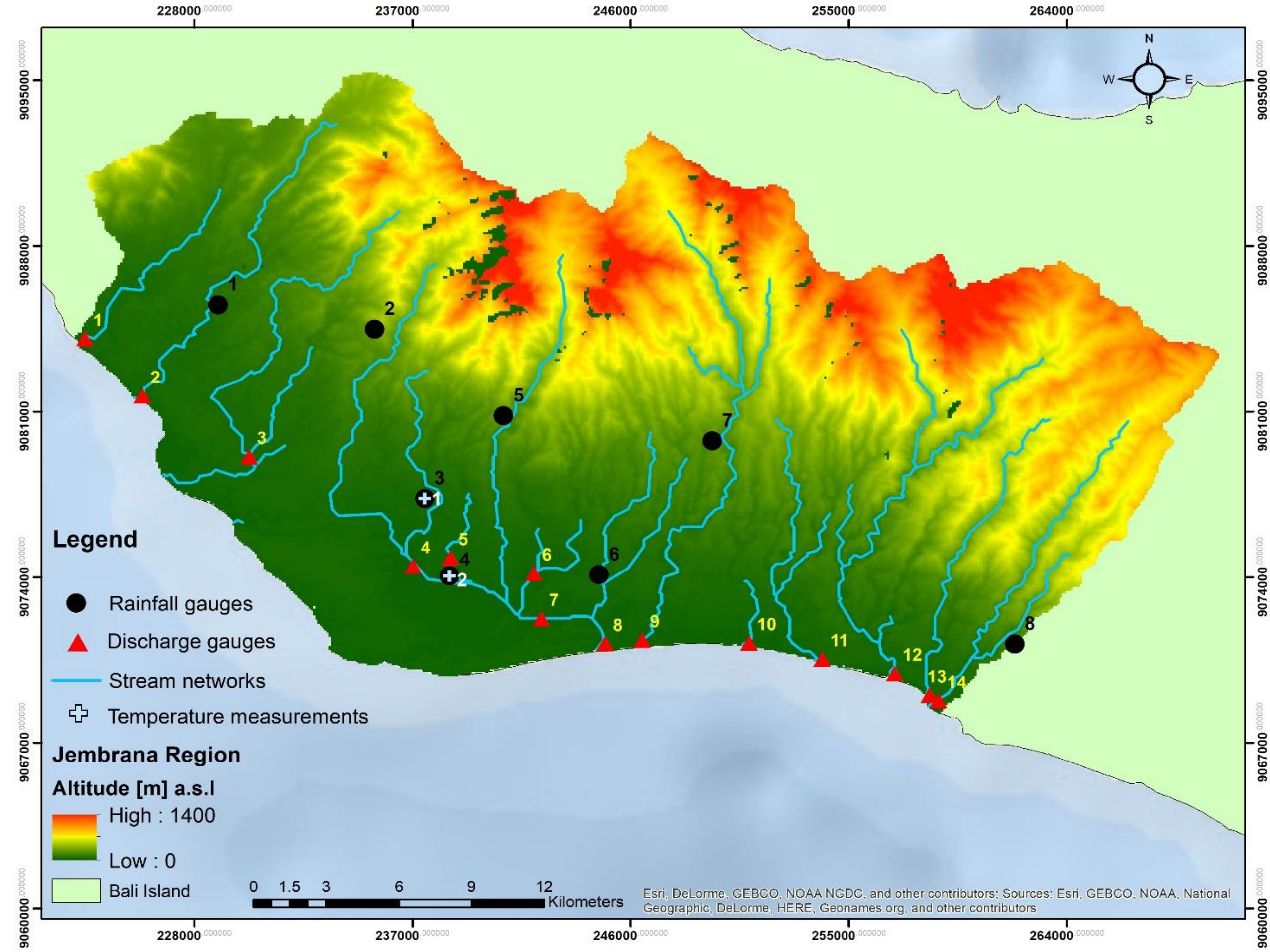

Figure 2. Monitoring networks of the Jembrana Region (J.R). For the name of rain gauges, stream discharge and temperature measurement see Appendix I,II and III.

2.3. Climate

Bali Island has a tropical climate characterized by two distinct seasons, dry and wet seasons. The dry season normally starts from April to September and the wet season from October to March. The rain from the northwest equatorial wind in the wet season is conveyed by the air mass, and during the dry season the wind comes from the southeast wind Australia produced a seasonal pattern in this area (Kayane et al. 1993). During the rainy season, rainfall divided into evapotranspiration by the plant, surface runoff, and the rest is infiltrated to the sub surface. The percentage of infiltration depends on the condition of geology, land use, vegetation cover and slope (Nielsen and Widjaya 1989b). The temperature in this island ranges from 27 – 30 ^{o}C and the humidity from 85% to 90% respectively. In this island, soil temperature declines at laps rate of 0.615 ^{o}C in every 100 m elevations, and the same behaviour with air temperature (Kayane et al. 1993). In Jembrana region, based on measurement from two stations from 2009 to 2013, the temperature ranges from 22 °C to 33°C with the average 27 °C.

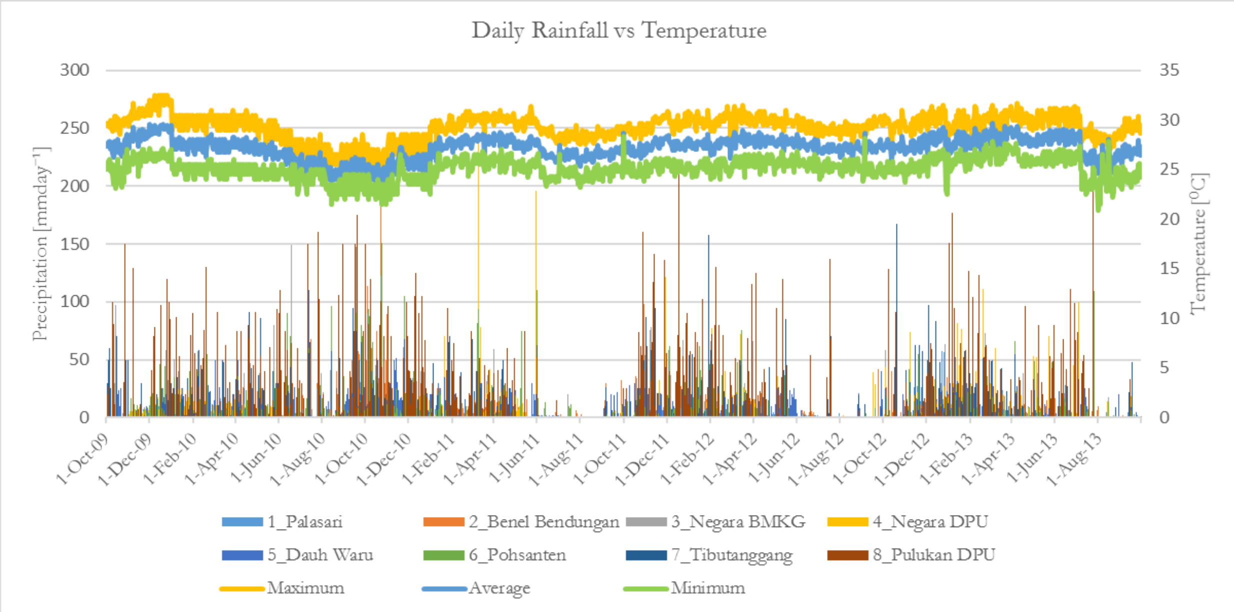

Figure 3. Daily rainfall vs temperature data from 2009 to 2013, rain gauges numbers are referred with Figure 2 (Data source: Agency of Climatology, Meteorology and Geophysics of Indonesia)

Based on in situ measurement from 2009 to 2013, the Jembrana region has an interesting pattern of rainfall distribution. It has variability distribution of rainfall and stream discharge where can be classified into three parts, high, middle and low distribution.

2.4. Land use and land cover

Bali is composed of volcanic rocks affecting island topography and land core. There are Quaternary volcanoes, active stratovolcanoes, thick tephra deposits, and pyroclastic flows. It is dominated by unconsolidated layer in the upper part and consolidated layer in lower part of the island. In the study area, based on the SRTM 90 m resolution DEM (Digital Elevation Model), the highest elevation located in the northern part and the lowest elevation located in the southern part of the catchment which is known as an outlet of the catchment.

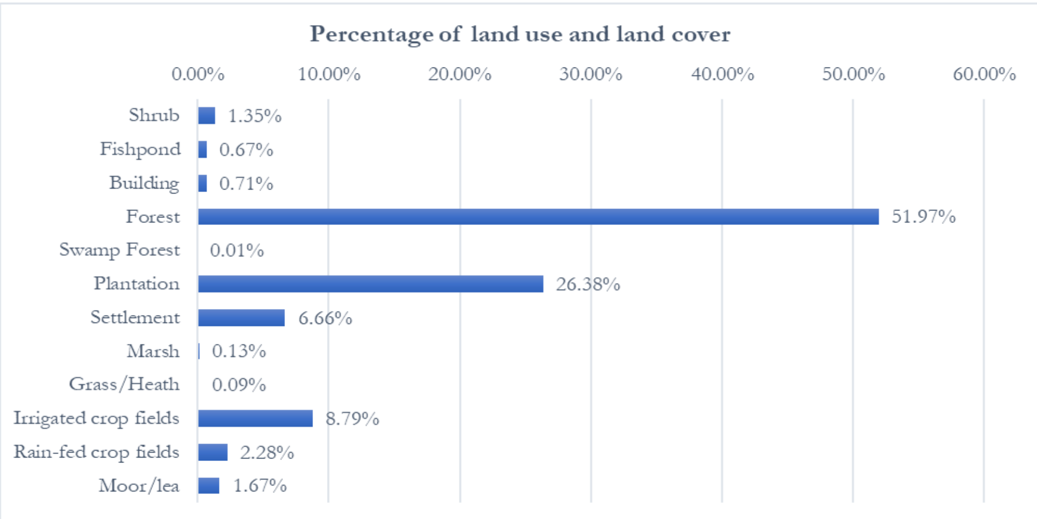

Figure 4. Percentage of land use and land cover in the Jembrana region

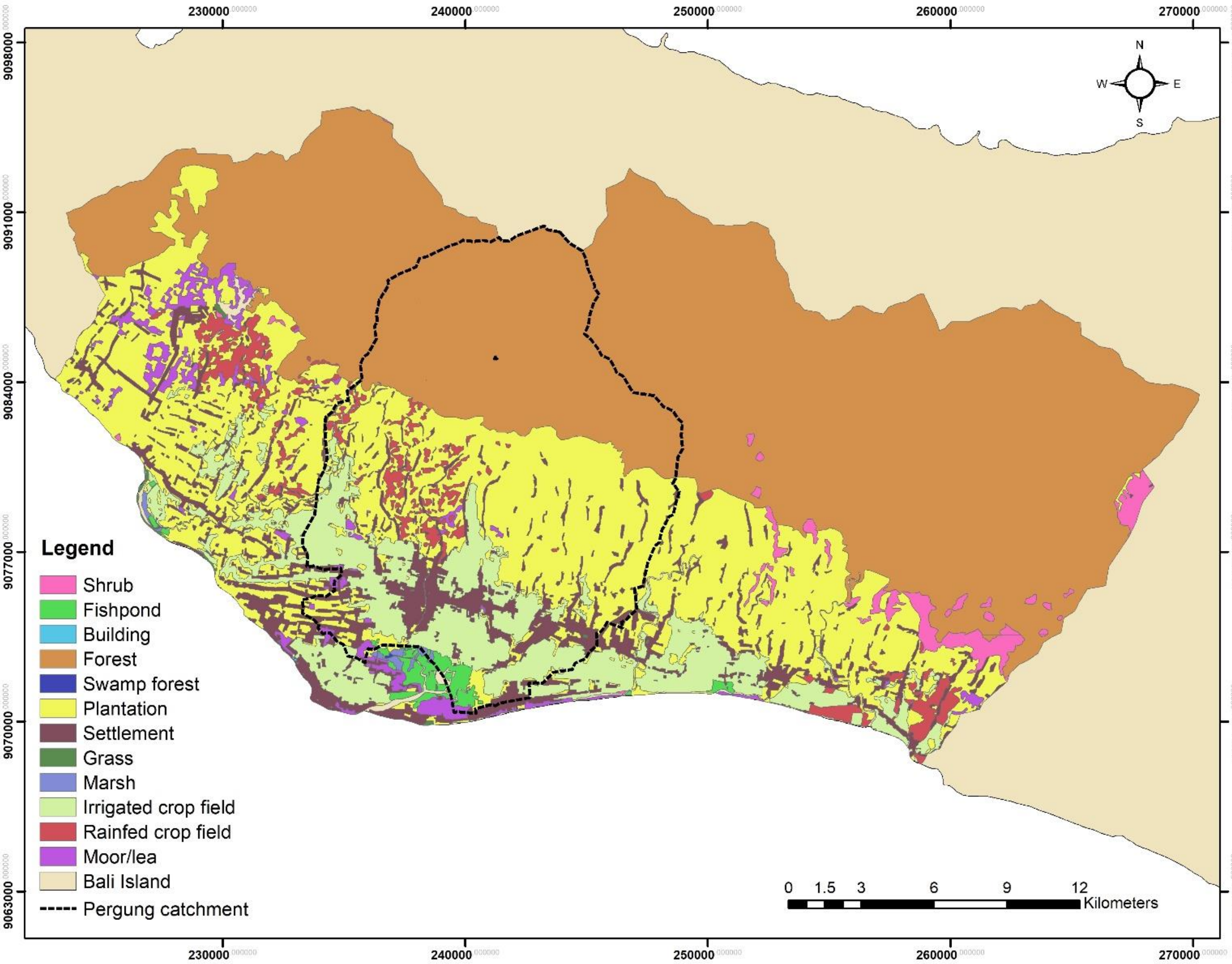

Figure 5. Land use and land cover map of the J.R
(Data source: Geo-Spatial Information Agency of Indonesia)

According to Figure 4 and 5, the land use and land cover of the J.R are characterized by forest (51.91%), plantation (26.34%), settlement and building (8.04%) and crop fields (12.72%), then shrub, grass and marsh (1.47%) respectively. Forest dominates the land cover of the J.R. It covers more than half of the catchment area, from northern part to middle area of the catchment. In Pergung catchment (P.C) which marked by dash line, Forest contributes 35.32 %, plantation (34.64%), settlement and building (10.68%), crops field (19.27%), marsh (0.06%) and grass (0.03%) respectively.

2.5. Hydrology

The study area is considered to be affected by monsoon pattern. Therefore, the hydrograph shapes are associated with the rainfall distribution; it means that when rainfall is higher during the rainy season (October to March) then river discharge are higher as well. In the dry season (April to September), the stream discharges tend to decline as rainfall decreases. This means that river dynamics is directly dependent on rainfall. The stream discharge data was coupled with DEM in ArcGIS software to extract the Jembrana catchments boundary. The Jembrana region consists of ten catchments as shown in Figure 6.

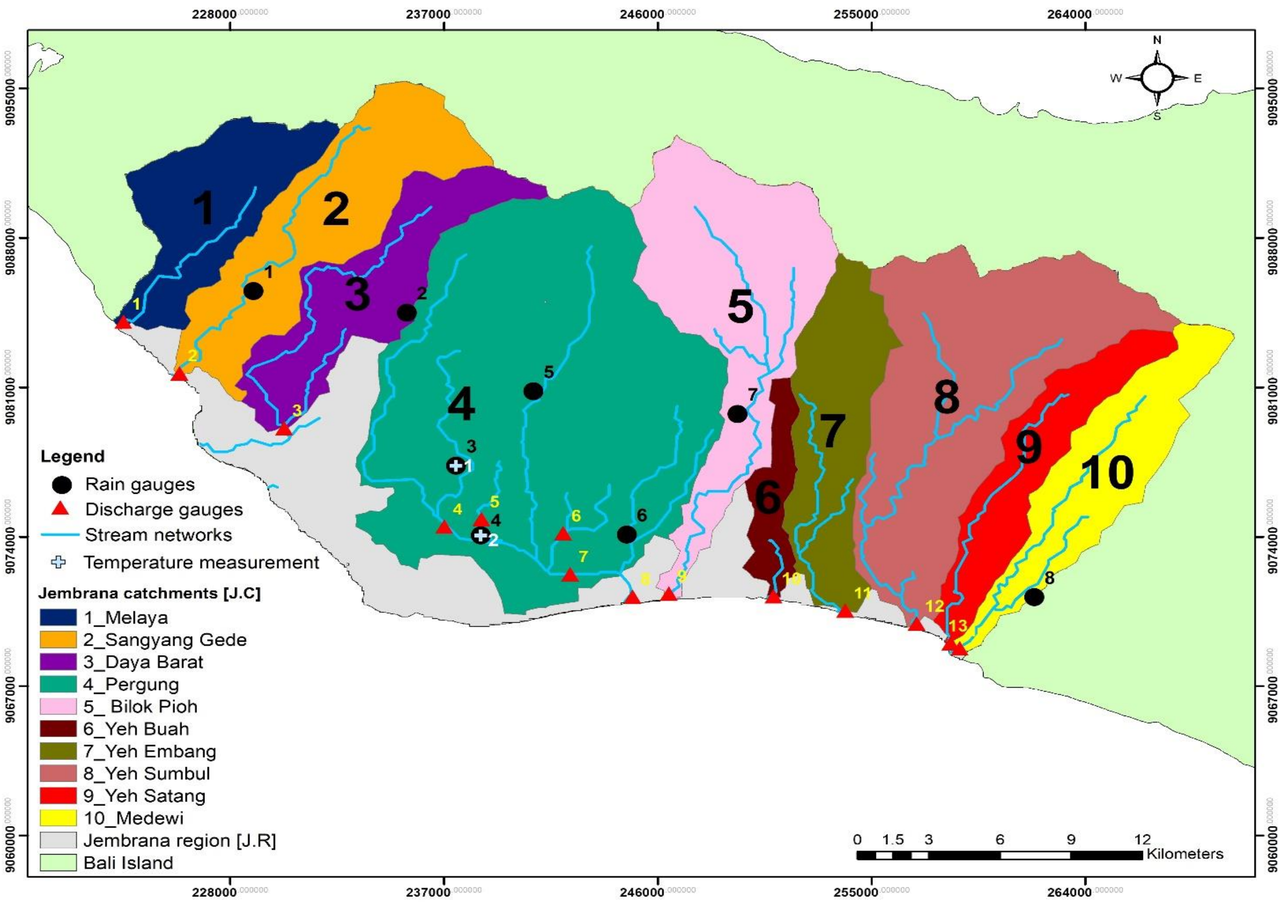

Figure 6. The Jembrana catchments boundary of the region

According to in situ data from 1st October 2009 to 31st September 2013, the daily mean river discharges vary from 0.12 m^3s^{-1} to 5.12 m^3s^{-1} in Melaya and Pergung catchment (Figure 6). Then, in the eastern part of the Jembrana region, the daily mean of stream discharges was 2.08 m^3s^{-1} which are located in Yeh Satang catchment.

Table 1. The Jembrana region catchments

No	Catchment	Au [m²]	Au [Km²]
1	Melaya	43652522	43.65
2	Sangyang Gede	64208503	64.21
3	Daya Barat	48121948	48.12
4	Pergung	212362627	212.36
5	Bilok Poh	82999159	83.00
6	Yeh Buah	13424654	13.42
7	Yeh Embang	47959868	47.96
8	Yeh Sumbul	109801817	109.80
9	Yeh Satang	36854894	36.85
10	Medewi	46110474	46.11
Total		**705496466**	**705.50**

The mean of stream discharge values has trend to decrease from eastern to western part of the catchment. It means that the eastern part is classified as wet area compared to the western part of the catchment which is the drier area. Based on Table 1, the largest catchment is Pergung Catchment. It is located in the middle of the J.R (see Figure 6). It covers ~212.36 km² and has four stream discharge gauges inside the catchment. Also, it is attributed with two temperature measurement and six rain gauges installed in the surrounding catchment. This catchment is considered as important catchment because a lot of stations are installed around this area. Then, the smallest catchment is Yeh Buah catchment, it covers ~13.42 km². Overall, the J.R covers ~705.50 km² for the whole catchment.

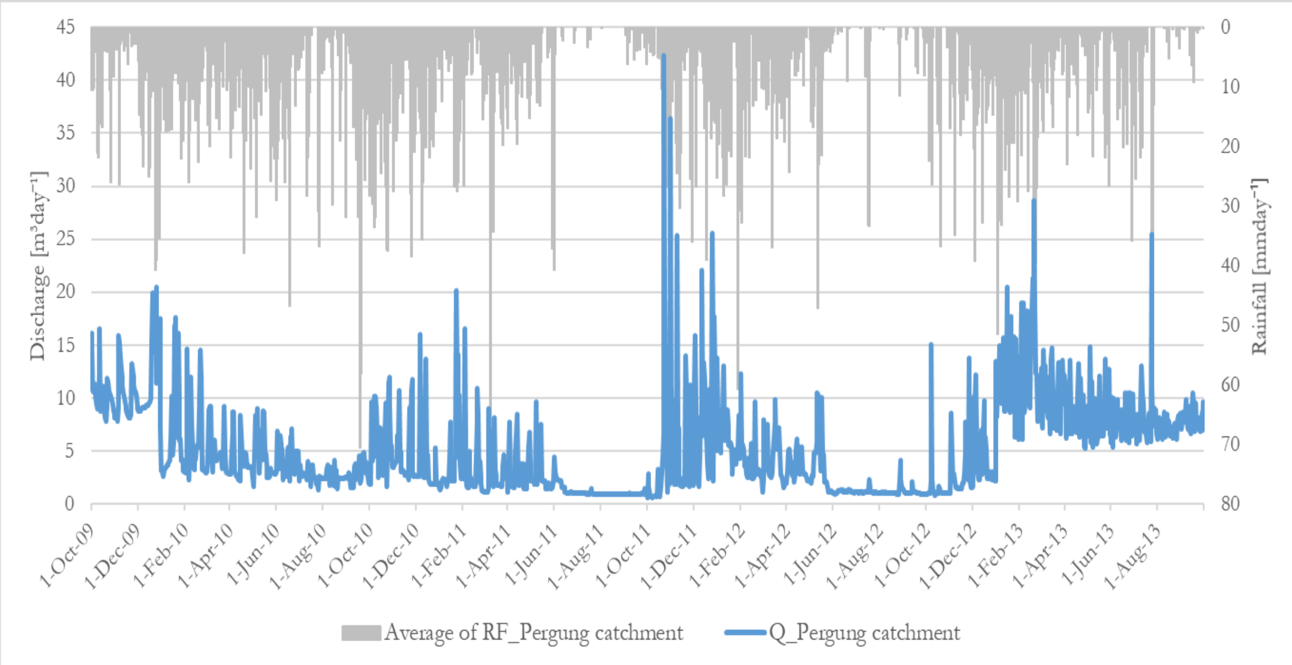

Figure 7. Daily rainfall distribution in the catchment compared to daily discharge (Q) in Pergung Catchment (Data source : Agency of Climatology, Meteorology and Geophysics of Indonesia, and Agency of Public works)

In general, the flow direction of streams in Jembrana Region is from north to south direction. Based on the result of preliminary assessment, the number of streams discharges gauges in the catchment are available from 14 locations. Rainfall is not the only sources contributing water to the stream flow. According to Teketel (2017), groundwater outflow also contributes to streams. From Figure 7, it can be observed that the distribution of amount stream discharges are vary in space and time; the stream discharges affected indirectly by rainfall distribution in the region and structured by the surface topography. In Pergung Catchment, the average of stream discharge was ~5.12 m^3s^{-1} with the average of rainfall ~6.08 $mmday^{-1}$.

2.6. Hydrogeology

The geology and hydrogeology of J.R from northern to the southern part are composed of volcanic products such as lava, volcanic breccia, and tuff (50.90%), Palasari formations which are conglomerates, sandstones and reef limestone (42.98%) and alluvial deposit (6.12%) respectively. This volcanic products are rich in mafic mineral, exhibits considerable relief (Purnomo and Pichler 2015). The northern part of the study area is occupied by mountains of major watershed divide, and hence it can be assumed that there is no flow from outside of boundary to the Jembrana Catchment. As stated earlier, data about cross sections, piezometers and wells are not available in the J.R for the period of 2009 to 2012. The transmissivity and boreholes data are available but lack of spatial distribution in this region. They are only spatially distributed in the southern part of the region and these data have been collected from May 2013 to January 2014 (Figure 8).

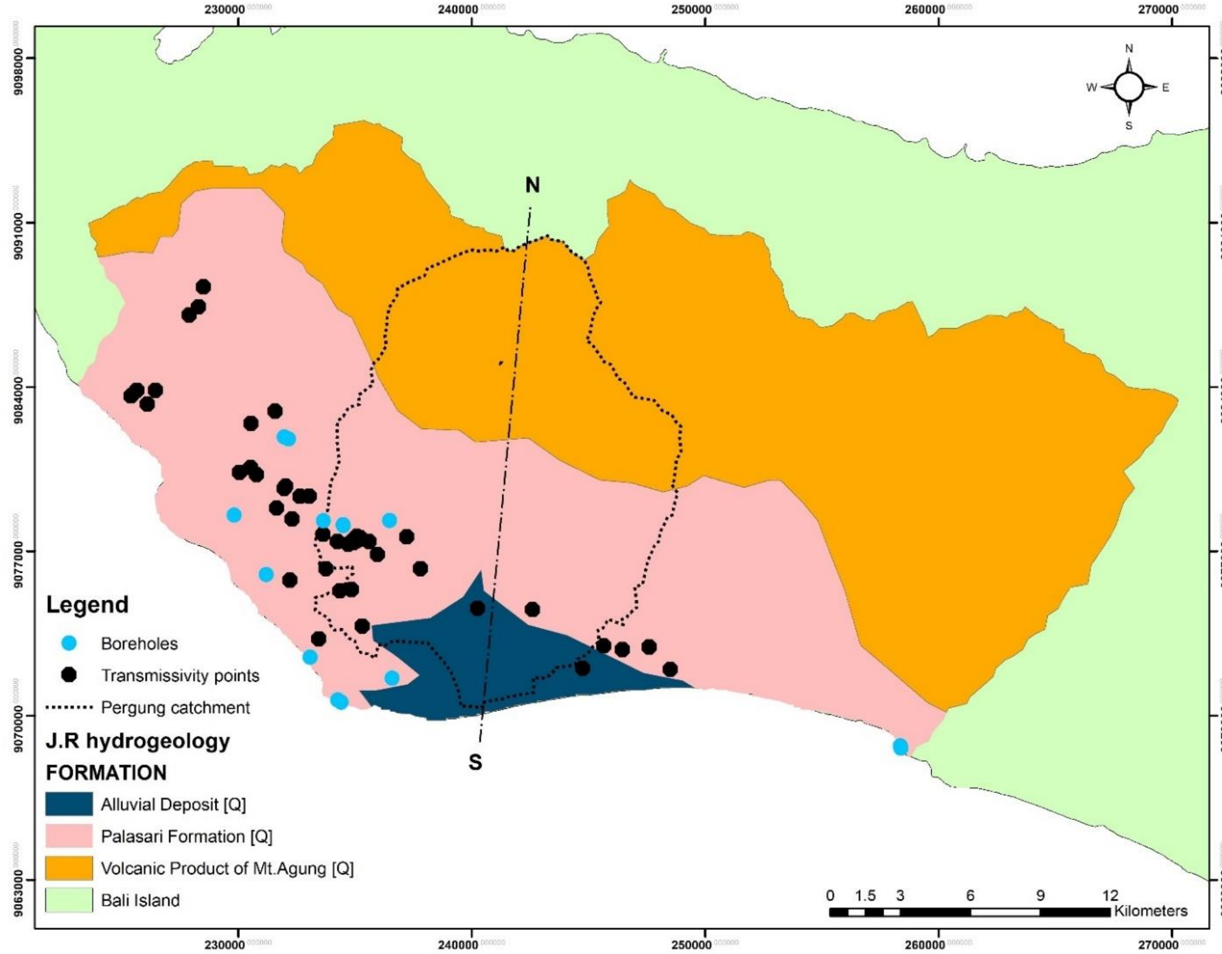

Figure 8. Hydrogeology map of J.R, boreholes and transmissivity distribution in J.R
(Data source : Ministry of Energy and Mineral Resources of Indonesia)

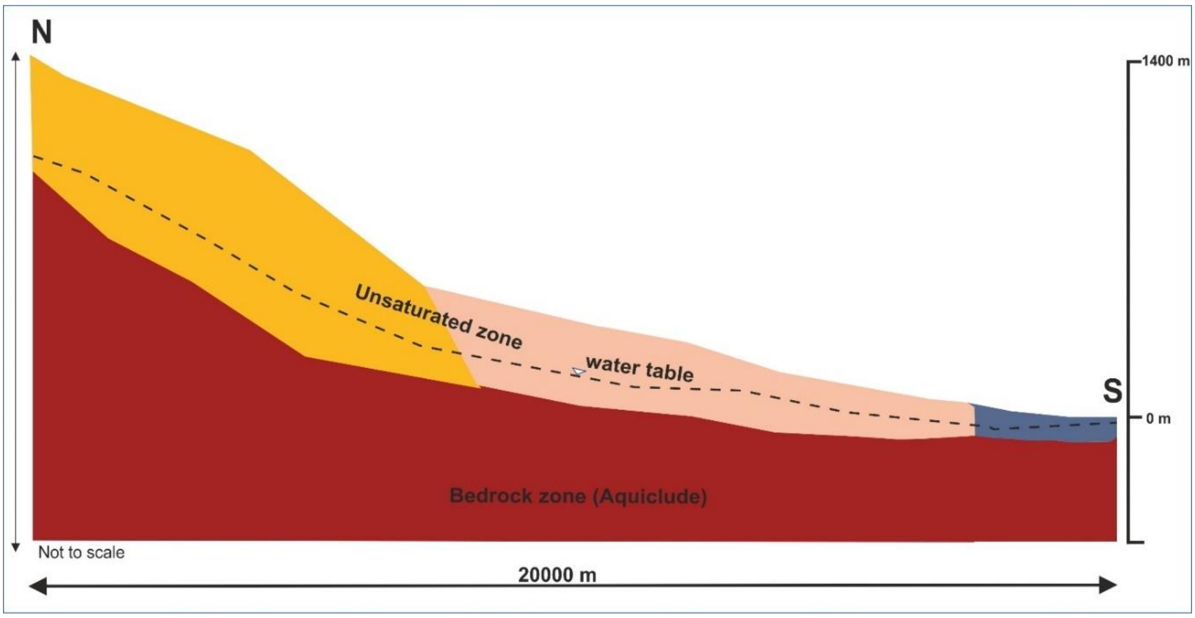

Figure 9. Sketch of hydrogeology cross section across the J.R

Table 2. Boreholes data distribution in the J.R.

No	Name	longitude [x]	Latitude [y]	Elevation of Boreholes [m]	Water table level [m]
1	Boreholes1	114° 33' 33,3"	08° 21' 05,6"	87.00	3.00
2	Boreholes2	114° 34' 53,7"	08° 19' 51,7"	94.00	30.00
3	Boreholes3	114° 48' 20,3"	08° 25' 11,4"	77.00	1.50
4	Boreholes4	114° 48' 19,8"	08° 25' 08,2"	79.00	1.40
5	Boreholes5	114° 48' 20,3"	08° 25' 11,4"	55.00	1.50
6	Boreholes6	114° 36' 26,4"	08° 19' 51,7"	70.00	5.00
7	Boreholes7	114° 36' 28,7"	08° 23' 30,3"	70.00	5.00
8	Boreholes8	114° 34' 05,5"	08° 17' 57,8"	70.00	7.00
9	Boreholes9	114° 33' 59,7"	08° 17' 55,0"	46.00	6.00
10	Boreholes10	114° 32' 49,1"	08° 19' 43,0"	37.00	8.00
11	Boreholes11	114° 35' 12,4"	08° 24' 00,3"	45.00	3.00
12	Boreholes12	114° 35' 17,2"	08° 24' 03,2"	40.00	3.00
13	Boreholes13	114° 34' 34,3"	08° 23' 00,7"	41.00	3.00
14	Boreholes14	114° 35' 21,3"	08° 19' 57,7"	40.00	27.00
15	Boreholes15	114° 35' 21,4"	08° 19' 57,3"	39.00	25.00
16	Boreholes16	114° 35' 21,6"	08° 19' 58,5"	40.00	27.00

Groundwater head observation in J.R was observed from the boreholes data, these data were taken from May 2013 to January 2014. It was found that there are 16 boreholes installed around the Jembrana Region. These data were collected from Public Works Agency of Bali province government, locally called 'DPU'. The hydraulic characteristics were observed by using pumping test data that spread sparsely located inside the Jembrana Region. The pumping test spots in Pergung Catchment counted 23 points out of 46 total spot. The range value of transmissivity is from 51.00 m^2day^{-1} to 4321.69 m^2day^{-1}, and the average was ~1876.64 m^2day^{-1}.

3. METHODS

3.1. Research workflow

Figure 10 illustrated steps that were done to attain the objective of this study. This study was divided into three steps which are preparation signed by (green colour), processing (orange), and the results and interpretations (yellow).

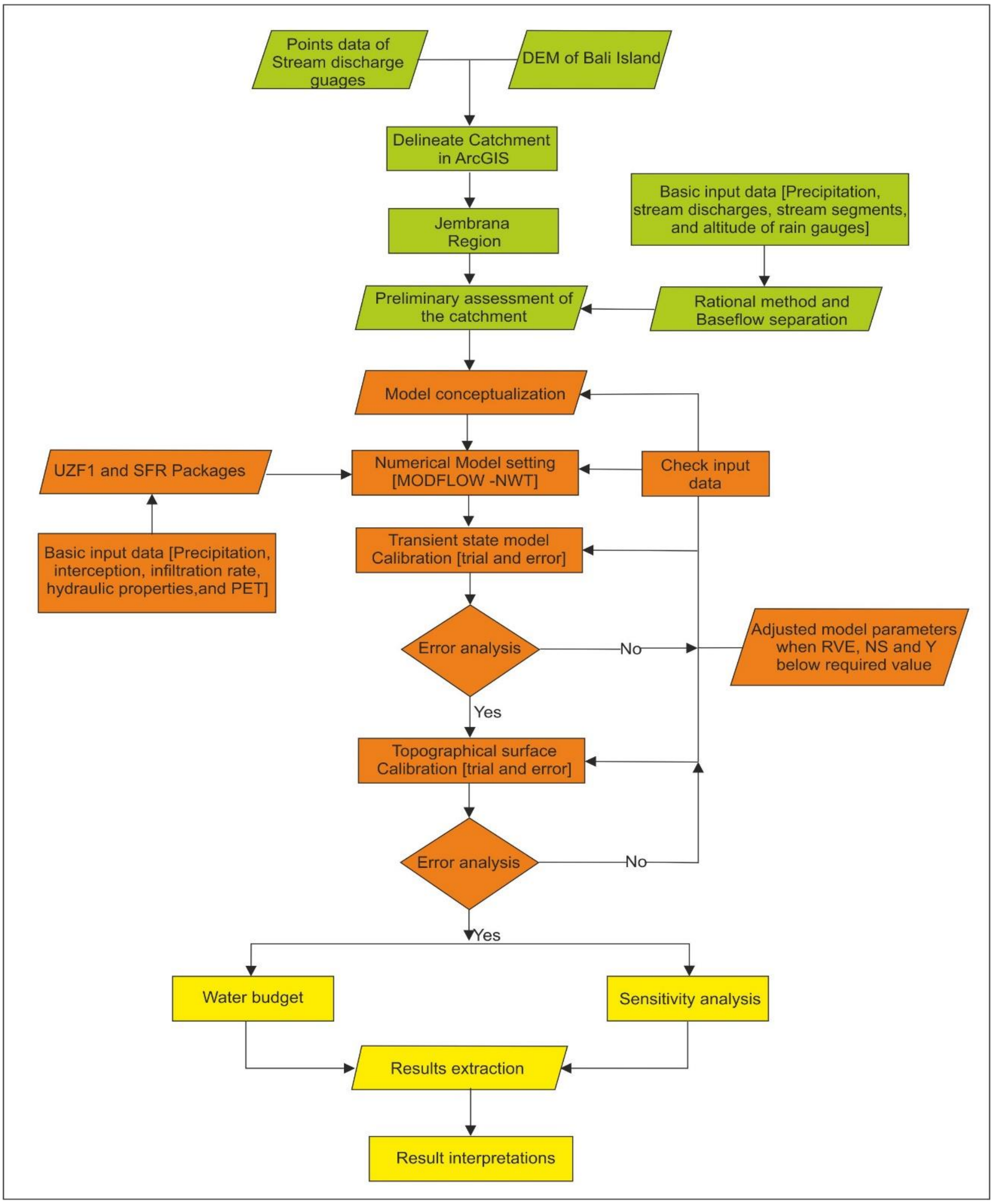

Figure 10. Flow chart of research

3.2. Data processing to select pilot catchment areas

Meteorological and hydrogeology data were required to generate a groundwater assessment model. In the J.R, four-years series of hydrologic year daily records of stream discharge and precipitation are available starting from 1st January 2009 till 31th December 2012. They are delivered from eight rain gauges and 14 stream discharge gauges which are spread sparsely over the region (see Figure 2). These data have been collected from Agency of Public Works or locally called "DPPU" and Meteorological and Geophysics Agency or locally called "BMKG" of Bali government. These data combined with DEM 90 m resolution from SRTM (Shuttle Radar Topographic Mission) of Bali Island have been used in the pre-processing which part of catchment assessment. The purpose of catchment assessment is to select the catchment for IHM simulation and calibration in Jembrana region.

Table 3. Data availability in Jembrana region

No	Required data	Available data	Available no of Stations	Frequency of available data	Units required
1	Digital Elevation Model (DEM)	V	X	X	m
1	Precipitation	V	8	Daily	$mday^{-1}$
2	Stream Discharge	V	14	Daily	$mday^{-1}$
3	Evapotranspiration	V	2	Daily	$mday^{-1}$
4	Groundwater level	V	16	X	m
5	Groundwater abstraction	X	X	X	m^3day^{-1}
6	Interception	X	X	X	$mday^{-1}$
7	Infiltration rate	X	X	X	$mday^{-1}$
8	K_s	X	X	X	m^2day^{-1}
9	S_y	X	X	X	m^2day^{-1}

Where V: data are available, X: Data are not available, Ks: Saturated hydraulic conductivity, and Sy: Specific yield.

The table above presents some data type required for MODFLOW-NWT. The existing data are considered as not complete of the data set because of eight datasets, only five datasets that already full fill the requirement. The rest are still needed to be adjusted, and some of them also have taken from literature sources. Then the available data were calculated through proper methods and then converted in such a way to be accepted as input parameters in the MODFLOW-NWT. Groundwater abstraction was not incorporated in the simulation and calibration of IHM because there is no data related to it in the study area. Also, other data such as piezometers which show groundwater level are not available in this region. However, there are sixteen bore hole data over the region; they are considered only one day data having daily records, but they show the groundwater level over the Jembrana region. However, these data have been collected by Agency of Public Works in different time ranged from May 2013 to January 2014 which is not part of the simulation period.

The data were processed through some hydrological procedures. First, checking the quantity and quality of precipitation and stream discharges was carried out by scanning of daily records of three years hydrologic years started from 1st October 2009 till 30th September 2012. It was found that there are some missing data of precipitation and it was solved by using rational method (Equation 3.1). The details of quantity and quality of the data can be seen in Appendices I. Second, checking the consistency of precipitation data and stream discharge was considered as critical issues in modelling and it was carried out by using a double mass curve method. Third, DEM data incorporated with point data location of discharge stations were used for delivering stream segments, Jembrana catchment and contributing area of each catchment using hydrology spatial analyst tools in ArcGIS software which consists of flow direction, flow accumulation, stream order, stream to feature, and watershed respectively. As the results, ten catchments were produced through those processes (Figure 6).

$$Q = c.I.A \tag{3.1}$$

Where Q is stream discharges of the catchment [$m^3 day^{-1}$], c is runoff factor, I is rainfall intensity [$mmday^{-1}$] and A is drainage area [m^2]. Stream discharge [Q] and precipitation [I] are available in daily records. Drainage area [Au] of each catchment (Table 2) was defined using spatial analyst tool in ArcGIS software.

3.2.1. The J.R. assessment

The first aim of J.R assessment is to select one catchment out of ten for IHM simulation and calibration. Also, the second is to know the characteristic of the catchment in terms of correlation of the rainfall distribution, streamflow and groundwater regime over the region. Hydrological data, such as precipitation, stream discharge, and DEM were involved in this assessment. This assessment was conducted through hydrological procedures using excel spreadsheet and ArcGIS software. The excel spreadsheet was used to estimate missing data of precipitation and stream discharge using rational method (Equation 3.1); and then spatial analyst tool ArcGIS was used to define the J.C. boundary and contributing area [Au] of each catchment by coupling DEM and stream discharge locations. As the results, ten catchments were produced over the J.R. The assessment has been carried out on these catchments using rational method and baseflow separation (Figure 6). The rational method was used to fill missing data of precipitation and stream discharge by assuming runoff factor constants over the region. This method is commonly used for estimating discharge in small watershed (Thompson 2006) it was originally developed by Kuichling (1889). Then baseflow separation was used for estimating surface runoff (Qs) and groundwater runoff (Qg) from estimated streamflow. Web-based Hydrograph Analysist Tool [WHAT] was selected for baseflow separation.

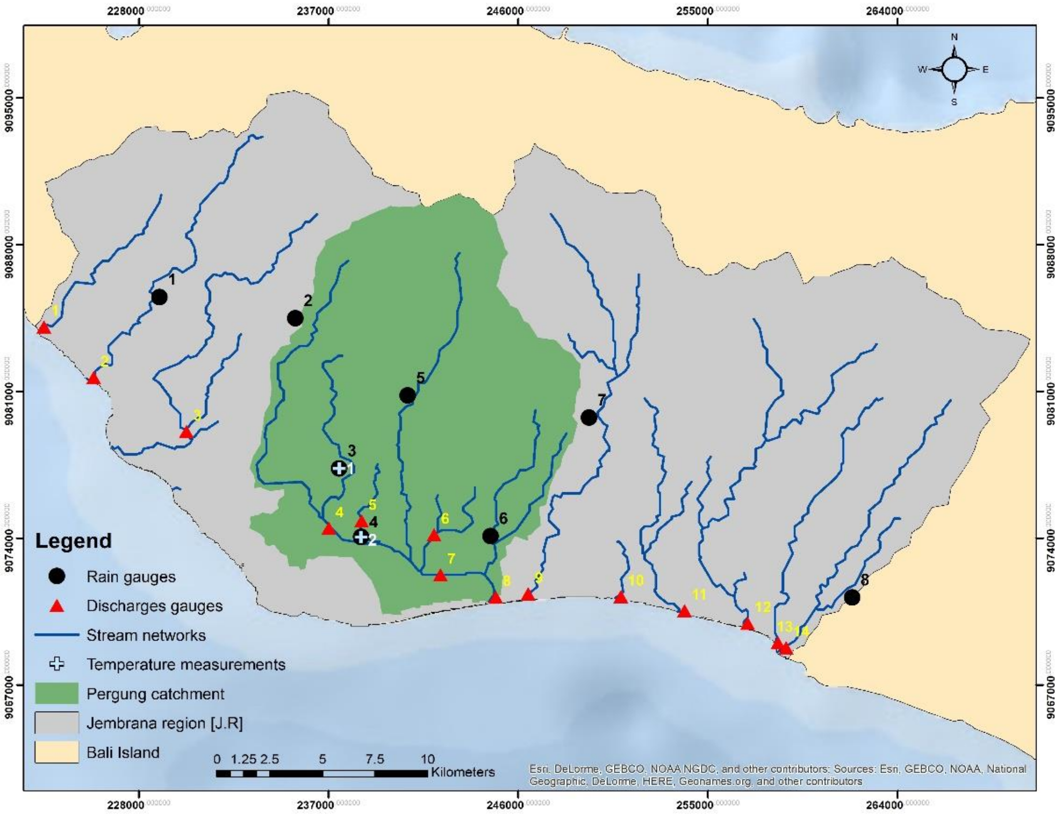

Figure 11. Selected catchment (Pergung catchment) after J.R assessment

One period hydrologic year (1st October 2009 to 30th September 2010) was selected to perform this assessment. As the results, Pergung catchment (P.C) was selected for IHM simulation and calibration. it covers ~212.36 km². This catchment was selected because a lot of monitoring stations are located around this area. Moreover, it is the biggest catchment in the J.R which also considered as transitions between drier and wet area and representative area of the region.

3.2.2. The Pergung Catchment (P.C) assessment

Pergung Catchment has four stream discharge gauges meaning that there are four sub-catchments in this catchment. By using similar methods with J.R assessment, rational method and baseflow separation were applied in this assessment to select sub-catchment for IHM simulation and calibration. Before going through the catchment assessment, the outlet stream segments P.C has checked using Google maps and RBI (base map of Indonesia). As the results, there is a deviation of the outlet of streams network SRTM 90 m resolution. Therefore, DEM data was shifted from SRTM 90 m resolution to ALOS PALSAR 12.5 m resolution. DEM ALOS was obtained from https://www.asf.alaska.edu/sar-data/palsar/terrain-corrected-rtc/. According to ALOS, Pergung catchment covers ~~221.76 km². By using the same method with J.R assessment, four sub-catchments were derived from P.C, namely Sebual, Jogading, Daya Timur and Pergung respectively (see Figure 12). After that, these sub-catchment were assessed using rational method and baseflow separation. As the results, Sebual and Jogading were performed dynamics of surface runoff and groundwater runoff.

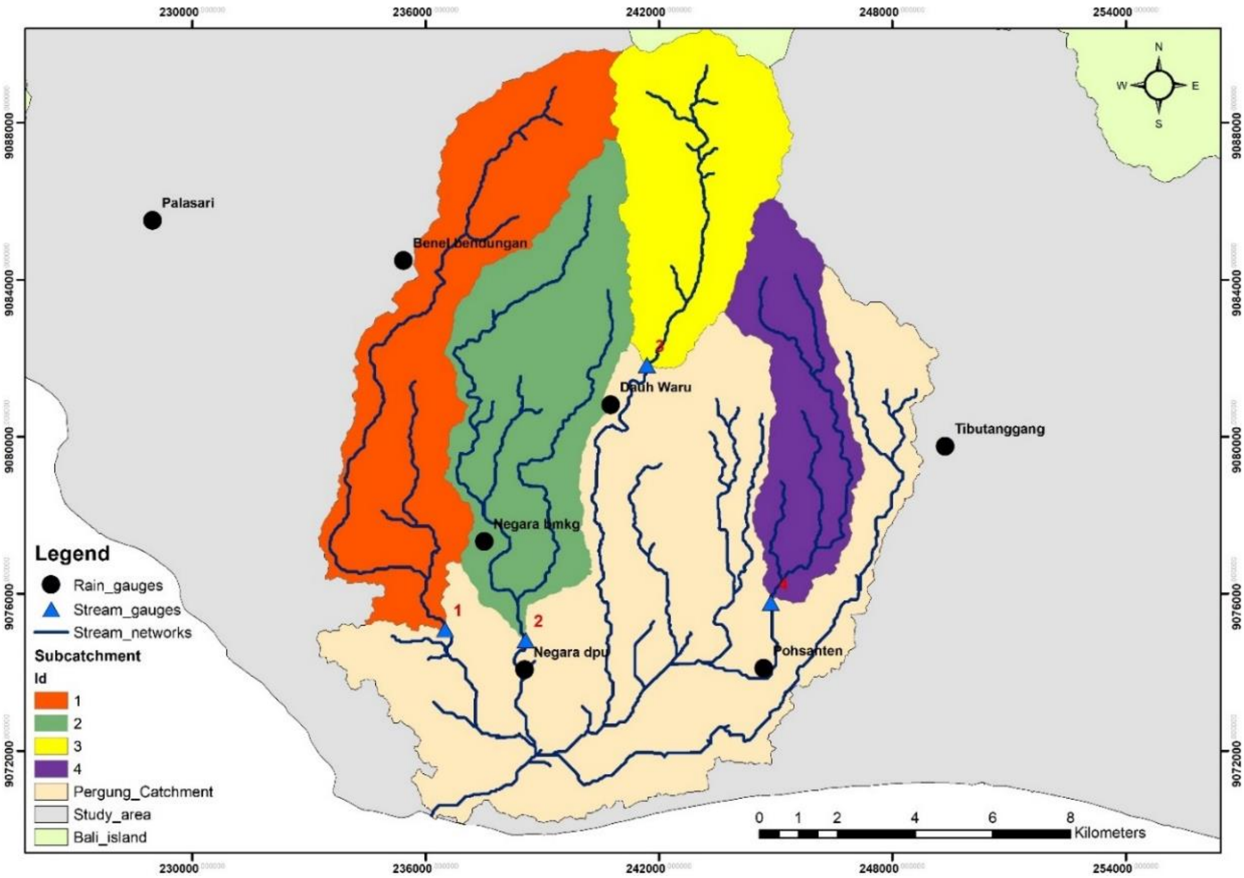

Figure 12. Selected sub-catchment (SC): (1) Sebual (2) Jogading after P.C assessment, (3) Daya Timur and (4) Pergung sub catchment

Sebual_SC covers ~41.00 km², Jogading_SC was~36.70 km², Daya Timur _SC was~27 km² and Pergung_SC was ~20 km² . Sebual and Jogading Sebual_SC considered to have lower groundwater runoff, but higher of surface runoff whereas Jogading_SC [~36.70 km²] was performed lower of surface runoff but higher in groundwater runoff. Therefore, these sub- catchments were selected for This dynamic interactions of surface and groundwater runoff in was being the main factor to select for IHM simulation and calibration

3.2.3. Baseflow separation

As stated earlier, baseflow separation [WHAT] was used for assessing J.R. and P.C to select the catchment for IHM simulation and calibration. It is public domain software which incorporated with a USGS geological survey webserver. It is web base software which is available at links https. //engineering.purdue.edu/mapserve/WHAT/. it was developed by Lim et al. (2005). This method is commonly used for validating hydrological components of a model. In principle, it uses a local minimum method with two digital filtering methods, BFLOW filter (Lyne and Hollick,1979) and the Eckahrdt filter (Eckhardt, 2005). Technically, there are three steps had to follow in executing this method. First, setting daily records of stream discharge in text file formatted, then uploaded them into the website and the direct runoff (Qs) and baseflow (Qg) were produced quickly in csv file formatted. Moreover, this method also generated the hydrograph of estimated streamflow, surface runoff and groundwater runoff respectively.

3.3. Precipitation

The consistency of precipitation records of eight rain gauges was checked using the double mass-curve method (Searcy and Hardison 1960) for the period of hydrologic year 2009 till 2011 (Equation 3.2). The principle of this method is that the cumulative value of target stations (y-axes) is compared to the nearby average a group stations (x-axis). The purpose of checking the consistency is to evaluate whether the data have good quality or not before incorporating them into the model. In general, they performed good consistency which means that data have good quality.

$$Pa = \frac{\delta a}{\delta b}\, Pb \tag{3. 2}$$

Where, Pa is adjusted precipitation, Pb is actual precipitation, δa is slope before break, δb is slope after break or where the precipitation records should be adjusted.

Precipitation data of rain gauges were used for catchment assessment over J.R. Then for IHM Sebual and Jogading, those data were interpolated using Inverse Distance Weighting (IDW) method in ArcGIS software with power was assigned to 1 and cell size was set to 100 m in daily basis (1096 days). Before using IDW interpolation, the average of precipitation 2009 from eight stations has been plotted against altitude to check whether there was any correlation or not between them. As the results, it was revealed that coefficient determination (R^2) was very low which is 0.045 meaning that there is no correlation between rainfall and the altitude. Then the average area of spatial data interpolation of precipitation was calculated in ArcGIS software using Model builder zonal statistics as table tools.

3.4. Stream discharge consistency

Instead of precipitation, stream discharge is the only one state variable of the IHM model. Therefore, it has to be managed properly to have good enough quality of consistency. The consistency of discharge data was checked and re-adjusted by using the double mass - curve method. According to observation results, the Sebual, Jogading and Daya Timur showed inconsistency of stream discharge records. Therefore, this method was applied for re-adjusting stream discharge records of Sebual, Jogading and Daya Timur.

3.5. Stream discharge validation

The amount of stream discharge data in Sebual and Jogading was validated with three hydrologic years (1 October 2009 till 30 September 2012) spatial data interpolation of rainfall in the those area. As the results, they performed good correlation between stream discharges (Q) and the rainfall (RF) distribution. It was clear that in the wet season the amount of stream discharge was higher compared to the dry season.

3.6. Estimation of missing data of stream discharges

The discharge data from 2009 to 2012 has been observed; however, some data in Jogading station from 1st January to 31st December 2011 were missing. This was might be due to no observation or measurement during that period. Therefore, these missing data must be estimated by the reliable method. In this case, rational method was used to fill missing stream discharge data, it was based on the nearby discharge station records.

3.7. Head observation

As stated earlier, there are no piezometers data for both IHM Sebual and Jogading. Therefore, head observations have been conducted by assigning fictitious piezometers using a Head observation package (HOB) in the MODFLOW-NWT. Nine fictitious piezometers were installed in Sebual and Jogading sub catchment to records the heads. Moreover, these piezometers have been used for observing calibrated heads distributions over the models. The observed heads were set equal to surface altitude [DEM] because they also were used for calibrating groundwater heads upon surface altitude.

3.8. Conceptual model

Anderson and Woessner (1992) defined a conceptual model is a descriptive representation of the groundwater flow system that integrated with hydrogeological conditions. To set up conceptual model, it needs good information about hydrogeology, hydraulic parameters, and boundary conditions. It is generated to figure out the complex field problem in a simplified way, then easy to formulate in the numerical model. Modelers need to pay more attention in generating conceptual model because commonly error occurred in formulating it, and if there is an error, it will be accumulated in the numerical model. There are four steps in developing the conceptual model; 1) Defining hydrostratigraphic units, 2) determining flow system, 3) defining preliminary water balance, 4) and determining boundaries of the model.

The conceptual model is the most important part in the groundwater modelling because commonly error and failure of the simulation and calibration model due to mistakes in figure out of the conceptual model. In this study, data regarding piezometers, wells, and cross-section were not available both in Sebual and Jogading sub catchment. Therefore, IHM of Sebual and Jogading were classified into one layer unsaturated zone of an unconfined aquifer.

3.8.1. Defining hydrostratigraphic unit

The Jembrana region is composed by upper Quaternary and lower Quaternary. The Upper Quaternary is volcanic sequence unconsolidated sand, gravel, volcanic ash, lava flow, breccia, clay, and tuff from Jembrana mountain. The lower Quaternary is Palasari formation which is composed of limestone, sandstone, reef limestone and alluvium (unconsolidated silt, clay, sand, gravel). Stratigraphic unit with the same hydrogeological characteristics can be combined into one hydrostratigraphic unit (Anderson and Woessner 1992). Therefore, either upper Quaternary or lower Quaternary can be considered as an unconfined aquifer. The top of the aquifer is water table, and the bottom can be assumed as aquiclude. Then beneath of the stream is considered as an unsaturated zone, which is one-dimensional vertical flow of Richards' equation. In this zone, it is possible to have interactions between stream and aquifer. The hydrostratigraphic units of Sebual and Jogading sub catchment was generated based on the hydrogeology bore hole data. In IHM, both Sebual and Jogading were set to have one layer of unconfined aquifer due to lack of data.

3.8.2. Defining the flow system

Groundwater flows from higher hydraulic head to lower hydraulic head (Fetter 2001). According to DEM, stream networks and stream discharge data in Figure 2, the flow direction in this catchment was described from north to the south part or considered from a higher altitude to lower altitudes in Pergung catchment.

3.8.3. Defining preliminary water balance

Based on the preliminary assessment above, precipitation is considered as the only sources in water balance components. However, interception, infiltration rate and evapotranspiration were used as driving forces in IHM of Sebual and Jogading sub-catchment. They have an important role in water balance components because around fifty percent of the catchment covered by forest, then agriculture, and grass cover.

3.8.4. Defining boundaries of the model

Model boundary set up has significant impact of the model results. Model conceptual boundaries consist of physical and hydrological boundaries. In this study, hydrological boundaries defined by mountain ranges from northern to southern part of the sub catchment were assumed as groundwater divides which can be represented as no-flow boundary. The bottom of unconfined aquifer contact with bedrock was assumed to be no-flow boundaries as well.

3.9. Numerical model setup

3.9.1. Software selection

MODFLOW-NWT was used in this study to generate the model for both Sebual and Jogading. The active packages were UZF1 and SFR2 to simulate daily data from 1st October 2009 to 30th September 2012. It is a Newton formulation of MODFLOW-2005 which is used for connecting saturated and unsaturated zone (Hassan et al. 2014). It has the ability to solve non linearities rewetting and drying problems of unconfined groundwater-flow equation (Niswonger et al. 2011). It works based on Upstream Weighting Package (UPW), and differs from Block Centered Flow (BCF), Layer Property Flow (LPF) and Hydrogeologic Unit Flow (HUF) packages in which heads in two adjoining cells are used to estimate the intercell horizontal conductance. Furthermore, The UPW package smoothes the horizontal-conductance function and the storage-change function during wetting and drying of a cell to give continues derivatives solution by the Newton method (Niswonger et al. 2011). MODFLOW-NWT is working under ModelMuse Graphical User interface (GUI) and merged with the Unsaturated zone flow (UZF1) package and stream flow routing (SFR2) packages. Therefore, in this study MODFLOW-NWT software was selected to generate the model because: (i) it is able to integrate SFR2 and UZF1 packages (ii) it is an international standard for groundwater modelling (iii) Open source software which is free of charge.

Unsaturated Zone Flow (UZF1) package

The (UZF1) package was used to simulate the flow and storage in the unsaturated zone and to separate flows into evapotranspiration and recharge. One dimension form Richard's equation is approximated by the kinematic wave equation to simulate the flow of water in vertical directions. A kinematic wave approximation to Richards' equation is solved by the method of characteristics to reproduce the vertical vadoze flow. The package assumes that unsaturated flow occurs in response to gravity potential gradients only and neglects negative potential gradients. Additionally, This package assumes uniform hydraulic properties in the unsaturated zone for each vertical column of model cells. The Brooks-Corey function is used to determine the correlation between unsaturated hydraulic conductivity and water content. Residual water content is estimated internally by this package on the basis the difference between saturated water content and specific yield (Niswonger et al. 2006). Infiltration rate is assigned as land surface instead of specified recharge rate directly to groundwater. The assigned infiltration rate is further restricted by the saturated vertical hydraulic conductivity. In case of ET, Evapotranspiration losses are first removed from the vadose zone above the evapotranspiration extinction depth, and if the demand is not met, water can be removed directly from groundwater whenever the depth to groundwater less than the extinction depth. Moreover, water is discharged directly to land surface whenever the altitude of the water table greater than land surface. Water that is discharged to land surface, as well as applied infiltration in excess of the saturated vertical hydraulic conductivity, may be routed directly as inflow to specified streams or lakes (Niswonger et al. 2006). This package requires input data, such as evapotranspiration, infiltration rate, extinction depth, and extinction water content.

$$\frac{\partial\theta}{\partial t} = \frac{\partial q}{\partial z} - i = \frac{\partial}{\partial z}\left|D(\theta)\frac{\partial\theta}{\partial z} - K(\theta)\right| - i \qquad (3.3)$$

$$q = -K(\theta) \qquad (3.4)$$

$$\frac{\partial\theta}{\partial t} + \frac{\partial K\,(\theta)}{\partial z} + i = 0 \qquad (3.5)$$

$$\frac{\partial\theta}{\partial t} + \frac{\partial K\,(\theta)}{\partial z}\frac{\partial\theta}{\partial z} = -i \qquad (3.6)$$

Where θ- volumetric water content [m^3m^{-3}], q is water flux [$mday^{-1}$], z- elevation in vertical direction [m], $D(\theta)$- hydraulic diffusivity [m^2day^{-1}], $K(\theta)$- unsaturated hydraulic conductivity [$mday^{-1}$], i - ET rate per unit depth [$mday^{-1}$], t- time [day].

Stream Routing Flow (SFR2) package

The SFR2 package uses a kinematic-wave approximation to Richards' equation which is solved by the method of characteristics to simulate the flow and storage in the unsaturated zone beneath the stream (Niswonger and Prudic 2005). The kinematic-wave approximation to Richards' equation ignores diffusive forces and flow is assumed to take place in the vertical-downward direction. Therefore, this package was filled unsaturated zone pores from top to down sequence and the saturated region below the stream will be relatively narrow. The method of characteristics is used to reduce the one-dimensional partial-differential equation deriving from the kinematic-wave approximation to an ordinary differential equation that is solved by analytical integration. Unsaturated flow is reproduced independently of saturated flow within each model cell meet a stream reach whenever the water table is lower than the elevation of the streambed. This simulation is also based on dimension Richard's equation which uses a kinematic wave approximation. The relation between unsaturated hydraulic conductivity and water content is determined by the Brooks-Corey function (Niswonger and Prudic 2005). In this package, unsaturated flow variables such as saturated and initial water content; saturated vertical hydraulic conductivity; and the Brooks-Corey exponent are determined independently for each stream reach. This package requires input variables such as saturated water contents and unsaturated zone, Brook-Corey exponents for the unsaturated zone, and vertical hydraulic conductivity.

$$\frac{\partial\theta}{\partial t} = \frac{\partial q}{\partial z} = \frac{\partial}{\partial z}\left|D(\theta)\frac{\partial\theta}{\partial z} - K(\theta)\right| \quad (3.7)$$

$$q = -K(\theta) \quad (3.8)$$

$$\frac{\partial\theta}{\partial t} + \frac{\partial K(\theta)}{\partial z} = 0 \quad (3.9)$$

$$\frac{\partial\theta}{\partial t} = \frac{\partial K(\theta)}{\partial z}\frac{\partial\theta}{\partial z} \quad (3.10)$$

Where θ- volumetric water content [m^3m^{-3}], q is water flux [$mday^{-1}$], z- elevation in vertical direction [m], $D(\theta)$- hydraulic diffusivity [m^2day^{-1}], $K(\theta)$-unsaturated hydraulic conductivity [$mday^{-1}$], i - ET rate per unit depth [$mday^{-1}$], t- time [day].

3.9.2. Aquifer geometry design

Aquifer geometry is discretized by the applied grid and tops and bottoms of model layers and water table distributions. In this study, the models were set the grid size to 100 m * 100 m. Sebual was set up with 46 column and 129 row while Jogading 49 column and 124 row respectively. Following the conceptual model, the numerical models of the two catchments simulated (Sebual and Jogading), consist in both cases of one unconfined layer because of hydrogeological data limitation; in both cases the top model is represented by DEM.

3.9.3. Driving forces

Precipitation, evapotranspiration, and infiltration rate were considered as the driving forces of IHM Sebual and Jogading sub catchment. These data were governed systematically into account of the MODFLOW-NWT. Both UZF1 and SFR2 packages were processed them to produce the results.

3.9.4. Precipitation

Precipitation is one of driving force input to the model. Spatial data interpolation of precipitation has been derived from eight rain gauges over the J.R. Inverse Distance Weighting [IDW] method was selected to interpolate daily records precipitation (1096 days). IDW method performed more reliable estimation than the other method (Kriging, Spline and ANUDEM) (Yang et al. 2015). This process was conducted in the Arc GIS software, and the method was specified to power 1 and cell size 100 m. Then, spatial data interpolation of daily records precipitation was imported to the model as raster ASCII files formatted in daily basis. The precipitation data were assigned in the UZF1 package as infiltration rate variable. It was set spatiotemporal variable during simulation and calibration period.

3.9.5. Interception and infiltration rate

Interception and infiltration rate of Sebual and Jogading were calculated spatially based land use and land cover map of the model area. According to land use and land cover map (Figure 5), it is clear that more than fifty percent of the area was covered by forest and vegetation. Therefore, interception and infiltration rate considered as important parameters in water balance components. They are also considered as driving forces of input data in IHM. The higher rainfall, the more interception will be captured by a canopy, and it will affect infiltration to the soil. Interception loss can be calculated with the following equation (Weldemichael 2016).

$$I = P*[I_f*A_f + I_{Agr}*A_{Agr}] \tag{3.11}$$

Where I is canopy interception per grid cell [mday^{-1}], P is precipitation [mday^{-1}], I_f and I_{Agr} is interception loss rate by forest and other land use [% of P], A_f and A_{Agr} is the ratio of forest and other land cover area. Then for infiltration rate in this catchment can be estimated based on equation below:

$$P_e = P - I \; ; \; \text{OR } P_e = P - [P*[I_f*A_f + I_{Agr}*A_{Agr}]] \tag{3.12}$$

Where P_e is effective infiltration rate per grid cell [mday^{-1}], P is precipitation [mday^{-1}], I_f and I_{Agr} is interception loss rate by forest and other land use [% of P], A_f and A_{Agr} is the ratio of forest and other land cover area. Infiltration rate was used in UZF1 package to calculate unsaturated zone evapotranspiration, unsaturated zone storage and groundwater recharge (Niswonger et al. 2006).

In this study, I_f and I_{Agr} were adjusted spatiotemporally variably between wet season (1st October to 31st March) and dry season (1st April to 30th September) because interception (I) correspond to rainfall (P); where P according to data was seasonally higher in the wet season and lower in the dry season. Therefore, I_f and I_{Agr} also were set higher in the wet season and lower in the dry season as (Table 4).

Table 4. Percentage of interception rate based on land use and land cover

Jembrana land cover	Interception loss	Adapted literature	Interception loss in Wet season	Interception loss in Dry Season
Forest	22.4 %	(Ghimire et al. 2012)	22.4%	20.16%
Agriculture	14.4%	(van Dijk and Bruijnzeel 2001)	14.4%	7.2 %
Grass	6.5%	(Corbett et al. 1968)	6.5 %	3.25%

Furthermore, satellite images were used to indicate spatiotemporally variably of interception in wet and dry season. As the results, a couple images with 30 m resolution were collected from https://earthexplorer.usgs.gov/ from Landsat 5 and 7; one image in wet period (15 March 2010) and the second image in dry periods (29 July 2013). Then, those images were processed in QGIS and ERDAS imagine software for removing clouds, atmospheric correction and NDVI calculation. After that, spatially interception and infiltration rate were applied in land use and cover map. The interception rate was calculated as rainfall multiplied with the rate of interception (Equation 3.11). Infiltration rate was estimated as rainfall subtracted by interception rate times rainfall (Equation 3.12).

3.9.6. Potential Evapotranspiration

Potential evapotranspiration [PET] is defined as the rate at which evapotranspiration will take place in the large area where covered by homogeneous growing vegetation which can take water from soil zone and without advection and heating effects (McMahon et al. 2013). According to several studies, ETo of FAO Penman-Monteith was considered as best estimation compared to another method (Wang et al. 2012). However, in this study only two temperature measurements are available for measuring a temperature in the catchment, which is in the station Negara BMKG and Negara DPU. They are located close to each other which is not enough either for calculating ETo FAO Penman-Monteith or spatial interpolation over the modelled area.

Therefore, the spatio-temporal PET data was taken from literature satellite images [MODIS] 1000 m resolution every eight days (after Rahmawati, 2017) in this study. The data was resampled into 100*100 m using Arc GIS software in order to match with the grid size of IHM Sebual and Jogading. Then, the cumulative values of eight days PET MODIS was converted into daily basis because MODFLOW-NWT required input daily data of PET. Thus, the values of PET was temporally constant in every eight days period. The original satellite data of PET MODIS 1000m with eight day temporal resolution can be obtained from web link http://files.ntsg.umt.edu/data/NTSG_Products/MOD16/MOD16A2.105_MERRAGMAO/Y2010/ .

3.9.7. Model parametrization

The models were simulated in the transient state in the period from 1st October 2009 to 30th September 2012, which UZF1 and SFR2 were set as active packages and applying fully "convertible option". Convertible option is another term of unconfined aquifer, which is available in MODFLOW-NWT layer group options. It was set to unconfined due to lack of hydrogeological data. IHM Sebual and Jogading have been set up in ModelMuse Graphical User Interface (GUI), using NWT solver which consists of Head Tolerance [HEADTOL] was set 0.0001 m^3, Flux Tolerance [FLUXTOL] was 900 m^3day^{-1}, Maximum number of outer iteration [MAXITEROUT] was set at 1000, Model complexity [OPTIONS] was set as Complex. Flows simulated in Upstream weighting (UPW) and Unsaturated zone flow (UZF1) packages.

UZF1 parameterizations comprise of the recharge and discharge location option [NUZTOP] was set as top active cell (3), vertical hydraulic conductivity source [IUZFOPT] was selected as specify vertical hydraulic conductivity (1), number of trailing wave [NTRAIL2] was assigned to 16, number of wave [NSET2] was set 20 because infiltration rate spatially and temporally vary in time, and then others parameters such as route discharge to streams, lakes or SWR reaches [IRUNFLG], simulate evapotranspiration [IETFLG], print summary of UZF budget terms [IFTUNIT], and calculate surface leakage [Inverse of NOSURFLEAK] were selected. The boundary conditions, General head boundary [GHB] and Stream Flow Routing package were selected in Head-dependant flux. The conductance [C] were calculated per unit length or area, it was set to 3 m^2day^{-1} for Sebual and 1 m^2day^{-1} for Jogading. Extinction water content for Sebual and Jogading were set to 0.35 m^3m^{-3} and 0.25 m^3m^{-3} respectively. UZF data properties comprise of Brooks Corey-Epsilon was set to 3.5 , the discharge routing was set to 1, Maximum unsaturated vertical conductivity was assigned to 0.05 $mday^{-1}$, saturated water content was set to 0.5 m^3m^{-3} for both models.

SFR parameters such as unsaturated flow [ISFROPT] was selected, streambed properties [ISFROPT] was set to specified streambed properties by reach (can't inactivate streams), tolerance [DLEAK] was set 0.0001 m^3day^{-1}, number of trailing wave increments [NSTRAIL] was assigned to 10, maximum number of trailing waves [NFSRSETS] was set to 30, maximum number of cells to define the unsaturated zone [ISUZN] was set to 10, use transient streamflow routing with kinematic-wave equation [IRTFLG] was selected, number of divisions per time steps kinematic waves[NUMTIM] was set to 1.The time weighting factor for the kinematic wave solution [WEIGHT] was set to 1, and closure criterion for the kinematic wave solution [FLOWTL] was set to 0.0001. Streambed top [STRTOP] was set to 0.6 m, stream slope [SLOPE] was assigned 0.025 m, streambed thickness [STRTHICK] was set to 0.5 m, streambed Kv [STRHC1] was assigned 0.7 times Kx, saturated volumetric water contents [THTS] was set to 0.5, initial saturated volumetric water content [THTI] was set to 0.1 m^3m^{-3}, Brooks-Corey exponent [EPS] was set to 3.5 and maximum unsaturated Kz[UHC] was set to 0.4, and stage calculation [ICALC] was set to specified stage (0). Specific yield [Sy] was set uniformly to 0.25 and 0.27 for Sebual and Jogading. Horizontal hydraulic conductivity zones [HK] were set from 0.05 to 2.5 $mday^{-1}$.

MODFLOW layer group setting consists of a layer group[aquifer] was set upper aquifer with thickness 170 m, layer type [LAYTYP, LTHUF] was set to convertible, method of calculating interblock transmissivity [LAYAVG] was selected as the harmonic mean (0), and method of specifying vertical hydraulic conductivity [LAYVKA] was set to vertical hydraulic conductivity (0). Model top was assigned to Digital elevation model [DEM].

Then stream networks of IHM Sebual and Jogading were extracted from DEM by using ArcGIS software hydrology spatial analyst tools imported as shapefile. Both Sebual and Jogading has seven stream networks and they were activated in SFR package. The raster data of DEM, precipitation, PET, interception and infiltration rate, and extinction depth were converted to ASCII file to be used as the input data in ModelMuse.

Extinction depth [EXTDP] of the models were generated based on land use and land cover map. From Figure 13, both Sebual and Jogading sub catchment dominated by forest. EXTDP is temporally invariable and spatially vary based on the percentage of land use and land cover (Figure 13). EXTDP for forest, was assigned to 2.5 m (Shah et al. 2007), agriculture and grass were set to 1.45 m (Mishra et al. 1999 & Francés et al. 2014) and the bare soil cover was set to 0.5 m (Francés et al. 2014) respectively.

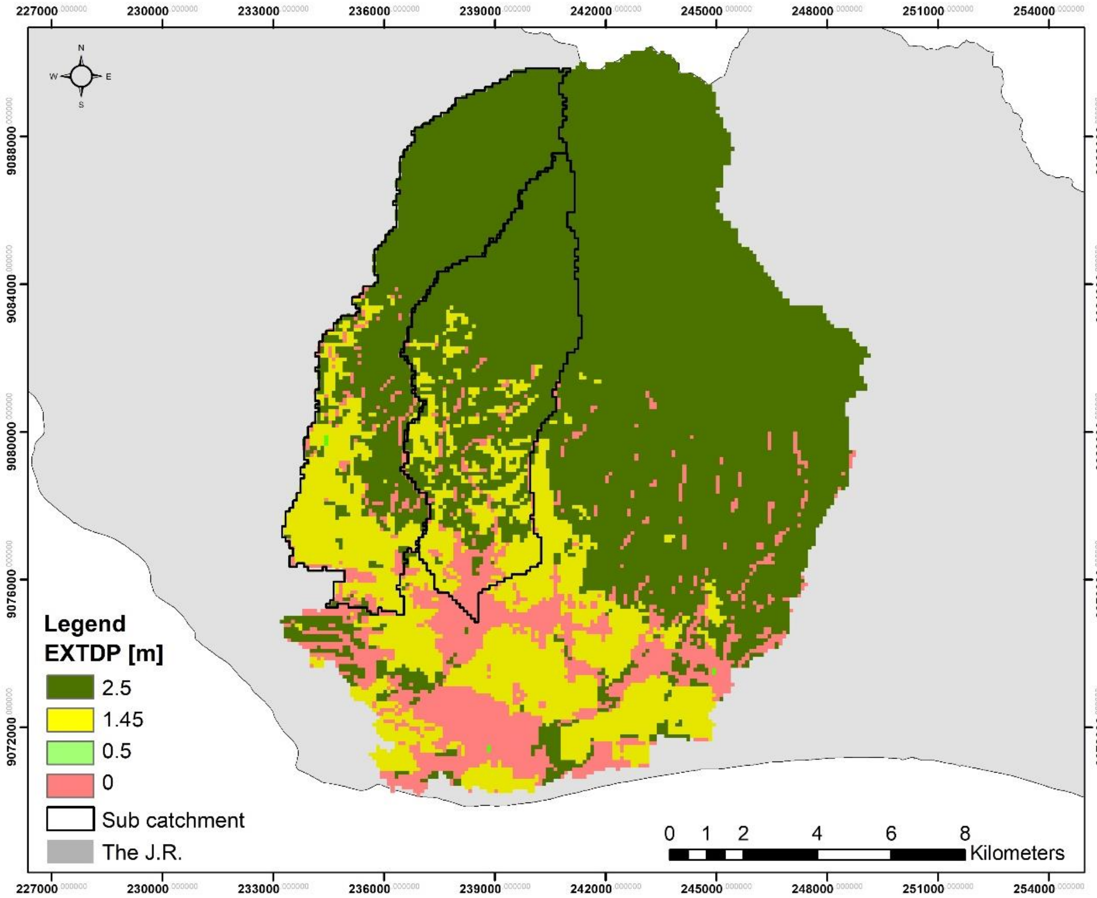

Figure 13. Spatially variable of extinction depth [EXTDP] of Sebual (western) and Jogading (eastern) Sub-catchment.

3.9.8. State variables

The state variables are system characteristics that have various values in the different set of time series. For this study, daily records of stream discharges were defined as the only state variable. It is available in three hydrologic years started from 1st October 2009 till 30th September 2012, and the records were from Sebual and Jogading stream discharges stations. All data were collected from Agency of Public Works, Bali province government. These data were used for model calibration in transient state for both models, instead of calibration with topographical surface [DEM].

3.9.9. Initial conditions

MODFLOW-NWT requires initial conditions variables. IHM Sebual and Jogading used water table from boreholes data for initial conditions. Water table from boreholes data were interpolated using IDW method, and imported to the model as raster ASCII files formatted. Initial unsaturated water content was set uniformly to 0.1 for both models.

3.9.10. Boundary conditions

The models were generated in two boundary conditions : no flow boundary and General Head Boundary [GHB] (McDonald and Harbaugh 1984). The no-flow boundary assumed that there is no flow neither inflow nor outflow between the model and outside area. Meanwhile, GHB was assigned to simulate lateral groundwater outflow from the model. No-flow boundary was assigned as inactive cells and GHB was assigned around the outlet of the sub catchment.

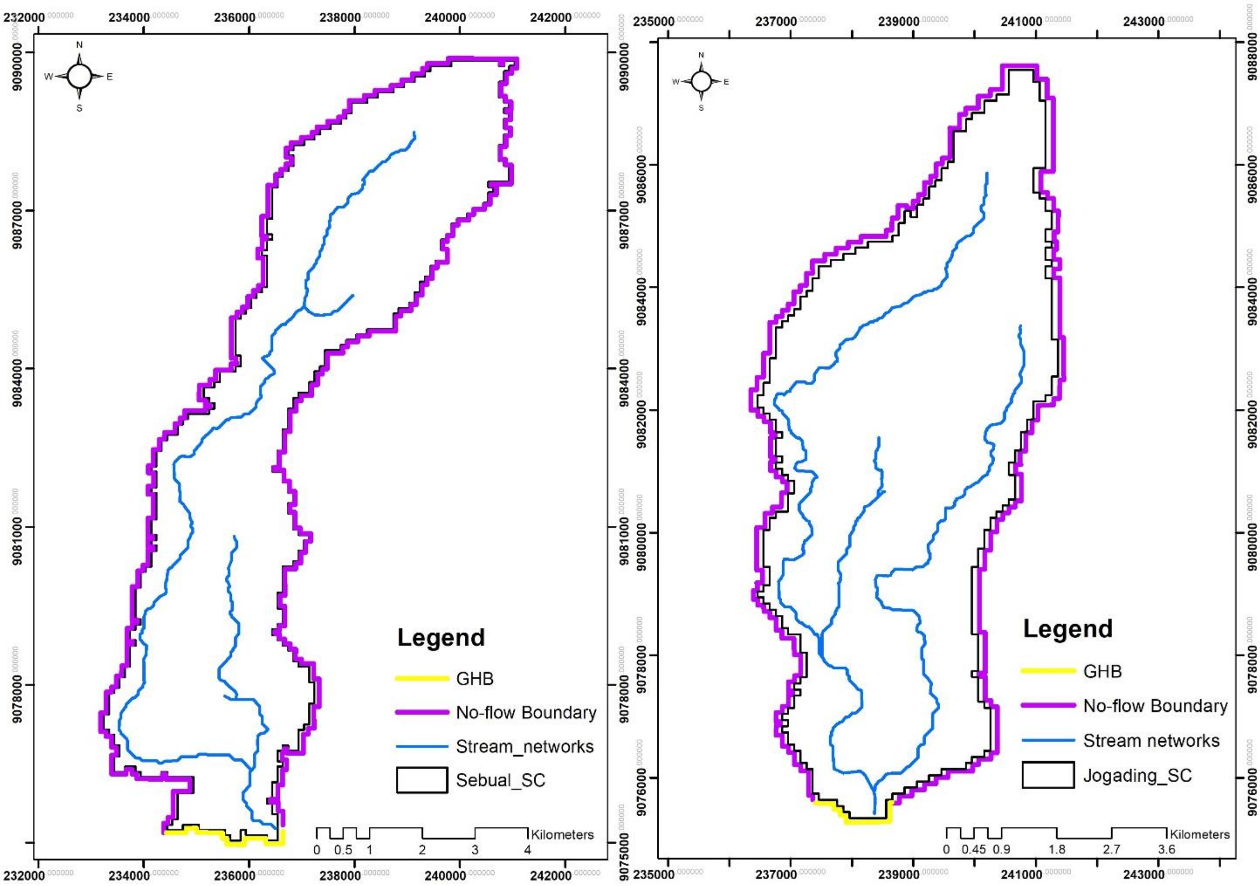

Figure 14. Boundary conditions: General Head Boundary (GHB) and No-flow boundary of IHM Sebual (left) and Jogading (right) Sub-catchment

3.9.11. Numerical Model calibration

The calibration model is also called model fitting or history matching (Barnett et al. 2012). In this steps, input parameters were adjusted till reach the best fit with observed values. In MODFLOW-NWT, calibration has been conducted with adjustment of UZF1 and SFR2 variables, hydraulic conductivity and specific yield. The IHM of Sebual and Jogading were simulated in transient state and calibrate with stream discharge and topographical surface. The aim of IHM transient calibration is to get minimize errors between simulated and observed of stream discharge. In this case, both Sebual and Jogading sub catchments have seven stream segments and all these segments were attributed in the calibration. The last stream segment where observed stream gauges are located was set as the last reach. Then daily output flow from SFR2 package was opened using TextPad software. After that those files were imported to excel spreadsheets to make a comparison between simulated and observed stream discharge. The calibration of IHM has been carried out manually by doing trial and error to understand the behaviour of the system input parameters. Calibration heads with topographical surface have been conducted by subtracted simulated heads that obtained from IHM with DEM map. If the results are positive values, it means that water table is below the surface but if the results show negative values, it means that water table is above the surface. To do this calibration, twenty-seven fictitious piezometers were installed inside Sebual and twenty-six in Jogading sub catchment. The observed heads were set equal to surface altitude [DEM]. These piezometers also are able to record the simulated heads resulted from IHM.

3.9.12. Calibration error

IHM performance of Sebual and Jogading was assessed by applying relative volumetric error [RVE], Nash-Sutcliffe Efficiency [NS] for streamflow after they reached calibrated condition. The objective formula (Equation 3.15 to 3.17) was recommended by Nash and Sutcliffe (1970); Seibert (1997); D. N. Moriasi et al. (2007) & Akhtar et al. (2009). They have used for evaluating the overall performance of fitting simulated hydrograph. The ranges value for RVE is from 0 to 1, 0 is considered no error and 1 is fully error. Inversely, NS is range from 0 to 1, 0 means that the model has very poor performance and 1 implies that the model is in very good performance. Then to evaluate of IHM groundwater heads performance, topographical surface was used to evaluate whether the heads are below or above the surface. In this case, the simulated heads were subtracted from DEM and as the results; all values of head are positive which means that heads below the surface or model has a good performance. The formula for RVE, NS, Y can be expressed in the following equation

$$RVE = \frac{\sum_{i=1}^{n}(Q_{sim} - Q_{obs})}{\sum_{i=1}^{n}(Q_{obs})} \tag{3.13}$$

$$NS = 1 - \frac{\sum_{i=1}^{n}(Q_{sim} - Q_{obs})^2}{\sum_{i=1}^{n}(Q_{obs} - Q_{mean})^2} \tag{3.14}$$

$$Y = \frac{NS}{1 + |RVE|} \tag{3.15}$$

Where Q_{obs}- observed stream discharge [m^{3}day^{-1}], Q_{sim}-simulated stream discharge [m^{3}day^{-1}], Q_{mean}-mean observed stream discharge [m^{3}day^{-1}], n- the number of time step, *i*- time step.

3.9.13. Sensitivity analysis

The sensitivity analysis was generated to check the model response over changing calibrated input parameters in reasonable ranges which can be analysed the sensitivity of each input parameters over the calibrated model. It also can detect which parameter has greater influence to the calibrated model. Therefore, the model can be improved based on this analysis. Also, it was conducted to determine the impacts of uncertainty parameter on the calibrated model. Practically, it was carried out by changing the parameter such as Brooks-Corey exponent, saturated water content, maximum unsaturated vertical conductivity, extinction water content, extinction depth, horizontal hydraulic conductivity, and specific yield. Those parameters were selected for this analysis because they impact the model. All the parameters were tested with range percentage factor start from -5% and +5% to 45% and -45% and fixed for the rest parameters. Each parameter has picked up to those percentage while other parameters remain constants.

3.9.14. Sebual and Jogading IHM water balance (WB)

MODFLOW-NWT integrated surface zone, vadose zone, and saturated zone. The diagram of water balance components of Jembrana catchment can be illustrated in Figure 28. The water balance of Sebual and Jogading sub catchment and daily flux for the surface, vadose zone, and saturated zone can be estimated by the following equation.

$$P = ET + q + q_g \pm \Delta S \tag{3.16}$$

Where ET- total evapotranspiration, q is stream discharge at the catchment outlet, q_g-lateral groundwater catchment outflow and ΔS-change in storage of the catchment

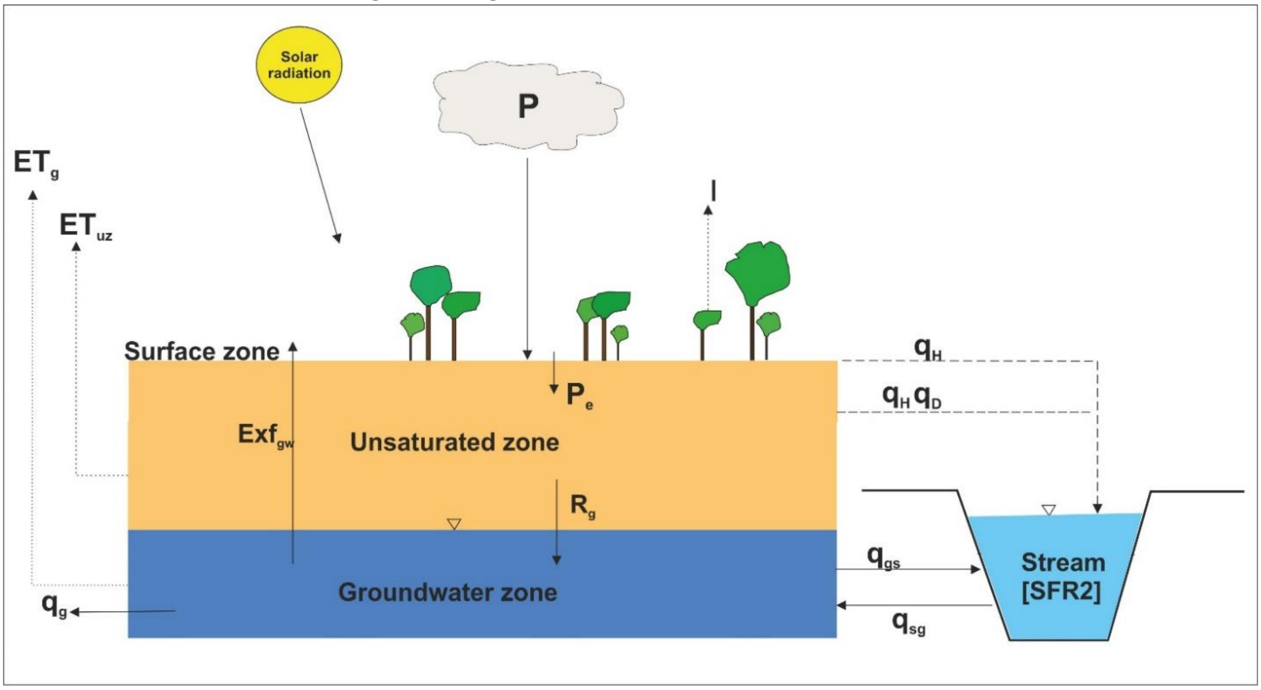

Figure 15. Schematic diagram of MODFLOW -NWT setup for Pergung catchment After (Hassan et al. 2014)

Where P is precipitation, I is interception from canopy, R_g is gross recharge, ET_g is evapotranspiration from groundwater, ET_{uz} is evapotranspiration from unsaturated zone, ET_s is evapotranspiration from surface zone, P_e is precipitation excess infiltration, q_{gs} is groundwater discharge to stream, q_{sg} is stream discharge to groundwater zone, q_g is lateral groundwater outflow, q_H is hortonian overland flow to the stream, q_D is Dunnian saturation excess runoff to the streams, Exf_{gw} is exfiltration from groundwater to soil zone.

ET and ΔS can be calculated as the below equations

$$ET = ET_{uz} + I + ET_g \tag{3.17}$$

$$\Delta S = \Delta S_{uz} + \Delta S_g \tag{3.18}$$

Where, ET_{uz} is Evapotranspiration from unsaturated zone, ET_g is evapotranspiration from groundwater zone, ΔS_{uz} is change in storage in vadose zone and ΔS_g is change storage in groundwater zone. Then surface and unsaturated zone balance can be expressed as the following equation.

$$P + Exf_{gw} = I + R_o + P_a \qquad \text{where } P_a = R_g + ET_{uz} + \Delta S_{uz} \tag{3.19}$$

$$P + Exf_{gw} = I + R_o + R_g + ET_{uz} + \Delta S_{uz}$$

Where R_o is total runoff of stream, P_a is actual infiltration rate. Eventually, groundwater balance can be estimated in below equations

$$R_g + q_{sg} = q_{gs} + q_g + ET_g + Exf_{gw} \pm \Delta S \tag{3.20}$$

where $R_n = R_g - ET_g - Exf_{gw}$ then final equation will be expressed as following formula:

$$R_n + q_{sg} = q_{gs} + q_g \pm \Delta S$$

Where, R_n is net recharge to the groundwater, estimating net recharge and total recharge is essential to know about sustainability and dynamics of groundwater resources (El-Zehairy et al. 2017;Hassan et al. 2014;Sophocleous 2005)).

3.10. Comparison of catchment WB obtained by IHM and Direct baseflow separation

At the end of this research, the results of baseflow separation [WHAT] of Sebual and Jogading were compared to the results of IHM MODFLOW-NWT. Then, the correlation and agreement between baseflow separation [WHAT] and IHM MODFLOW-NWT in terms of hydrological components were analysed. In this case, the parameters that were compared are groundwater run off (q_g) and stream runoff (q_s) from baseflow separation and from IHM model. The Rs from the model was estimated from stream discharges of the model [q_{sfr}] subtracted by groundwater to the stream [q_{gs}].

4. RESULTS

4.1. Precipitation

Precipitation data (1st October 2009 to 30th September 2011) from eight rain gauges over the J.R. were checked using Double-mass curves to analyse the consistency of data. It was proceed by plotting the cumulative rainfall at station x (y-axes) against the average cumulative rainfall of seven rainfall stations (x-axes) and all the units presented in mm. As shown by Figure 16, thee data performed good consistency (straight line of scatter plot) for whole rain gauges. It means that data have good performance either in quality or quantity.

A. Double-mass curve of BMKG Station (3)

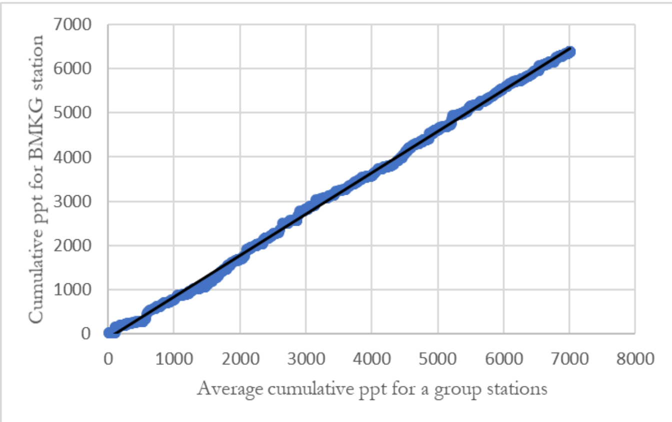

B. Double-mass curve of Dauh Waru station (5)

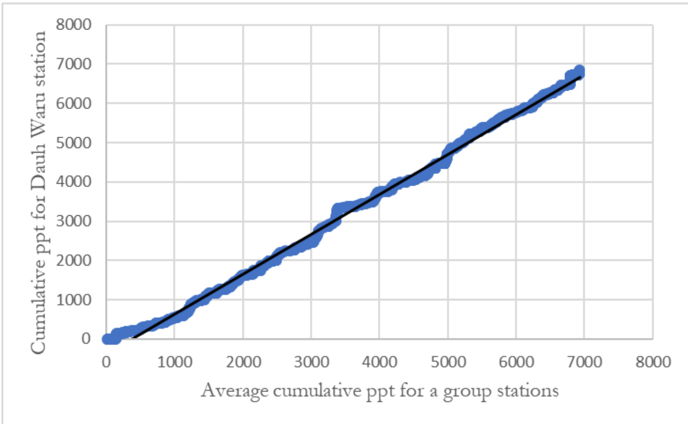

C. Double-mass curve of Tributanggang station (7)

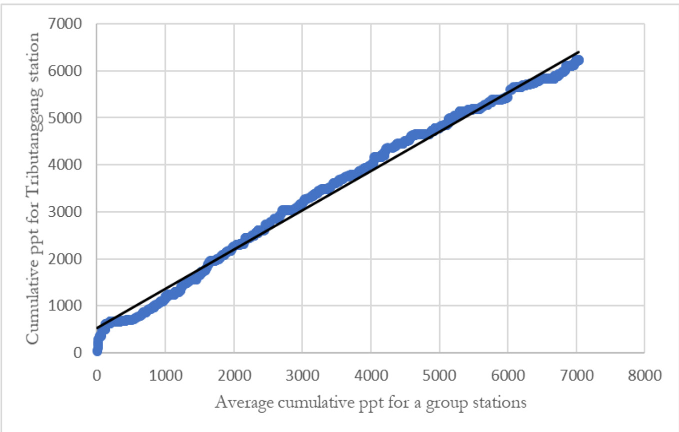

D. Double-mass curve of Pulukan DPU station (8)

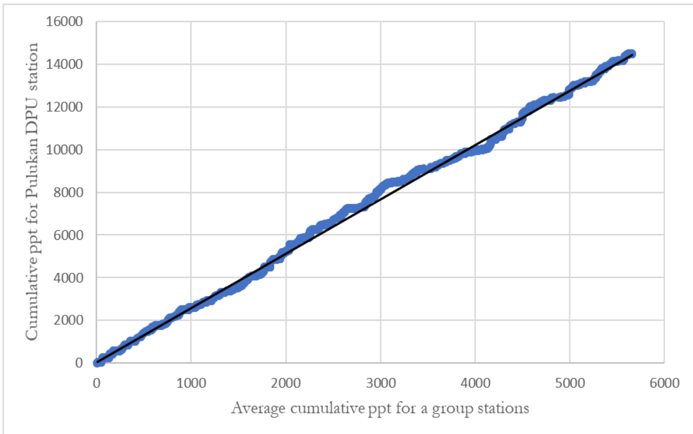

Figure 16. Precipitation records consistency [units in mm] of rain gauges around Pergung Catchment [P.C] and J.R. For location of the rain gauges see Figure 2.

From figure 16, BMKG and Tributanggang stations were performed slightly shifted in the beginning of period, but overall they performed good consistency record. Meanwhile, in Dauh Waru and Pulukan DPU performed slightly shifted in the middle of period, but in general they performed good consistency data as well.

Pergung Catchment surrounded by six rainfall stations (see Figure 19). The yearly three hydrologic years (1st October 2009 to 30st September 2012) of six rainfall stations around Pergung catchment were ~8.58 mmday^{-1}, ~6.50 mmday^{-1}, and ~6.05 mmday^{-1} respectively.

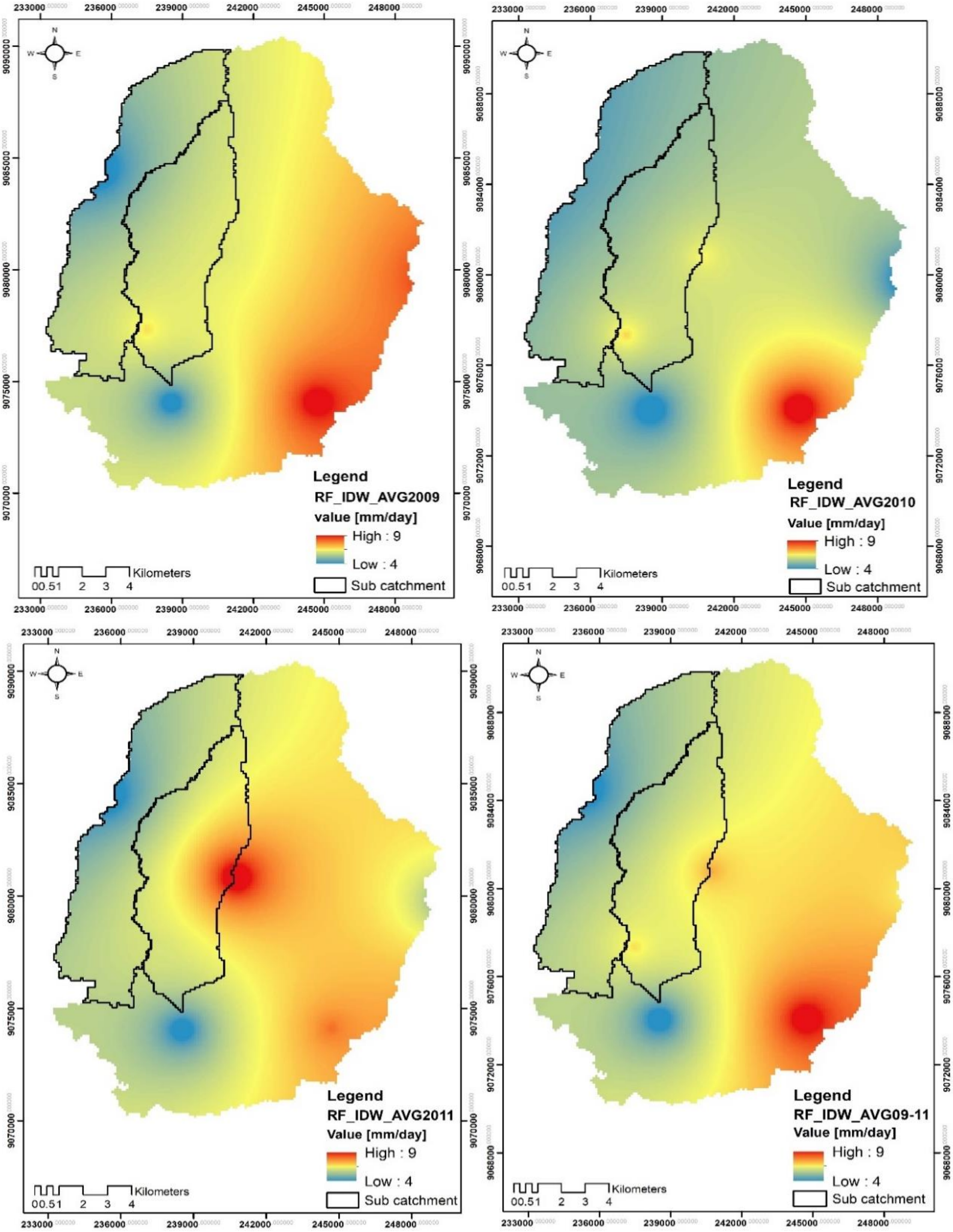

Figure 17. Spatially variable interpolated yearly averages of precipitation using IDW method for 2009, 2010, 2011 and the average of three years period in Sebual and Jogading sub-catchments

Figure 17 shows the results average of daily spatial interpolation of rainfall. It can be observed that the distribution of rainfall from 2009 to 2011 in general have the same pattern which was higher in eastern part and lower in western part in Pergung Catchment. In addition, Jogading has higher rainfall distribution compared to Sebual. The yearly average of spatial data interpolation in P.C within three hydrologic years (2009 to 2011) was ~ 6.51 mmday^{-1}, ~5.60 mmday^{-1}, and ~ 4.70 mmday^{-1} respectively. Overall, the average range of three hydrologic in P.C was ~6 mmday^{-1}. In Sebual_SC, the yearly average (2009 to 2011) of spatial data interpolation of precipitation was ~5.94

mmday⁻¹, 5.39 mmday⁻¹, and 4.37 mmday⁻¹ respectively. Meanwhile, Jogading_SC was performed higher than Sebual, it was ~6.28 mmday⁻¹, ~5.28 mmday⁻¹ and ~4.69 mmday⁻¹ respectively.

4.2. Stream discharges consistency

Similar treatment as with precipitation was applied, the stream discharge data in Pergung Catchment was checked using the Double- mass curve analysis. As the results, Sebual, Jogading and Daya Timur were re-adjusted using the Double- mass curve to reach a good consistency, whereas Pergung_SC performed with less consistency compared to the others. It was deviated in the initial of the period before reaching good consistency (Figure 18).

1. Double-mass curve of Sebual

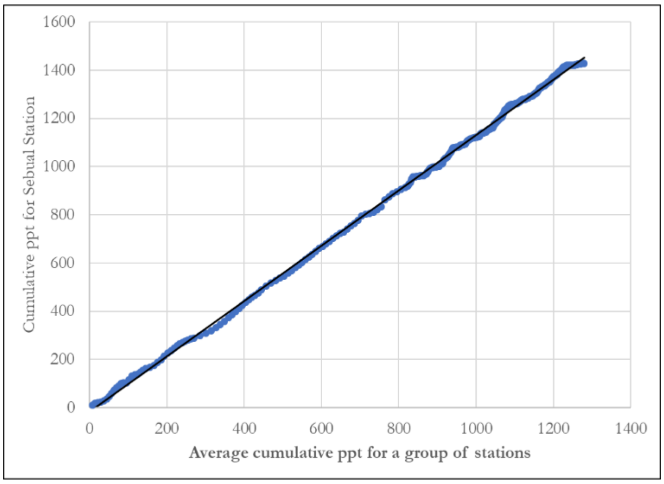

2. Double-mass curve of Jogading

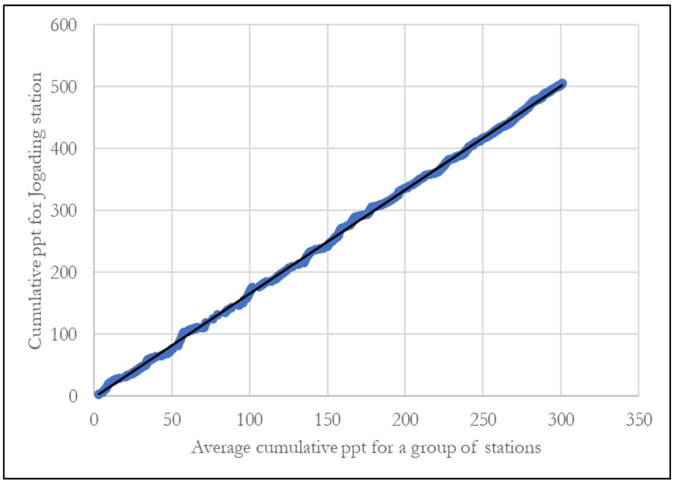

3. Double-mass curve of Daya Timur

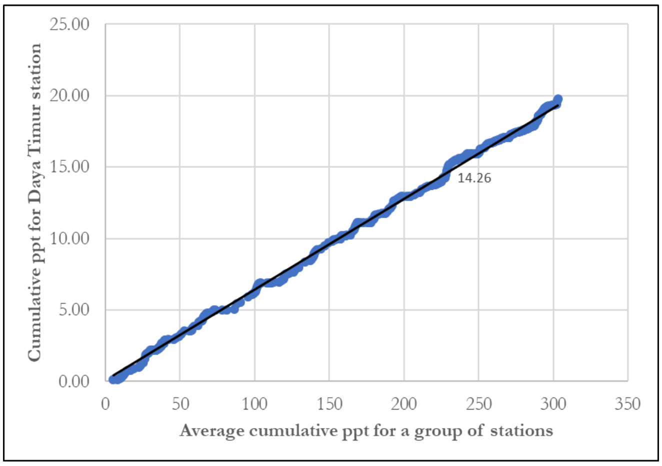

4. Inconsistency data of Pergung sub-catchment

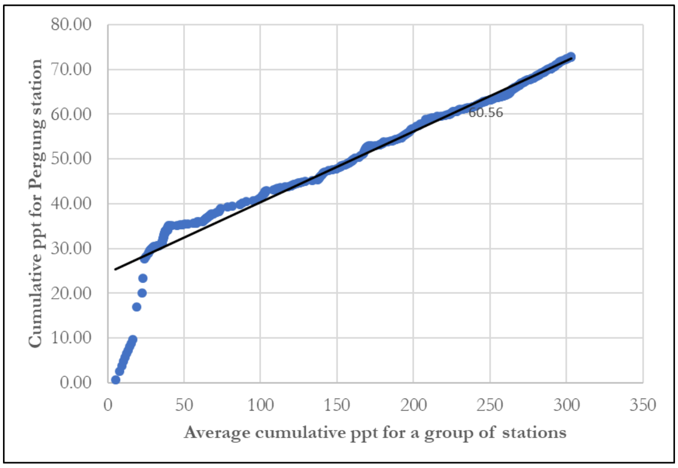

Figure 18. Double-mass curves analysis [units in mm] of Sebual, Jogading, Daya Timur and Pergung sub catchment. Where (y-axes) represents cumulative rainfall data at station which was tested and (x-axes) average cumulative of seven rainfall station (group). For location of the stream gauges see Figure 19.

4.3. Stream discharges validation

From Figure 19, P.C has four stream discharges gauges that were located sparsely in the catchment. According to in situ data, Sebual and Jogading had different amount of stream discharges even though they were close to each other. It was found that the amount of stream discharge both Sebual and Jogading has depended on rainfall distribution as shown in Figure 20. It means that the amount of stream discharge tends to be higher in the wet season and lower in dry season. In Sebual_SC, the yearly average of three hydrologic years (2009 to 2011) of stream discharges was ~2.29 m^3s^{-1}, ~1.67 m^3s^{-1}, and ~2.19 m^3s^{-1} respectively. Then in Jogading_SC, the yearly average of stream discharge was ~1.6 m^3s^{-1}, ~1.40 m^3s^{-1} and ~2.04 m^3s^{-1} for 2009, 2010 and 2011 respectively. The details correlation between rainfall (RF) and stream discharges (Q) in Sebual and Jogading can be observed in Figure 20 below.

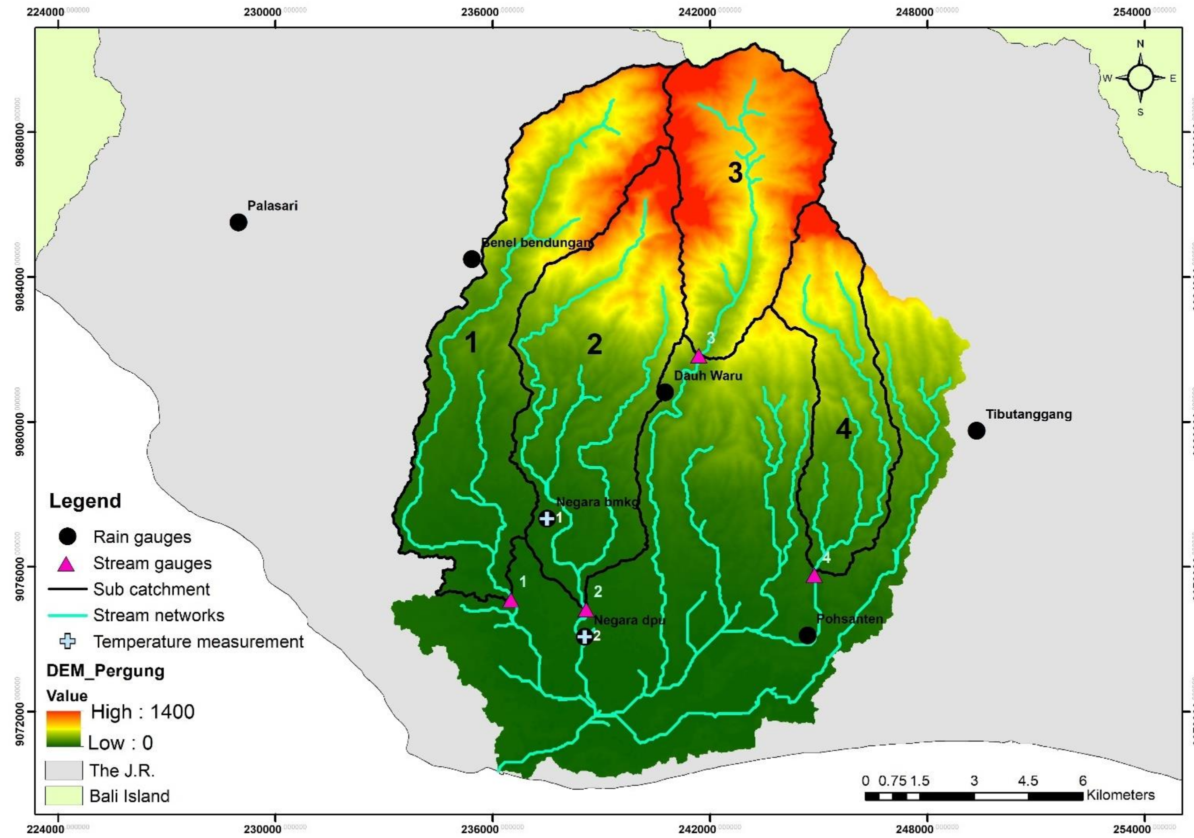

Figure 19. Stream networks and contributing areas of sub-catchments: (1) Sebual, (2) Jogading, (3) Daya Timur and (4) Pergung

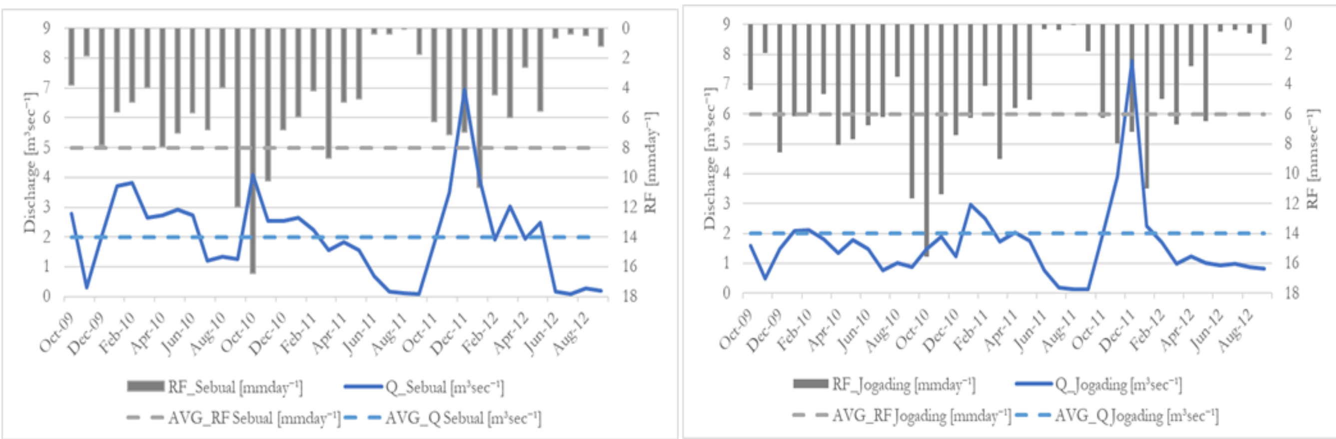

Figure 20. Relation of stream discharges (Q), rainfall (RF), average stream discharges (AVG_RF), average of rainfall (AVG_RF) in Sebual and Jogading sub catchment for the period of 1st October 2009 to 30th September 2012.

The distribution of rainfall in Sebual and Jogading has the same pattern and it was high in wet season and low in dry season. The shape of hydrograph of stream discharges responded to rainfall distribution where it was higher in the wet season and lower in dry season. Then, the average of three years stream discharges in Sebual was ~2.05 m^3sec^{-1} higher than Jogading was ~1.67 m^3sec^{-1} respectively.

4.4. Preliminary catchment assessment

The assessments of J.R and P.C have been conducted based on the precipitation and stream discharge data using rational method and baseflow separation [WHAT] method (Lim et al. 2005). As mentioned in the previous chapter, the single hydrologic year of 2009 (1st October 2009 to 30st September 2010) was selected to carry out this assessment.

4.4.1. Hydrological assessment of J.R.

The J.R. was assessed using rational method and baseflow separation. As the result, the estimated streamflow [q_t] ranged from ~0.14 mmday^{-1} to ~6.57 mmday^{-1}, groundwater fluxes [q_g] from ~0.06 mmday^{-1} to ~4.20 mmday^{-1}, and direct surface runoff [q_s] from ~0.02 mmday^{-1} to ~2.37 mmday^{-1}. Overall, the proportion of q_g was covered more than 60% of total estimated runoff in each catchment. Meanwhile, the proportion of q_s was from 13% to 38% of total estimated runoff. These results were used to make selection of one catchment for running and simulation IHM. Finally, the P.C. was selected for IHM as it was considered as the biggest catchment, also a lot of monitoring stations are located in this catchment. The following table are the results of this assessment. In this catchment, q_t, q_g and q_s were ~2.39 mmday^{-1}, ~1.69 mmday^{-1}, and ~0.70 mmday^{-1} respectively.

Table 5. Total estimated stream flow (Qt) for hydrologic year 2009

No	Catchments	Au [m²]	Au [Km²]	Pu [mmday⁻¹]	Q [m³day⁻¹]	q_t= Q/Au [mmday⁻¹]	fr=q_t/Pu [%]
1	Melaya	43652522	43.65	3.06	6050	0.14	4.58
2	Sangyang Gede	64208503	64.21	2.01	51856	0.08	3.98
3	Daya Barat	48121948	48.12	8.37	12100	0.25	2.99
4	Pergung	212362627	212.36	6.69	508211	2.39	35.72
5	Bilok Poh	82999159	83.00	8.29	87466	1.05	12.67
6	Yeh Buah	13424654	13.42	6.36	39971	2.98	46.86
7	Yeh Embang	47959868	47.96	7.11	85078	1.77	24.89
8	Yeh Sumbul	109801817	109.8	5.02	190249	1.73	34.46
9	Yeh Satang	36854894	36.85	11.16	241953	6.57	58.87
10	Medewi	46110474	46.11	3.61	61397	1.33	36.84

Table 6. Surface runoff [Q_s] estimated for hydrologic year 2009

No	Catchment	Au [m²]	Au [Km²]	Pu [mmday⁻¹]	Qs [m³day⁻¹]	q_s = Qs/Au [mmday⁻¹]	fs= q_s/P_u [%]	q_s/ q_t [%]
1	Melaya	43652522	43.65	3.06	1220	0.02	0.65	13.46
2	Sangyang Gede	64208503	64.21	2.01	1156	0.02	1.00	21.37
3	Daya Barat	48121948	48.12	8.37	3815	0.07	0.84	29.9
4	Pergung	212362627	212.36	6.69	148992	0.7	10.46	29.4
5	Bilok Poh	82999159	83.00	8.29	32993	0.39	4.70	37.72
6	Yeh Buah	13424654	13.42	6.36	12273	0.92	14.47	30.7
7	Yeh Embang	47959868	47.96	7.11	27144	0.56	7.88	31.9
8	Yeh Sumbul	109801817	109.8	5.02	42647	0.39	7.77	22.42
9	Yeh Satang	36854894	36.85	11.16	87278	2.37	21.24	36.07
10	Medewi	46110474	46.11	3.61	17464	0.38	10.53	28.72

Table 7. Groundwater runoff [Q_g] estimated for hydrologic year 2009

No	Catchment	Area [m²]	Area [Km²]	Pu [mmday⁻¹]	Q_g [m³day⁻¹]	$q_g = Q_g/Au$ [mmday⁻¹]	fg = q_g/P_u [%]	q_g/q_t [%]
1	Melaya	43652522	43.65	3.06	5236	0.12	0.04	86.54
2	Sangyang Gede	64208503	64.21	2.01	4078	0.06	0.03	78.63
3	Daya Barat	48121948	48.12	8.37	8482	0.18	0.02	70.1
4	Pergung	212362627	212.36	6.69	358809	1.69	0.25	70.6
5	Bilok Poh	82999159	83.00	8.29	54477	0.66	0.08	62.28
6	Yeh Buah	13424654	13.42	6.36	27698	2.06	0.32	69.3
7	Yeh Embang	47959868	47.96	7.11	57937	1.21	0.17	68.1
8	Yeh Sumbul	109801817	109.8	5.02	147604	1.34	0.27	77.58
9	Yeh Satang	36854894	36.85	11.16	154673	4.2	0.38	63.93
10	Medewi	46110474	46.11	3.61	43762	0.95	0.26	71.28

Where Au is upstream contributor area [m²], Pu is daily mean of precipitation [mmday⁻¹], Q is daily mean of discharge estimated [m³sec⁻¹], q_t is total runoff estimated from streams [mmday⁻¹], q_g is groundwater runoff estimated [mmday⁻¹], q_s is direct surface runoff estimated [mmday⁻¹], fr is streamflow factor [0<fr<1], fg is groundwater runoff factor [0<fr<1], and fs is direct runoff factor [0<fs<1].

From Table 6 and 7, the distribution of rainfall and stream discharges varied within the catchments. Yeh Satang catchment has the highest of groundwater runoff (~4.20 mmday⁻¹) compared to the others. Moreover, it is around twenty times higher than catchment of Daya Barat (~0.18 mmday⁻¹). The rainfall distribution ranged from ~2.01 mmday⁻¹ to ~11.16 mmday⁻¹ respectively.

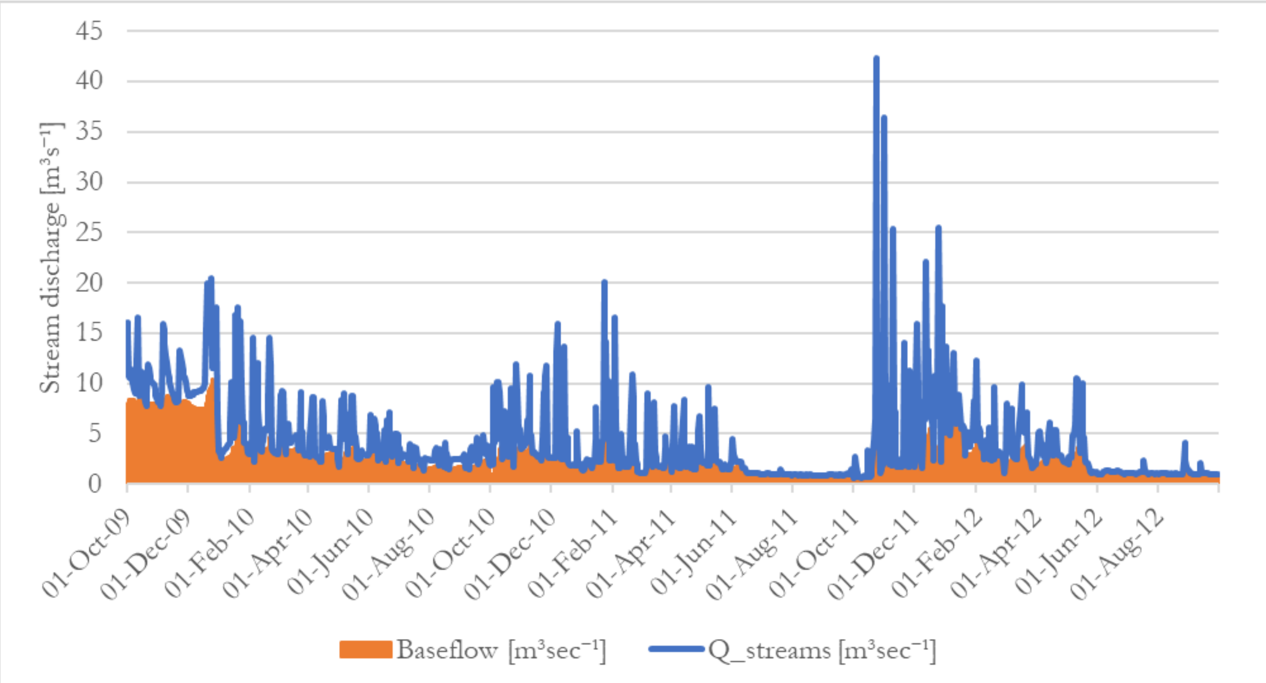

Figure 21. Long-term baseflow separation of P.C using Automated Web Based GIS method [WHAT]

Based on Figure 21, the flow was converted into direct runoff and baseflow. It was clear that in the wet season the stream discharge tends to be higher compared to the dry season. Consequently, the baseflow also was higher in wet season than in the dry season. This means that flows depends on the rainfall distribution and catchment characteristics contrasting partitioning of flow into surface and groundwater, represented by baseflow.

4.4.2. Hydrological assessment of the P.C

Similar way as with J.R, rainfall distribution in each sub catchment was defined by using rational method and baseflow separation [WHAT]. Rainfall of 2009 (hydrologic year) was selected to carry out analysis in each sub catchment in Pergung catchment. Rational method has been used for both Sebual and Jogading sub catchment to define rainfall distribution in the area (Au).

Table 8. Total estimated streamflow (Qt) of sub catchments in 2009

No	Sub catchment	Au [m²]	Au [Km²]	Pu [mmday⁻¹]	Q_t [m³day⁻¹]	q_t= Q/Au [mmday⁻¹]	fr=q_t/Pu [%]
1	Sebual	40999526	41.00	8.00	197856	4.83	60.32
2	Jogading	36672824	36.67	6.00	138240	3.77	62.83
3	Daya Timur	27279809	27.28	5.00	62208	2.28	45.61
4	Pergung	19912493	19.91	8.00	11232	0.56	7.05

Table 9. Direct runoff estimated (Qs) for each sub catchment in 2009

No	Sub catchment	Au [m²]	Au [Km²]	Pu [mmday⁻¹]	Qs [m³day⁻¹]	q_s= Qs/Au [mmday⁻¹]	fs=q_s/Pu [%]	q_s/q_t [%]
1	Sebual	40999526	41.00	8.00	99360	2.42	30.29	50.22
2	Jogading	36672824	36.67	6.00	30240	0.82	13.74	21.88
3	Daya Timur	27279809	27.28	5.00	19872	0.73	14.57	31.94
4	Pergung	19912493	19.91	8.00	2592	0.13	1.63	23.08

Table 10. Groundwater runoff estimated (Qg) for each sub catchment in 2009

No	Sub catchment	Au [m²]	Au [Km²]	Pu [mmday⁻¹]	Qg [m³day⁻¹]	q_g= Qg/Au [mmday⁻¹]	fg=q_t/Pu [%]	q_g/q_t [%]
1	Sebual	40999526	41.00	8.00	98496	2.40	30.03	49.78
2	Jogading	36672824	36.67	6.00	108000	2.94	49.08	78.13
3	Daya Timur	27279809	27.28	5.00	42336	1.55	31.04	68.06
4	Pergung	19912493	19.91	8.00	8640	0.43	5.42	76.92

From the Table 8, the Sebual_SC was defined as the biggest area with ~41 km², and the smallest is Pergung_SC with ~19,91 km². The total runoff estimated (q_t) ranges from ~0.56 mmday^{-1} to ~4.83 mmday^{-1}, q_g was 0.43 mmday^{-1} to ~2.94 mmday^{-1} and q_s was from ~0.13 mmday^{-1} to ~2.42 mmday^{-1}.

Based on Table 9 and 10, three out of four sub-catchments have a proportion of groundwater runoff (q_g) more than 60% and the rest, which is Sebual_SC has ~50% of direct runoff (q_s) and ~50 % for groundwater runoff (q_g). The proportion of q_s over q_g was found to vary within the sub catchments. In Sebual, it was like 1:1 (2.42 vs 2.40), Jogading 1:3.6 (0.82 vs 2.94), Daya Timur 1:2.1(0.75 vs 1.55) and Pergung 1:3.3 (0.13 vs 0.43) respectively.

4.5. Interception and infiltration rate

Interception and infiltration rate were adjusted to spatio-temporally variable for both models. Spatially based on land use and land cover and temporally vary in wet and dry season. This adjustment was based on rainfall distribution and NDVI values of Landsat image five and seven after correction and processing in QGIS and ERDAS image software. It was noticeable that NDVI values higher in the wet season compared to the dry season (Figure 22).

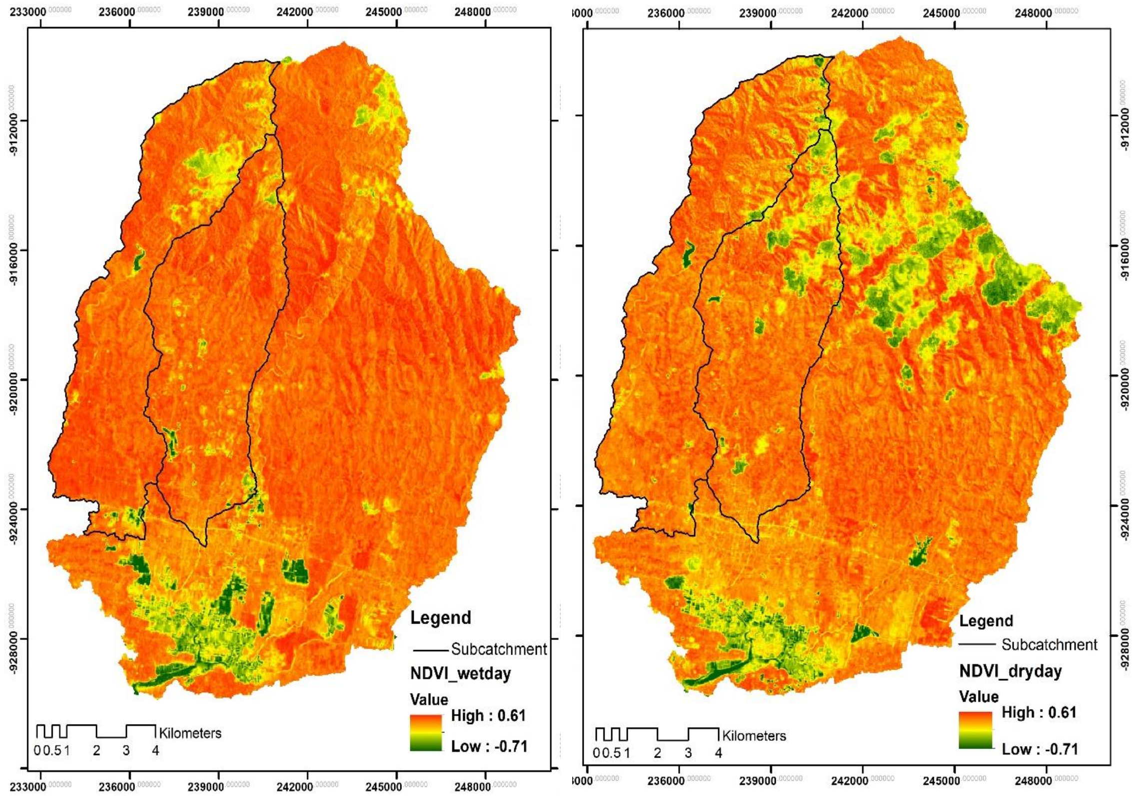

Figure 22. Spatially variable NDVI values of Landsat images for wet period (15th March 2010) and dry period (29th July 2013) over Sebual and Jogading sub catchments

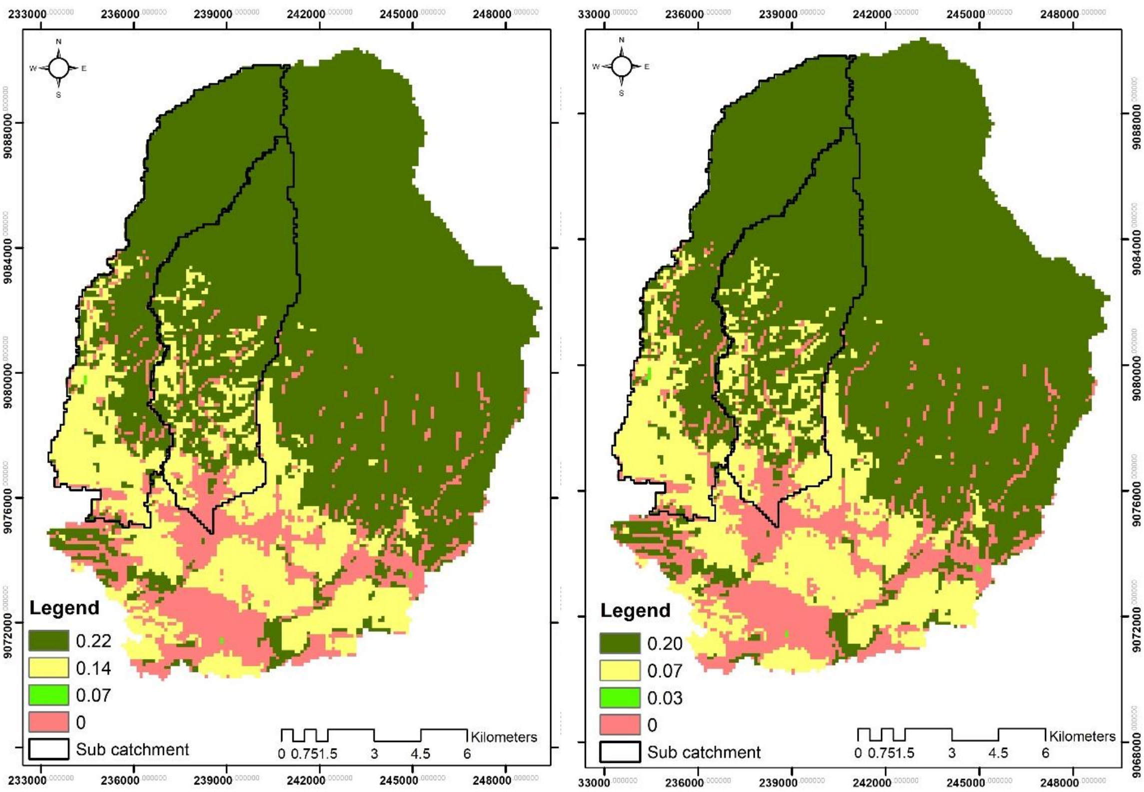

Figure 23. Spatially variable interception rate for wet and dry periods over Sebual and Jogading_SC

From Figure 23, The interception rate was set from 0 to 0.22 during wet season (1st October to 31st March) and from 0 to 0.22 during dry season (1st April to 30th September), it was spatially variable for both Sebual and Jogading sub catchment. Both Sebual and Jogading was dominated by forest (0.22 in wet period and 0.20 in dry period), agriculture was set (0.14 in wet and 0.07 in dry periods) and small percentage of settlement and building in Jogading (0 interception rate).

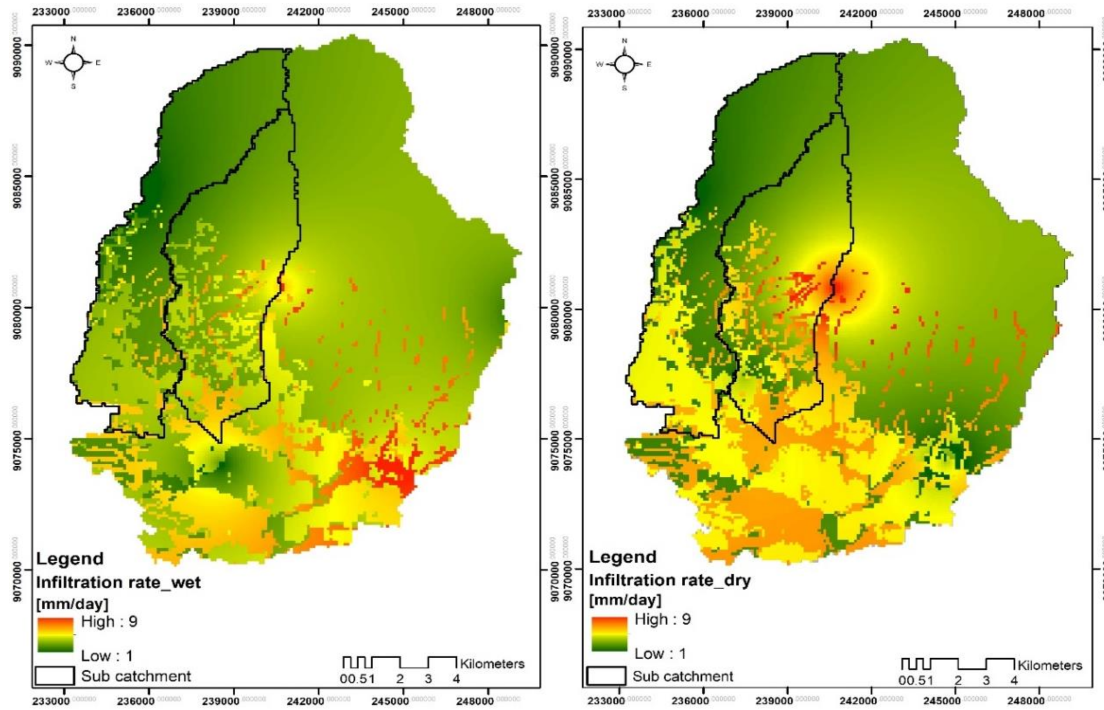

Figure 24. Spatially variable average infiltration rate during wet season (left) and dry season (right) in Sebual, Jogading and P.C in 2010 (hydrologic year).

Figure 24 presents the spatio-temporal distribution of effective infiltration rate [Pe] in hydrologic year 2010; it was ranged from ~1 mmday^{-1} to ~9 mmday^{-1}. During wet season infiltration was higher than dry season. In wet season, the mean infiltration rate in P.C, Sebual and Jogading was ~6.02 mmday^{-1}, ~5.60 mmday^{-1}, and ~5.97 mmday^{-1} respectively. In dry season it was ~1.76 mmday^{-1}, ~1.68 mmday^{-1}, and ~1.79 mmday^{-1} respectively.

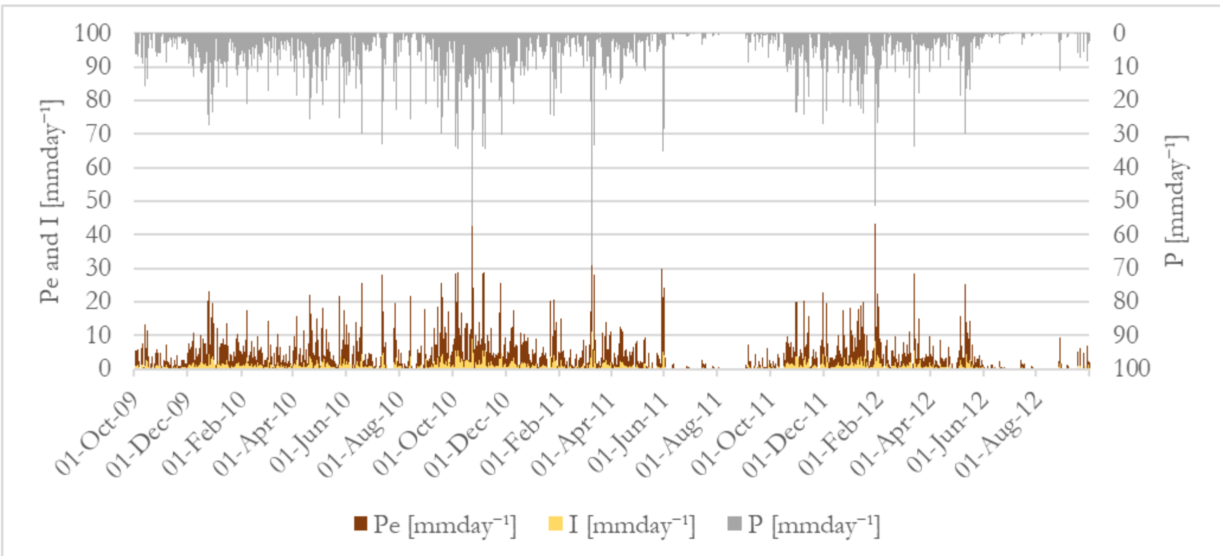

Figure 25. Long-term average interception [I] and effective infiltration rate [Pe] against precipitation [P] in Pergung catchment.

Based on NDVI values and seasonal rainfall distribution, the interception rate of IHM Sebual and Jogading were adjusted as spatiotemporally variably between wet and dry seasons (Figure 22). The infiltration rate was estimated from rainfall subtracted with interception loss. For IHM Sebual and Jogading, the calculation of interception and infiltration rate can be executed either in ArcGIS or MODFLOW-NWT using formula tools. In a three year period, average of rainfall, interception and infiltration rate in Pergung catchment were defined ~5.55 mmday^{-1}, 0.87 mmday^{-1}, and ~4.68 mmday^{-1} respectively. In MODFLOW-NWT, interception and infiltration rate was inputted in the UZF package.

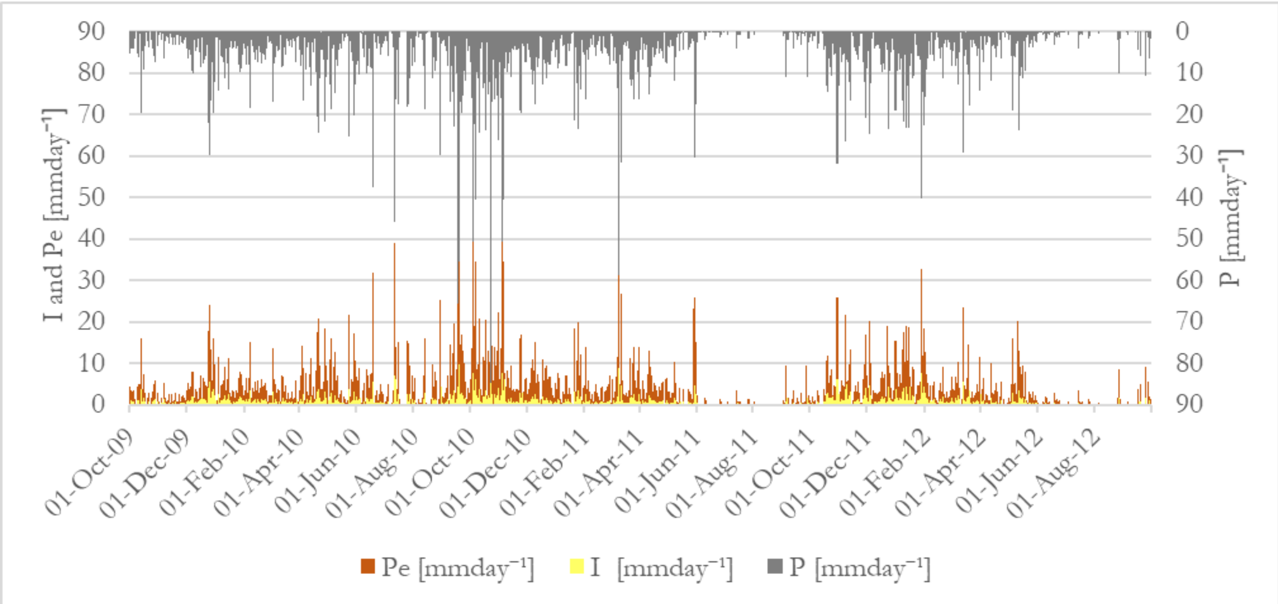

Figure 26. Long-term average interception [I] and effective infiltration rate [Pe] against precipitation [P] in Sebual

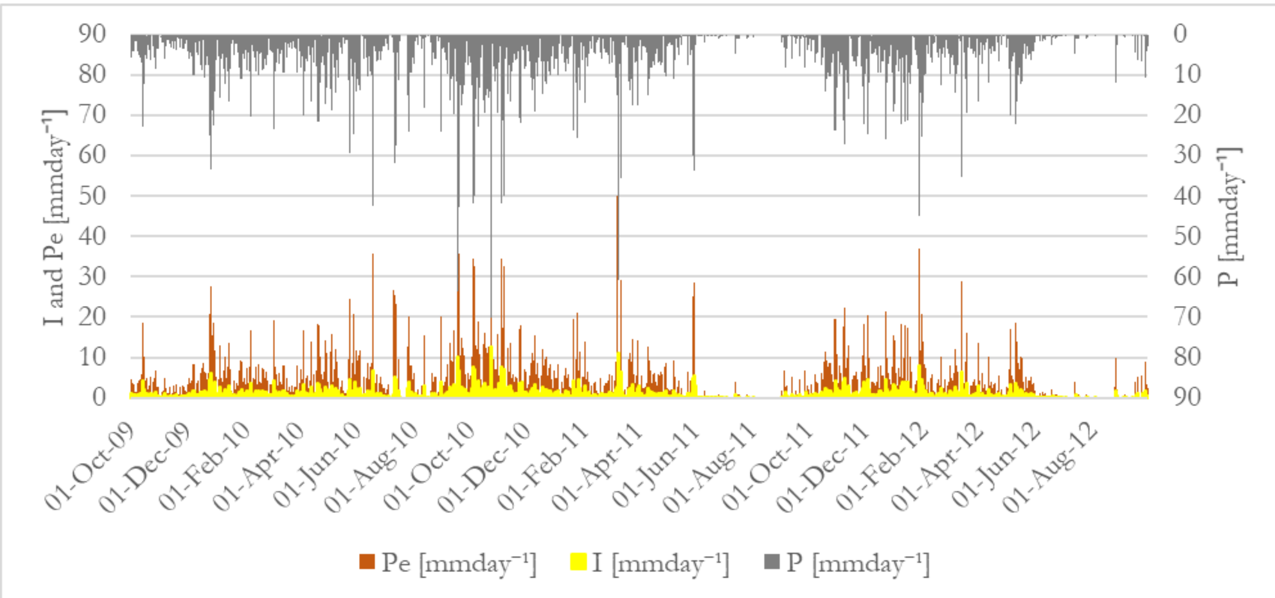

Figure 27. Long-term average interception [I] and effective infiltration rate [Pe] against precipitation [P] in Jogading

According to Figure 26 and 27, interception and infiltration rate was defined as not much different between Sebual and Jogading sub catchment. The average three hydrologic years of interception and infiltration rate in Sebual were ~0.86 mmday^{-1} and ~ 4.37 mmday^{-1} while in Jogading was slightly higher ~0.95 mmday^{-1} and ~4.56 mmday^{-1} respectively.

4.6. Potential evapotranspiration [PET]

As stated earlier, potential evapotranspiration [PET] of IHM Sebual and Jogading was generated based satellite images [MODIS] 100 m resolution (resampling products) on a daily basis. From Figure 30, it can be observed that the PET was higher in dry season compared to wet season. The average of three hydrologic years PET over Pergung Catchment was ~5.02 mmday^{-1}.

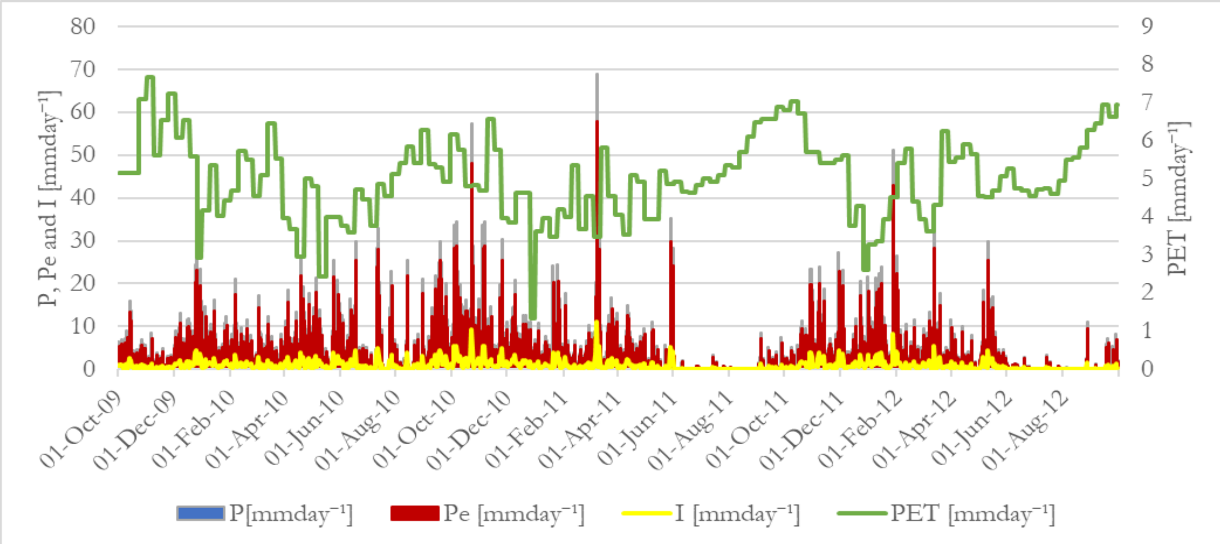

Figure 28. Long-term relation of precipitation, effective interception [Pe], effective infiltration rate and potential evapotranspiration [PET] in Pergung Catchment.

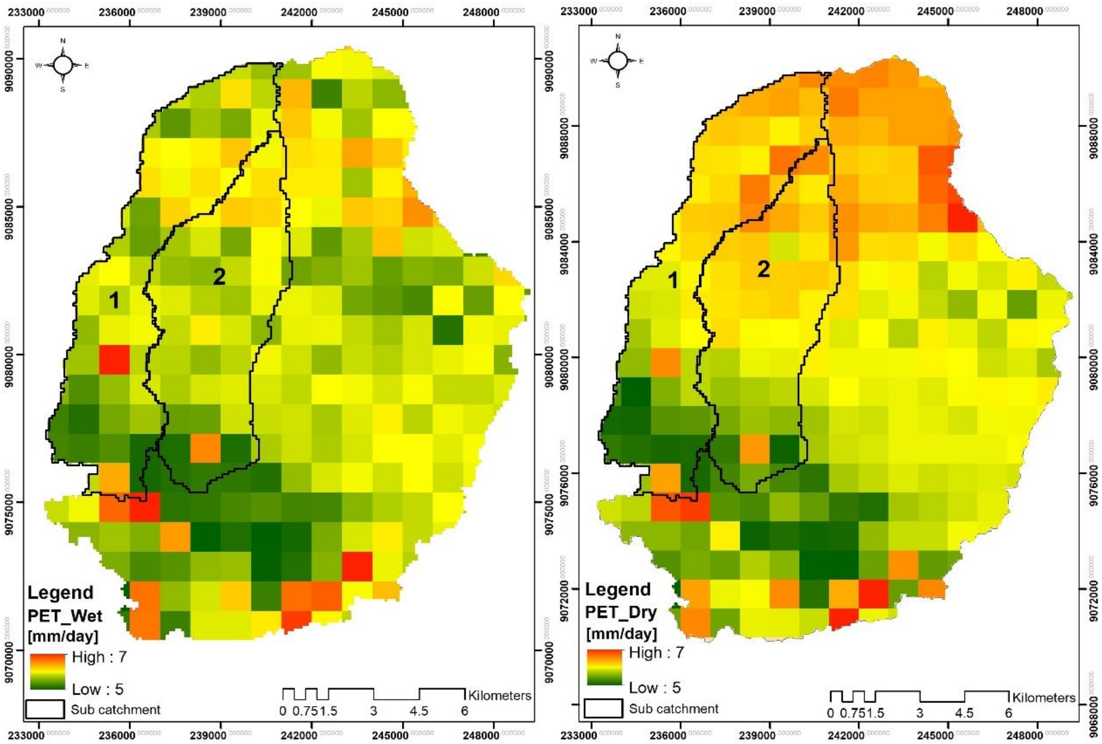

Figure 29. Spatially variable of average potential evapotranspiration [PET] in wet and dry season in (1) Sebual and (2) Jogading sub catchment

From Figure 30, PET spatially distributed high in mountain and low in the downstream area. In wet season, it was found slightly lower than dry season. In P.C, the range of PET in wet season was from ~5.30 mmday^{-1} to ~6.47

mmday^{-1} with the average of ~4.77 mmday^{-1} whereas in dry season was from ~5.83 mmday^{-1} to ~6.60 mmday^{-1} with the average of 6.20 mmday^{-1} respectively. In Sebual and Jogading sub catchments, the range of PET was from ~0 to ~6.40 mmday^{-1} and ~0 mmday^{-1} to 5.02 mmday^{-1} in wet season while dry season was ~5.87 mmday^{-1} to 6.54 mmday^{-1} and ~5.87 mmday^{-1} to ~6.45 mmday^{-1} respectively. In addition, the average of PET in Sebual and Jogading were ~5.06 mmday^{-1} and ~5.02 mmday^{-1} in wet season and in dry season ~6.20 mmday^{-1} and ~5.21 mmday^{-1} respectively.

4.7. Transient state model calibration

IHM of Sebual and Jogading was set up and running separately in transient state condition. Transient calibration has been conducted based on stream discharge data and surface altitude. The aim of transient state calibration was to match patterns between simulated stream discharges and observed stream discharge of Sebual and Jogading sub catchments. The calibration has been carried out manually in three hydrologic years started from 1st October 2009 till 30th September 2012 or it is equal to 1096 days. Both Sebual and Jogading sub-catchments were calibrated using four zones of horizontal hydraulic conductivity (K_h) but they were assigned in different range values. In this stage, all the input parameters were adjusted in order to reach model convergence; and then after several trials and errors, the models reached convergence. Additionally, there was no any error notification message during running the models meaning that the models were in well setup.

4.7.1. Warming up period

Before going through to IHM transient calibration, warming up period has been conducted in varying periods such as three months, six months then continue to one year period. The aim of warming up period was to know the behaviour of changing parameters in the model to assign realistic initial head. IHM Sebual and Jogading have been set up in the steady state condition at first stress period, then continue directly to transient state condition till the end of stress period.

4.7.2. Stream discharge calibration and error assessment

Transient state model calibration was carried out to match the pattern between simulated and stream observed stream discharges of Sebual and Jogading sub-catchments. The models were calibrated in three hydrologic years started from 1th October 2009 to 30th September 2012 (1096 days) or equal to 1096 stress periods and time steps.

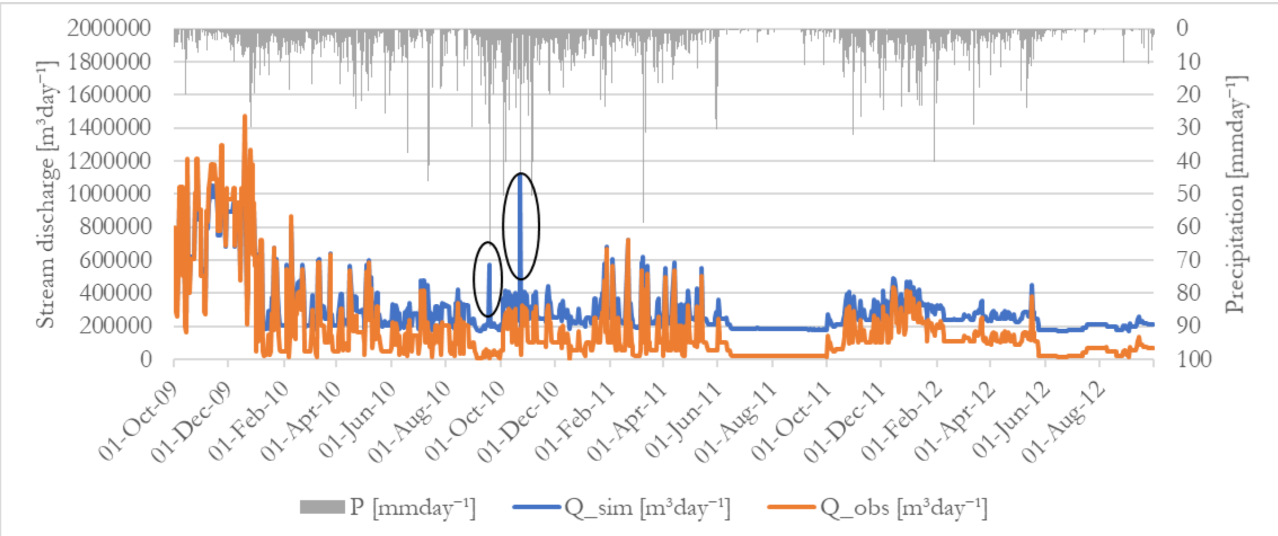

Figure 30. Long-term relation of simulated stream discharges [Q_sim], observed stream discharge [Q_obs] and precipitation [P] in Sebual_SC (calibrated stream discharge of IHM Sebual)

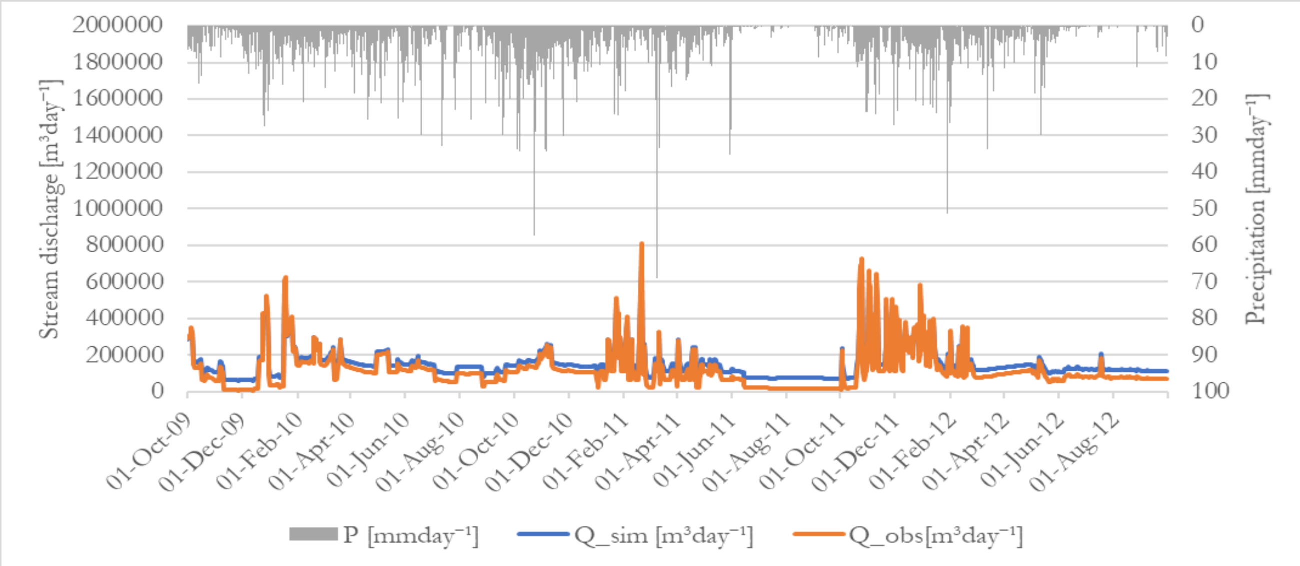

Figure 31. Long-term relation of simulated stream discharges [Q_sim], observed stream discharge [Q_obs] and precipitation [P] in Jogading_SC (calibrated stream discharge of IHM Jogading)

From Figure 30 and 31, the simulated stream discharges in Sebual and Jogading were found higher than observed stream discharges. In addition, there are two spots that the pattern of simulated did not match (marked by oval symbols) with observed stream discharges. However, simulated stream discharges generally was produced the same pattern with observed, meaning that the model was performed reasonably well. In Jogading_SC, simulated stream discharges pattern matched well with observed stream discharges, meaning that this model also performed well. Then, the error assessments of the results were carried out using relative volumetric error [RVE], Nash-Sutcliffe coefficient efficiency [NS] and overall model performance [Y].

Table 11. Error assessment of IHM Sebual and Jogading sub catchment.

Station	X_utm	Y_utm	RVE	NS	Y
Sebual_SC	236501.208	9075081.496	0.66	0.56	34.00
Jogading_SC	238575.138	9074812.540	0.29	0.91	71.00

Based on Table 11, it can be stated that IHM Jogading performed better than Sebual in terms of RVE, NS, and Y calibrated parameters. However, in general the pattern of hydrograph simulated and observed were performed in the same path for both Sebual and Jogading. Also, the pattern of hydrograph follows the path of rainfall, which means that the stream discharge followed well the rainfall temporal distribution.

4.7.3. Calibrated heads against surface altitude

The adjustment of heads to keep them below topographic surface at realistic depth below ground surface has been conducted simultaneously with stream discharge calibration. However, it had to found the balance between stream discharge and the adjusted heads because in several cases, the models reached good stream discharges calibration, but the water table was above the surface. Therefore, the aim of this calibration was to make sure that the positions of the water table was below the surface altitude [DEM]. To do this calibration, twenty-six fictitious piezometers were assigned in both Sebual and Jogading to records calibrated heads in the whole period of simulation. In addition, they were also installed along the stream segments to record the heads beneath the streams. As mentioned earlier, the heads in these piezometers were set equal to the surface water altitude. The calibration was conducted manually by subtracting simulated heads from surface altitude. The results of subtracting heads had to be positive,

which means that the depth of groundwater was beneath the ground surface. After several trials and errors, the model performed all simulated heads spatiotemporally below the surface altitude (Figure 33, 34 and 35).
Figure 32. Spatially distribution of assigned fictitious piezometers in Sebual and Jogading sub catchment
Figure 33. Spatially variable distribution of groundwater depth [m] after subtracting heads from DEM in the last

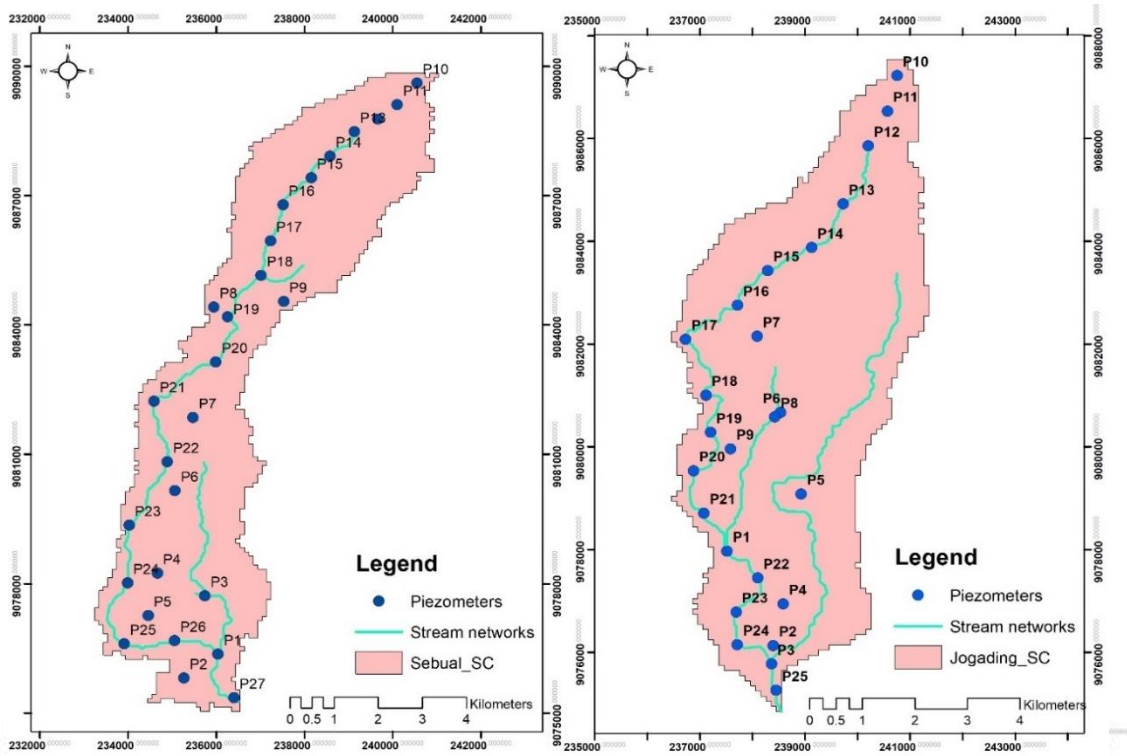

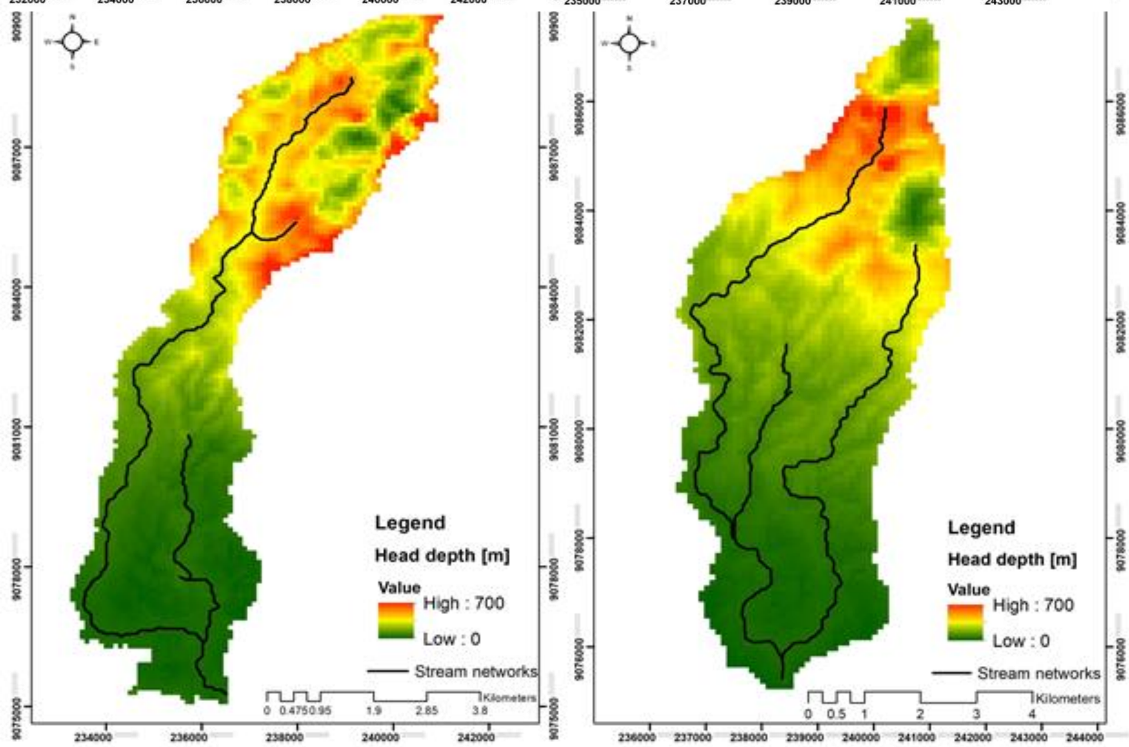

stress period for IHM Sebual and Jogading
The simulated heads from each stress period of Sebual and Jogading were subtracted from DEM, and in all cases they gave positive values, meaning that spatially the positions water table was always below the ground surface. From Figure 36, groundwater depth ranges from ~1.40 m to ~487.30 m in Sebual while in Jogading was from

~1.60 m to 707.40 m below the surface altitude. Also, simulated heads along the stream segments in both Sebual and Jogading performed beneath the surface altitude.

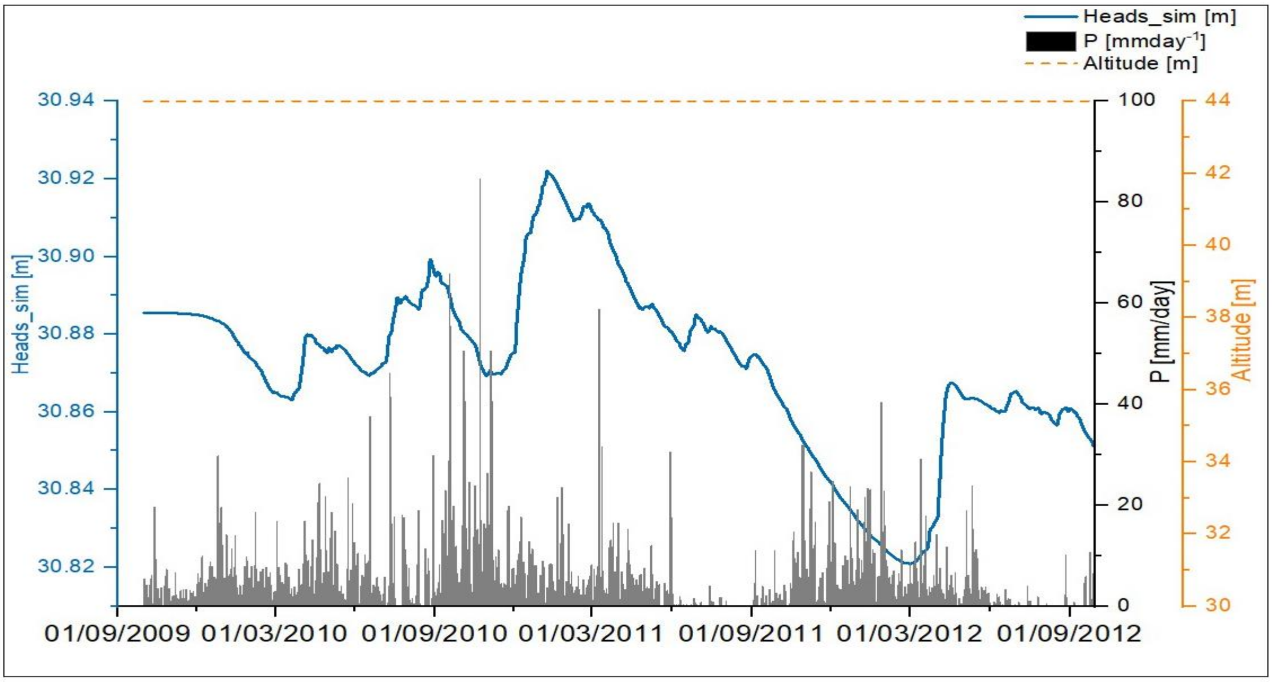

Figure 34. Long-term relation of simulated heads in P1(see Figure 32), precipitation [P], and surface altitude [DEM] in Sebual_SC

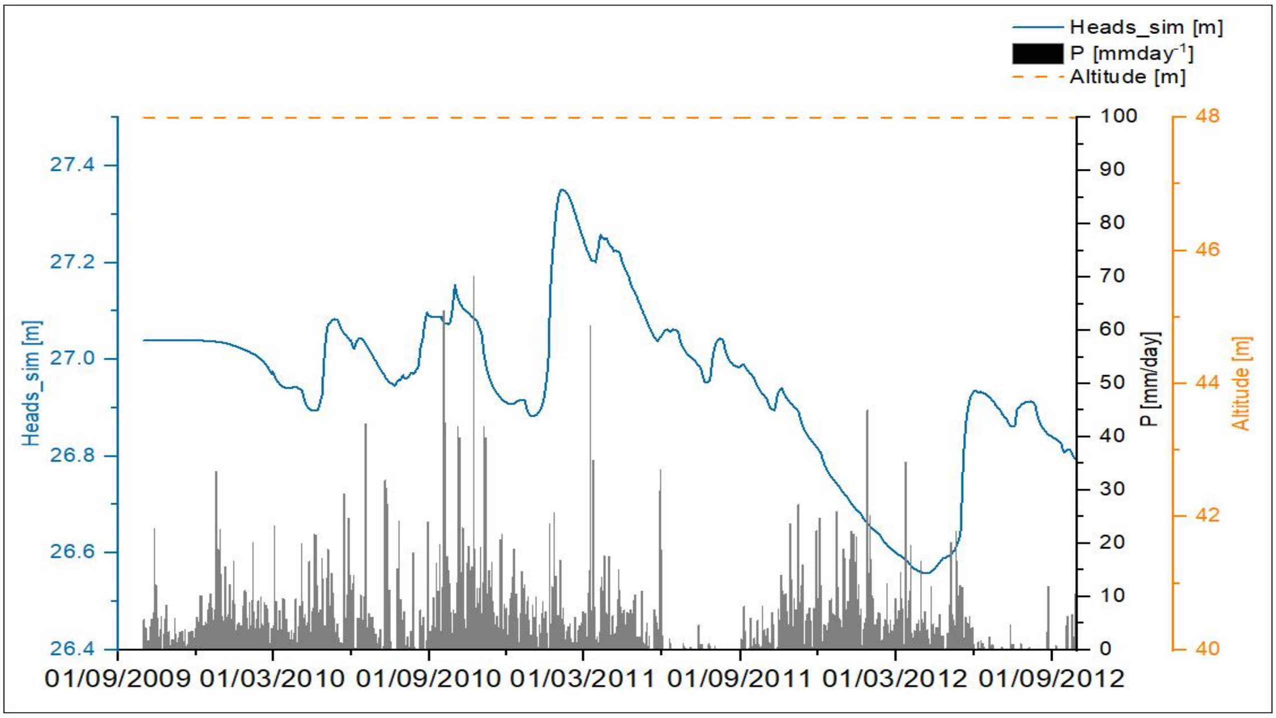

Figure 35. Long-term relation of simulated heads in P2(see Figure 32) and precipitation [P], and surface altitude [DEM] in Jogading_SC

From Figure 34, the simulated heads that was ~31 m obtained from fictitious piezometer 1 (P1 Figure 32) follow the pattern of rainfall distribution in Sebual, it was lower in wet season and tends to be higher in the dry season. It means that the simulated heads were affected by rainfall distribution. In Jogading, the simulated heads was ~26 to 27 m which derived from P2 (see Figure 32) also follow the path of rainfall distribution as shown in Figure 35.

Also, it can be observed that the simulated heads in Sebual and Jogading were checked against surface altitude in fictitious piezometer records. As the results, the simulated heads performed beneath the surface.

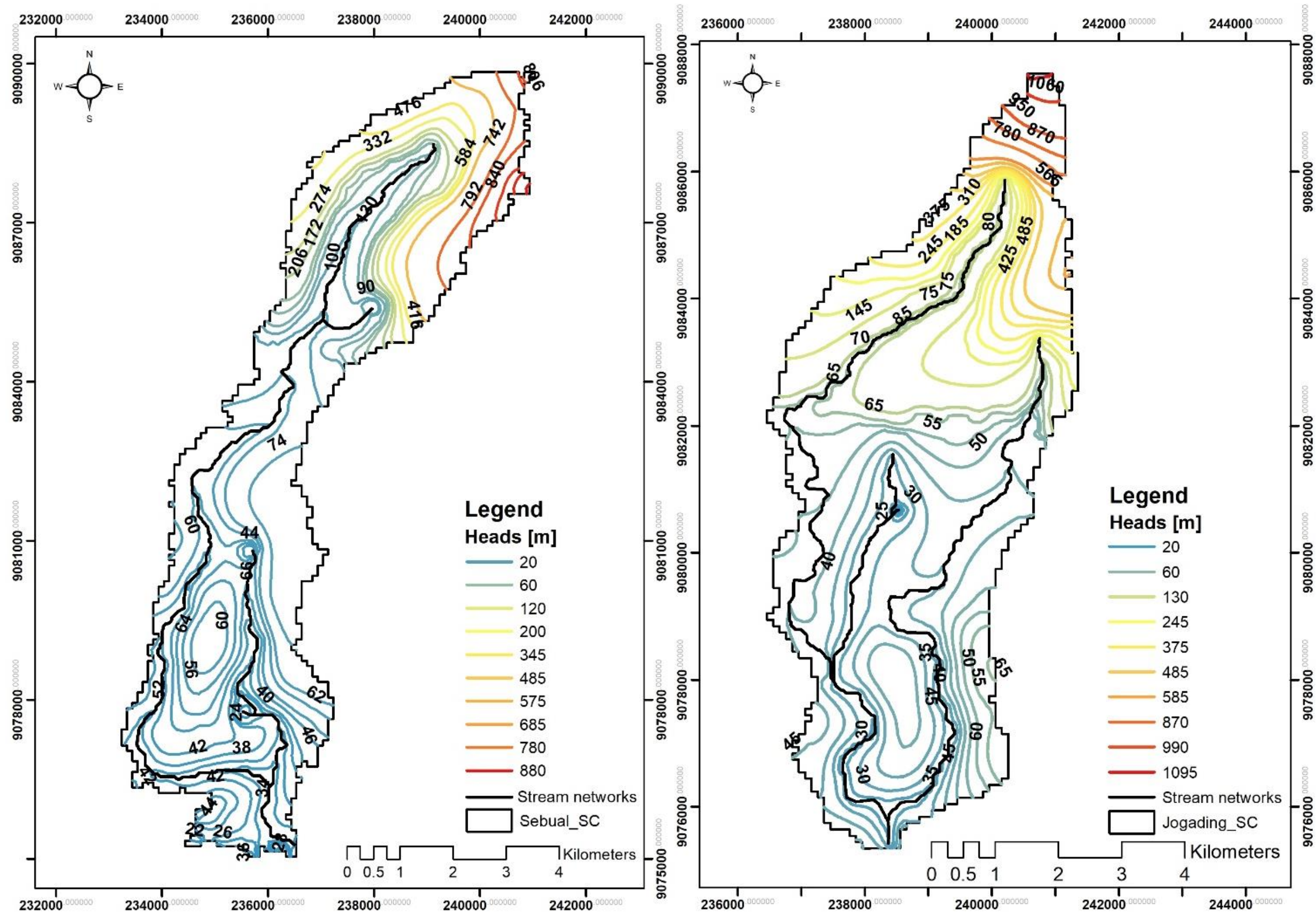

Figure 36. Potentiometric surface with stream segments map obtained from the last stress period (1096) of simulation IHM Sebual and Jogading

According to Figure 36, the water table was lower in the downstream area and higher in the mountain area for both Sebual and Jogading. In Sebual, the range of groundwater heads was from~20 m to ~885 m a.s.l while in Jogading from ~20 m to ~1095 m a.s.l. Additionally, the distribution of groundwater depth (Figure 33) was spatially varied in each cell of the models. In downstream area, water table relatively shallow compared to mountain area for both Sebual and Jogading sub catchment.

4.7.4. Hydraulic conductivity and specific yield

During the calibration period, IHM of Sebual and Jogading sub catchment was managed in four zones of horizontal hydraulic conductivities (K_h). Four zones were only used because of limitation hydrogeologic data in the study area., by doing in this fashion a comparison between the K_h values of two sub catchments was possible.

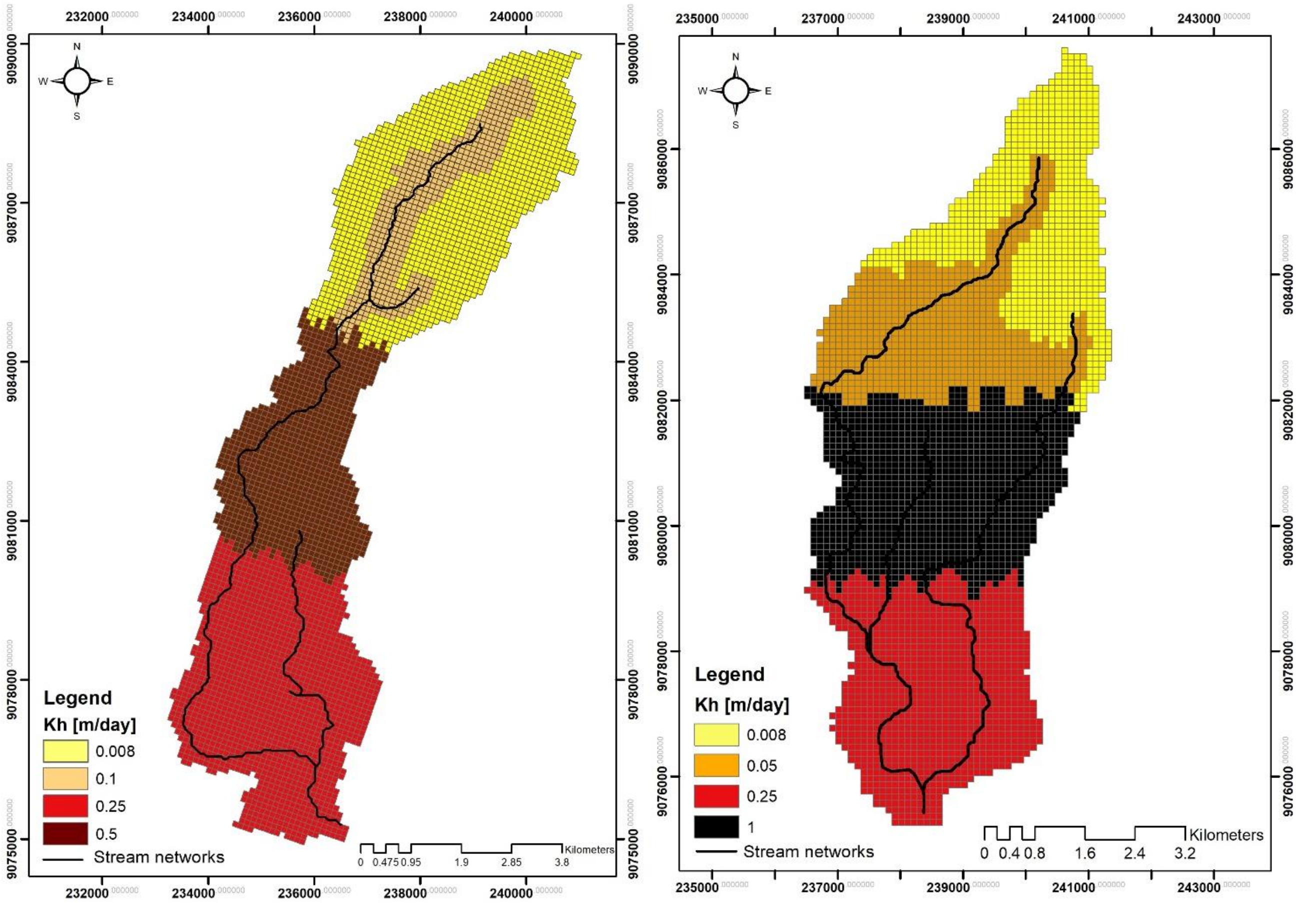

Figure 37. Calibrated horizontal hydraulic conductivity (K_h) of Sebual (left) and Jogading (right) sub catchment.

Table 12. Calibrated parameters of IHM Sebual and Jogading sub catchment, where EXTDP-extinction depth, EXTWC-extinction water content, THTS-saturated volumetric water content, THTI-initial volumetric water content, STRTOP-streambed top, STRTHICK-streambed thickness, SLOPE- stream slope,STRHC1-streambed Kv, Kh-horizontal hydraulic conductivity, Sy-specific yield, C-conductance, and Str depth-stream depth

Vertical zones	Parameters	Min value	Max value	Str discharges calibration	Sensitivity analysis	Assigned [A]	Calibrated [C]	units
Unsaturated zone	EXTDP	0	2.5	EXTDP	EXTDP	EXTDP		m
(MODFLOW-NWT, UZF1)	EXTWC	0.45	0.55	EXTWC	EXTWC		EXTWC	m^3m^{-3}
	Kvun	0.05	0.05	Kvun	Kvun		Kvun	$mday^{-1}$
Streams								
(MODFLOW-NWT, SFR2)	THTS	0.5	0.5	THTS		THTS		-
	THTI	0.1	0.4	THTI		THTI		-
	STRTOP	0.6	0.6	STRTOP		STRTOP		m
	STRTHICK	0.5	0.5	STRTHICK		STRTHICK		m
	SLOPE	0.025	0.025	SLOPE		SLOPE		-
	STRRHC1	0.2	0.49	STRRHC1		STRRHC1		$mday^{-1}$
	K_h	0.08	1	Kh	Kh		Kh	$mday^{-1}$
	S_y	0.27	0.30	Sy	Sy		Sy	-
	C	3	3	C		C		m^2day^{-1}
	Str depth	20	100	Str depth			Str depth	m

The ranges of calibrated (K_h) in Sebual were set from 0.008 mday^{-1} to 0.5 mday^{-1} whereas Jogading from 0.08 mday^{-1} to 1 mday^{-1} respectively (Figure 42). River bed hydraulic conductivity of Sebual was assigned from 0.1 to 5 mday^{-1}, and for Jogading was from 0.1 to 0.25 mday^{-1}. Then specific yield (Sy) for Sebual and Jogading were assigned using only uniformly one zone, and it was 0.30 and 0.27 for Sebual and Jogading respectively.

4.7.5. Temporal variability of unsaturated zone and groundwater fluxes

IHM Sebual and Jogading numerical models resulted unsaturated zone and groundwater components which were converted to be the fluxes by dividing with the area in the model itself. In Sebual, the estimated average of three years of actual evapotranspiration [P_a] was ~4.76 mmday^{-1} while in Jogading was ~4.52 mmday^{-1} respectively. Meanwhile, the average PET in Sebual was ~5.02 mmday^{-1} and Jogading was slightly lower ~4.98 mmday^{-1} (see Figure 38 and 39).

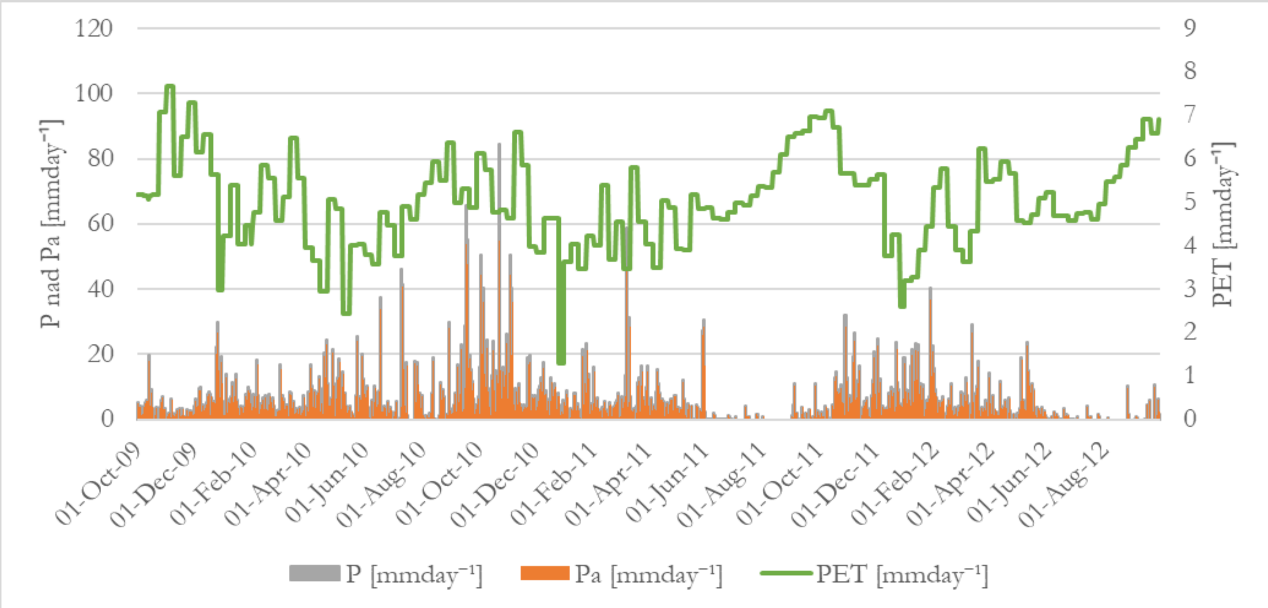

Figure 38. Temporal variability of precipitation [P], actual infiltration [Pa] and PET in Sebual sub catchment

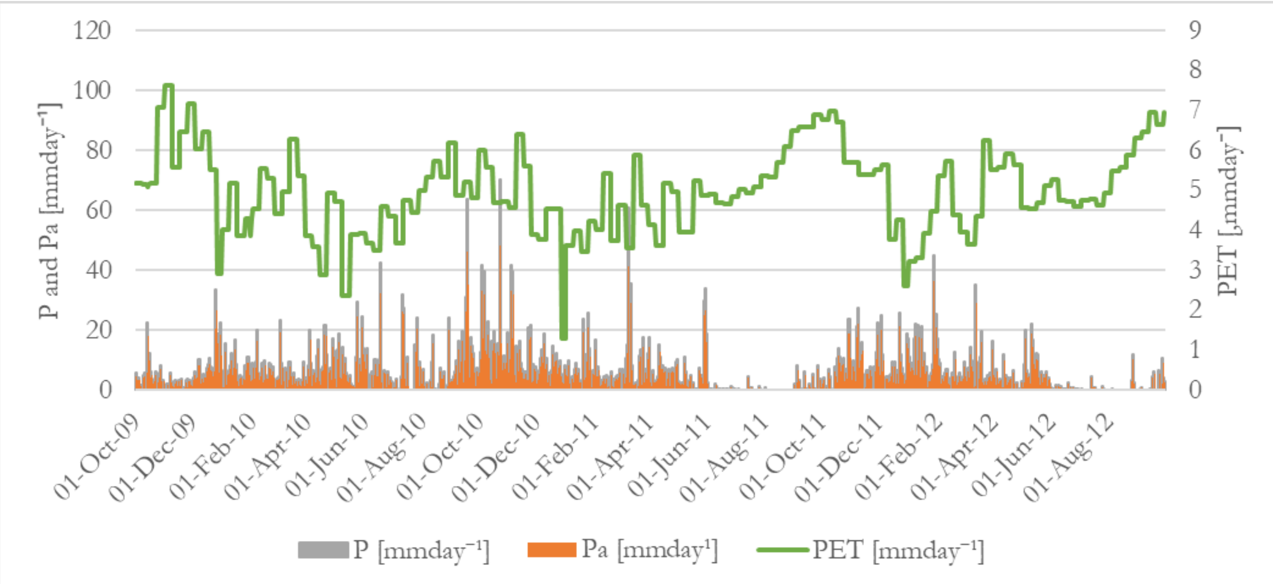

Figure 39. Temporal variability of precipitation [P], actual infiltration [Pa] and PET in Jogading sub catchment

IHM Sebual and Jogading also produced unsaturated zone components (actual infiltration and unsaturated zone evapotranspiration). From Figure 40 and 41, it can be observed that the hydrograph shapes of unsaturated zone evapotranspiration [ETuz] of Sebual and Jogading performed based on of seasonal rainfall, being quite high during high rainfall distribution but very low in low rainfall. In Sebual, [ET_{uz}] performed just slightly higher than Jogading, and the average of three years of [ET_{uz}] in Sebual and Jogading was 0.05 $mmday^{-1}$ and 0.04 $mmday^{-1}$ respectively. The temporal variabilities of unsaturated zone evapotranspiration [ET_{uz}] and actual infiltration [Pa] can be observed in Figure 40 and 41. In Sebual and Jogading, ET_{uz} followed the pattern of rainfall distribution

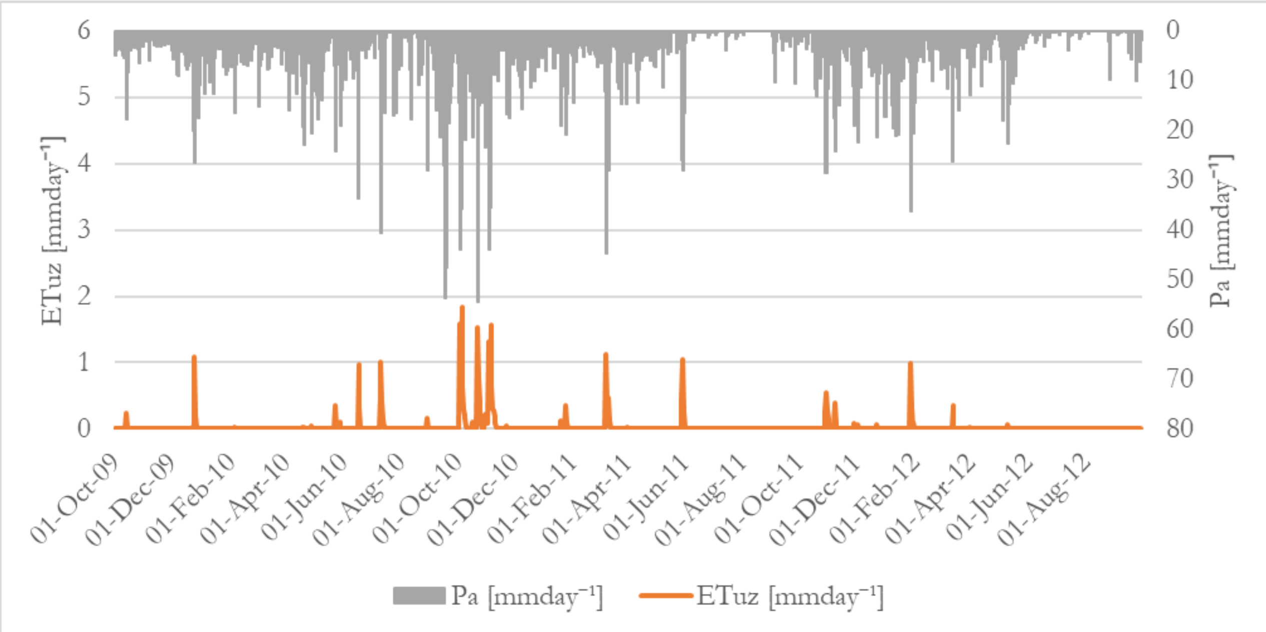

Figure 40. Relation of actual infiltration [Pa] and unsaturated zone evapotranspiration [ETuz] in Sebual

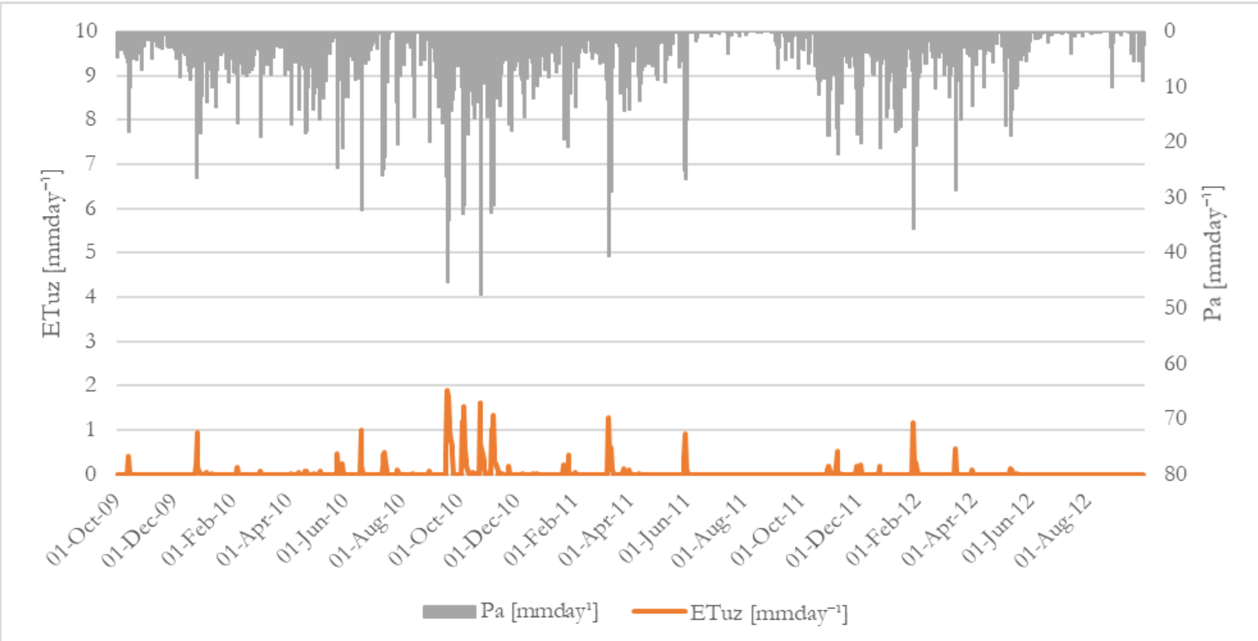

Figure 41. Relation of actual infiltration [Pa] and unsaturated zone evapotranspiration [ETuz] in Jogading

The temporal variability of groundwater fluxes of gross recharge [R_g] and net recharge [R_n] of the two models is presented in Figure 42 and 43. It can be observed that the pattern of net recharge [R_g] nearly matched well with gross recharge [R_g] and those patterns follow rainfall patterns.

In Sebual, the net recharge was considerably lower than the gross recharge while in Jogading was only slightly lower with gross and the averages of three hydrologic years of R_g and R_n in Sebual were ~4.18 mmday^{-1} and ~4.03 mmday^{-1} and Jogading, ~4.39 mmday^{-1} and ~4.35 mmday^{-1} respectively. Because of distribution ET_g and Exf_{gw} were considered quite low in both models; therefore, R_g and R_n were pretty similar [Equation 3.20]. The temporal variabilities of ET_g and Exf_{gw} for Sebual and Jogading presented in figure 45 and 46 respectively.

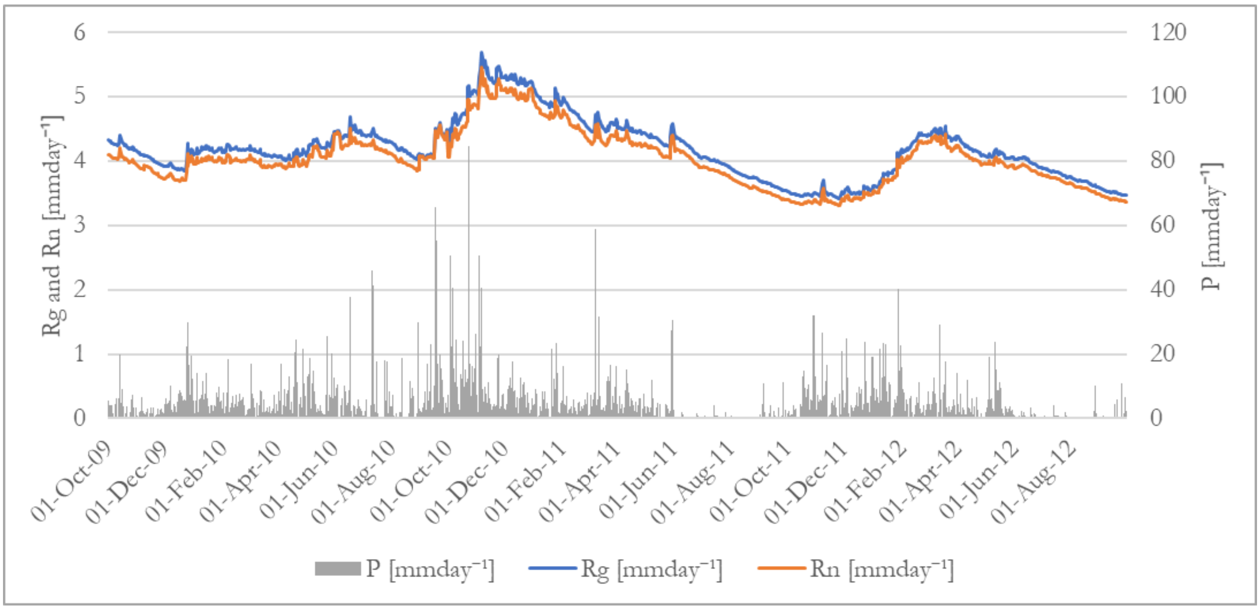

Figure 42. Long-term relation of precipitation [P], gross recharge [R_g] and net recharge [R_n] in Sebual_SC

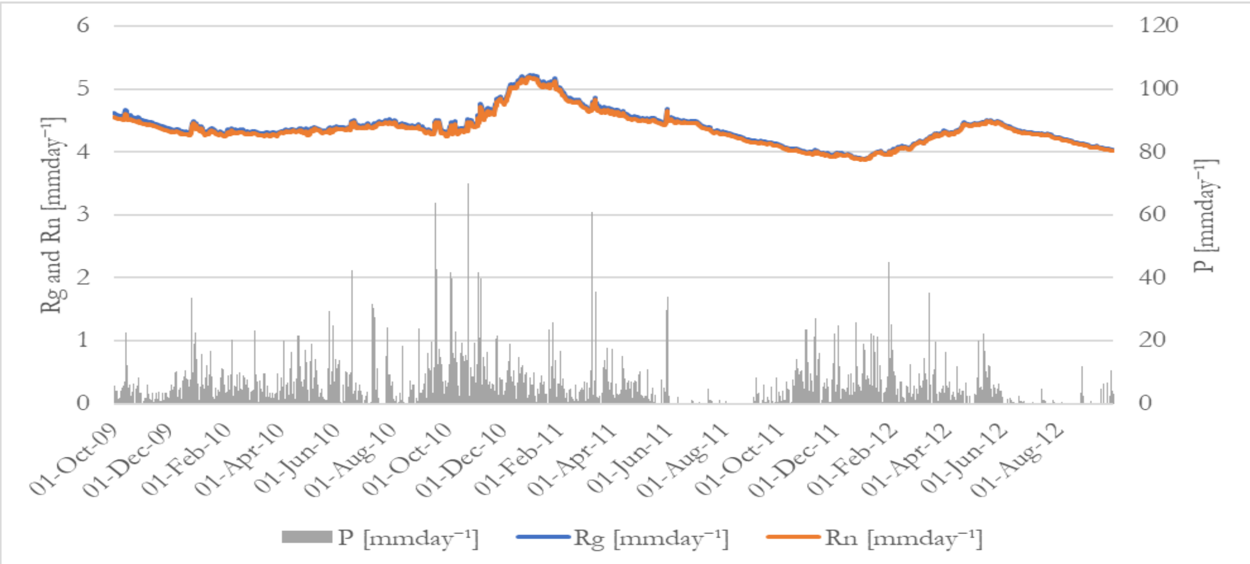

Figure 43. Long term relation of precipitation [P], gross recharge [R_g] and net recharge [R_n] in Jogading_SC

In Sebual, R_g defined slightly higher than R_n but in Jogading nearly equal to R_n (Figure 47 and 48), this condition occurred due to lower ET_g and *Exfgw*m (Equation 3.20). From Figure 44 and 45, in general the pattern of ET_g and *Exfgw* followed the path of rainfall distribution both in Sebual and Jogading. However, the graphs of ET_g and *Exfgw* in Sebual were performed different than Jogading. Both ET_g and *Exfgw* defined higher in wet season and lower in the dry season. In Sebual, the average of three years ET_g was ~ 0.13 mmday^{-1} while in Jogading was ~0.03 mmday^{-1}. Then, the average of three years *Exfgw* in Sebual was ~0.02 mmday^{-1} whereas in Jogading was < 0.01 mmday^{-1}.

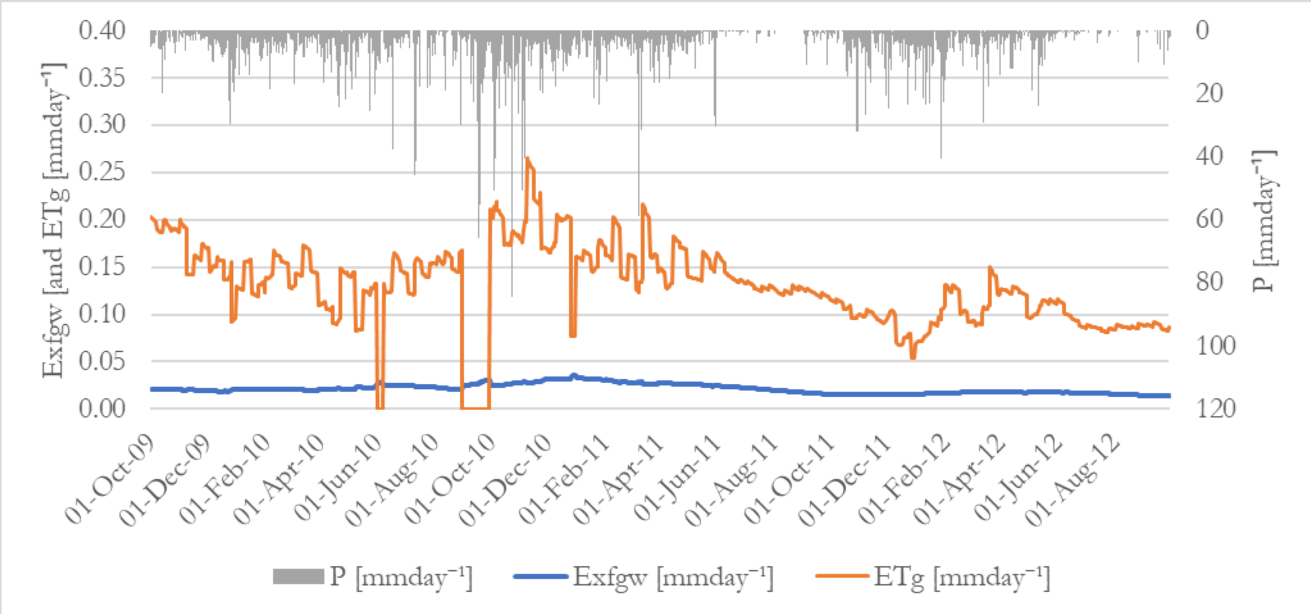

Figure 44. Long term relation of precipitation [P], surface leakage [Exf_{gw}] and groundwater evapotranspiration [ET_g] in Sebual sub catchment

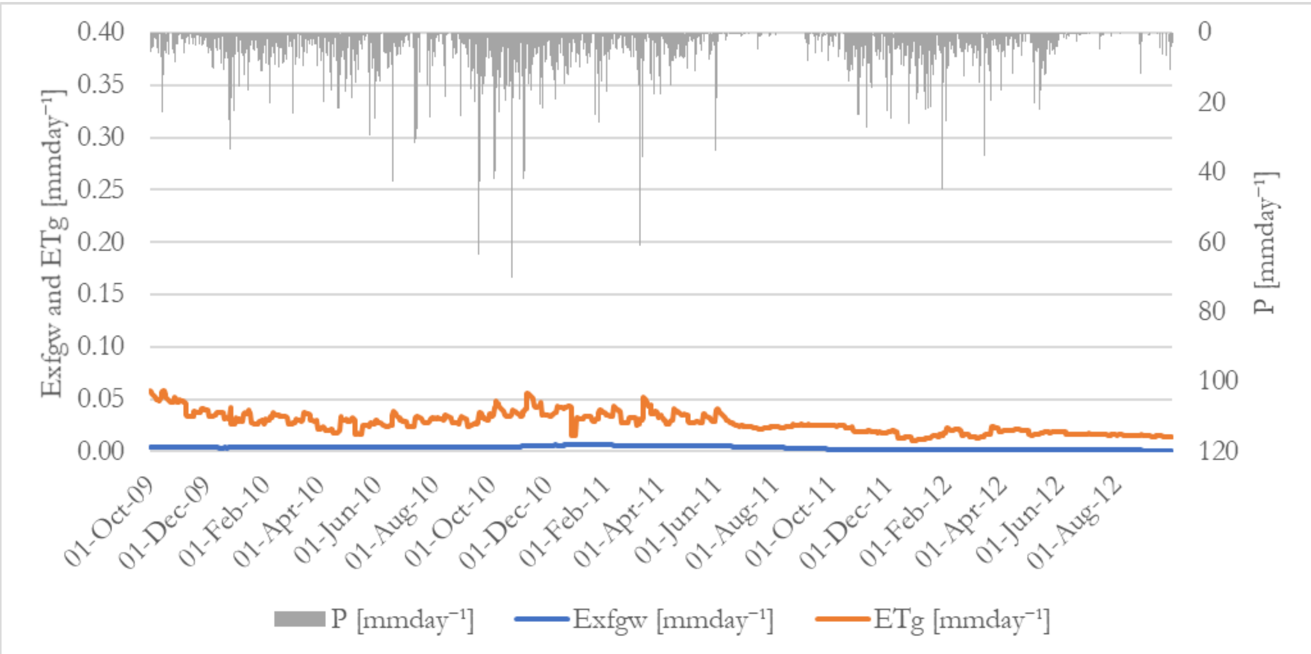

Figure 45. Long term relation of precipitation [P], surface leakage [Exf_{gw}] and groundwater evapotranspiration [ET_g] in Jogading sub catchment

4.7.6. Spatial variability of groundwater fluxes

In MODFLOW-NWT, the spatial variability of groundwater fluxes can be extracted from the output files. Figure 46 presented the spatial distribution of net recharge [R_n] which was obtained from wet period (3rd January 2010) in Sebual and Jogading. It can be observed that the higher spatial distribution of net recharge [R_g] was completely different between Sebual and Jogading sub catchment. In Sebual, the lower of R_n was located at the northeast, northwest and central of downstream area.. Then, the higher of R_n in Sebual was distributed from middle to lower middle of the modelled area. Also, it followed the track of the stream segments till reach the outlet of the catchment. In Jogading, the lower of R_n was distributed in the northwest, northeast and central of downstream of the modelled area. Additionally, it also spotted at the eastern part in the middle area of the modelled area. The same condition with Sebual, the higher of Rg was located at the central of the area, following the path of the stream segments till reach the outlet of the sub catchment. For stream segments path of Sebual and Jogading (see Figure 38).

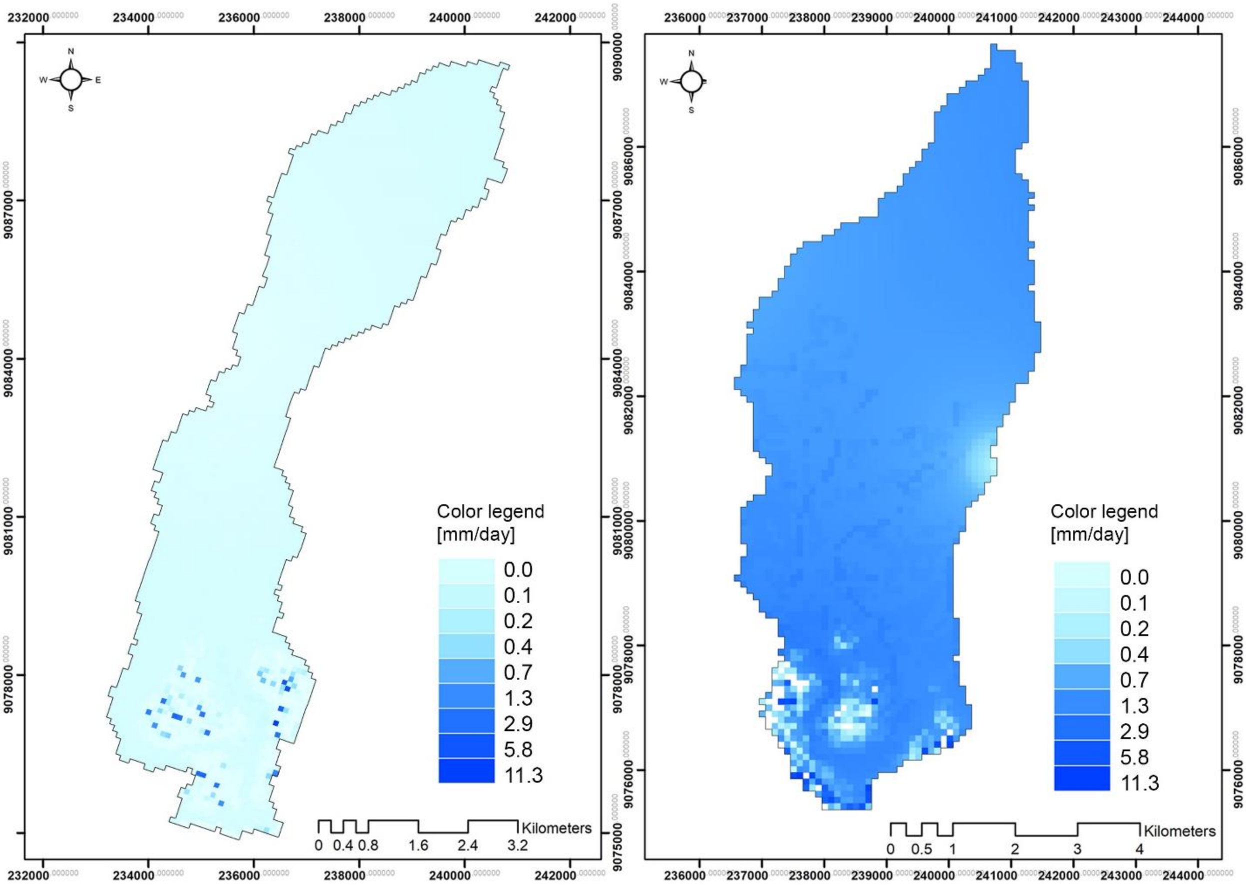

Figure 46. Spatial distribution of net recharge [R_n] in [mmday^{-1}] in wet period (3rd January 2010) in Sebual (left) and Jogading (right)

In this period, the range of R_n in Sebual was from 0 to ~11.3 mmday^{-1} while Jogading was slightly lower from 0 to ~11.0 mmday^{-1} respectively. However, R_n distribution in the upstream area (north area) of the models performed quite different, it was ~0.10 mmday^{-1} in Sebual and Jogading ~0.70 mmday^{-1}. In addition, its distribution in Sebual tends to be higher in downstream area while in Jogading distributed uniformly over the modelled area and higher in downstream as well. The spatio-temporal distribution of R_n in both sub catchments were mainly governed by rainfall distribution in the modelled area (see Figure 42 and 43).

In order to make comparison between the periods, the spatial R_n distribution also was taken from dry period (17th August 2011) for both models (see Figure 47). In Sebual , the lower areas of R_n distribution in dry period have the same pattern with the wet period. Moreover, the lower spots R_n in the western part of the middle area getting larger compared to wet period. Then, the higher of R_n clearly distributed in the downstream area, following the path of stream networks till get the outlet of the sub catchment. The range of R_n in dry period was range from 0 to ~0.0039 mmday^{-1} which means almost three times lower than wet period. The upstream area and the upper of downstream area performed the same values which was from ~ 0.0009 to ~0.0013 mmday^{-1} respectively.

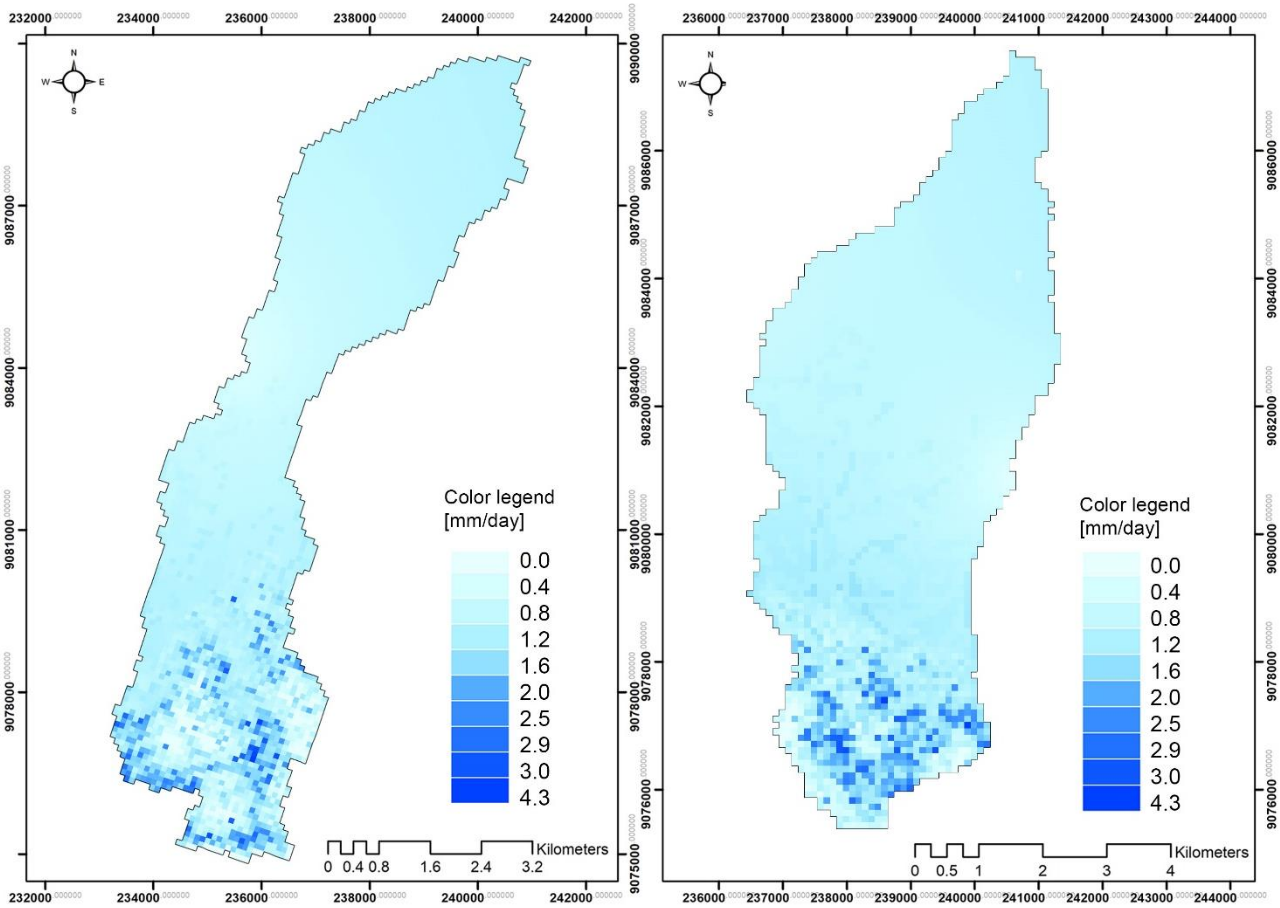

Figure 47. Spatial distribution of net recharge [Rn] in [mmday^{-1}] in dry period (17th August 2011)

In Jogading, there are three spots were considered as the lower of *Rn* distribution in the dry period, they are located in northwest, northeast and eastern part in the middle area of the model. Meanwhile, the higher of R_n was located in the central of the downstream area, following the path of stream lines till reach the outlet of the model. In that area, it was estimated ~0.30 mm day^{-1} which means three times lower than wet period. Also, if compared with Sebual, R_n in Jogading still has higher values of R_n distribution. Then, in the upstream area (north area), it was performed smoothly in the same values, it was ~0.8 mm day^{-1}.

4.7.7. Comparison of catchment WB from IHM and Direct baseflow separation

In this study, hydrological components such as groundwater runoff [q_g] and direct surface runoff of the stream [q_s] were estimated using two methods, baseflow separation [WHAT] and IHM MODFLOW-NWT. A single hydrologic year (2009) was selected for this comparison. The aim of this comparison was to see the agreement between them. The comparison of the results can be observed in Table 13 and 14 below.

Table 13. Estimation of q_t, q_g and q_s using [WHAT] in 2009

No	Sub catchment	Au [m²]	Au [Km²]	Pu [mmday⁻¹]	Qs [m³day⁻¹]	q_s= Qs/Au [mmday⁻¹]	fs=q_s/Pu [%]	q_s/q_t [%]	Qg [m³day⁻¹]	q_g= Qg/Au [mmday⁻¹]	fg=q_g/Pu [%]	q_g/q_t [%]
1	Sebual	40999526	41.00	8.00	99360	2.42	30.29	50.22	98496	2.40	30.03	49.78
2	Jogading	36672824	36.67	6.00	30240	0.82	13.74	21.88	108000	2.94	49.08	78.12

Table 14. Estimation of q_t, q_g and q_s using IHM MODFLOW-NWT in 2009

No	Sub catchment	Au [m²]	Au [Km²]	Pu [mmday⁻¹]	Qs [m³day⁻¹]	q_s= Qs/Au [mmday⁻¹]	fs=q_s/Pu [%]	q_s/q_t [%]	Qg [m³day⁻¹]	q_g= Qg/Au [mmday⁻¹]	fg=q_g/Pu [%]	q_g/q_t [%]
1	Sebual	40999526	41.00	8.00	224439	5.47	68.37	57.89	163199	3.98	49.75	42.11
2	Jogading	36672824	36.67	6.00	20440	0.55	9.16	11.12	161270	4.39	74.00	88.88

To sum up, q_g in Sebual performed lower than Jogading either using [WHAT] or IHM MODFLOW-NWT (Table 13 and 14). Inversely, q_s performed higher in Sebual than Jogading either in WHAT or IHM MODFLOW-NWT.

In WHAT method ,the yearly average of q_g in Sebual and Jogading was ~2.40 mm day^{-1} and ~2.94mm day^{-1} respectively. Then, In Sebual q_s was 2.42 mm day^{-1} whereas Jogading was 0.82 mm day^{-1}. The proportion of q_g in Sebual and Jogading was 49.78% and 78.12% while q_s was~ 50.22% and 21.88% of total estimated flow.

From IHM MODFLOW-NWT, the yearly average of q_g in Sebual and Jogading were ~3.98 mm day^{-1} and ~4.39 mm day^{-1} respectively. Meanwhile, q_s in Sebual was ~5.47 mm day^{-1} and ~0.55 mm day^{-1} respectively. The proportion of q_g in Sebual and Jogading was 42.11% and 88.88% while q_s was 57.89% and 11.12 % of total estimated flow.

4.8. Sensitivity analysis

The sensitivity analysis was conducted to the parameters of IHM in MODFLOW-NWT such as Brooks-Corey Epsilon, maximum unsaturated vertical conductivity, saturated water content, extinction water content, extinction depth, and horizontal hydraulic conductivity over relative volumetric error [RVE], NS the calibrated heads over Sebual and Jogading.

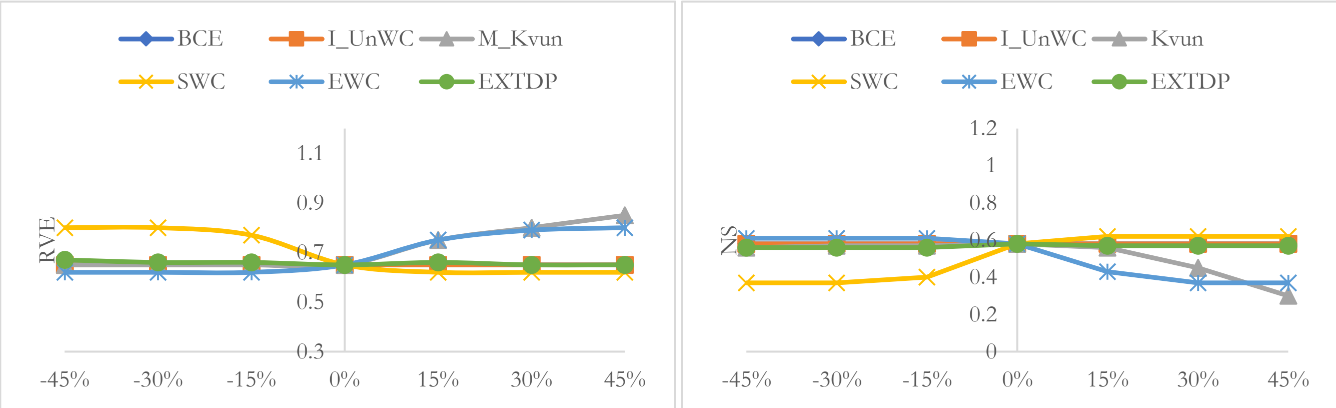

Figure 48. Sensitivity analysis of IHM Sebual sub catchment, where BCE [Brooks -Corey Epsilon, I_UnWC [Initial unsaturated water content], M_Kvun [Maximum unsaturated vertical conductivity], SWC [Saturated water content], EWC [Extinction water content], and EXTDP [Extinction depth].

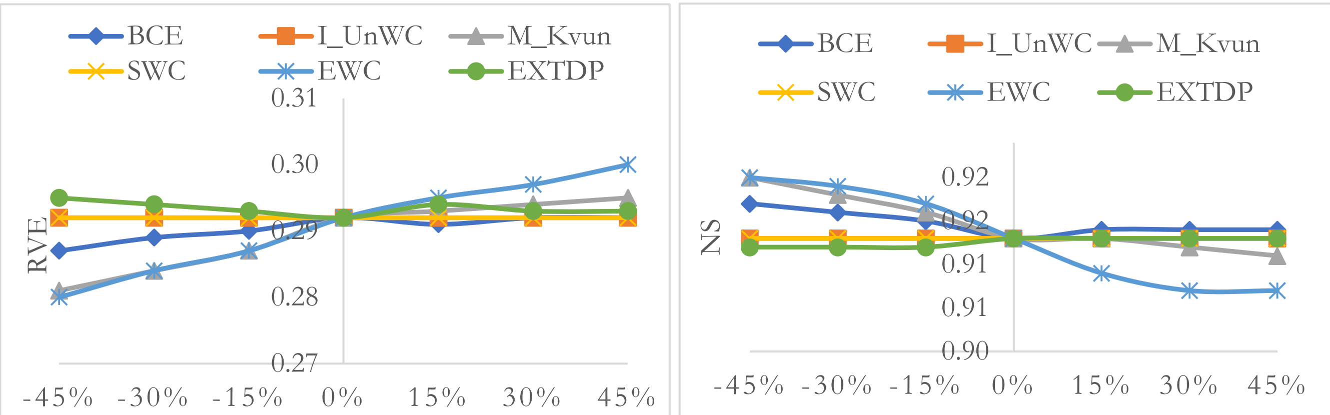

Figure 49. Sensitivity analysis of IHM Jogading sub catchment, where BCE [Brooks -Corey Epsilon], I_UnWC [Initial unsaturated water content], M_Kvun [Maximum unsaturated vertical conductivity], SWC [Saturated water content], EWC [Extinction water content], and EXTDP [Extinction depth].

According to sensitivity analysis (Figure 48 and 49), the models gave responses to RVE and NS values after changing parameters such as Brooks Corey Epsilon [BCE], maximum vertical hydraulic conductivity [M_Kvun], saturated water content [SWC], extinction water content [EWC], and extinction depth [EXTDP]. However the models did not react on changing parameter of initial unsaturated water content [I_UnWC]. In addition, RVE and NS also was influenced by specific yield [Sy] as shown in Figure 50 and 51. By reducing the specific yield [Sy], the models performance improved gradually and vice versa. The Infiltration rate decreased gradually while decreasing M_K_{vun} parameters and vice versa (Figure 53). Also, the simulated heads in Sebual and Jogading was reacted by changing parameters of K_h in both models (Figure 52). It can be observed that the simulated head decreased while increasing the K_h values and vice versa condition

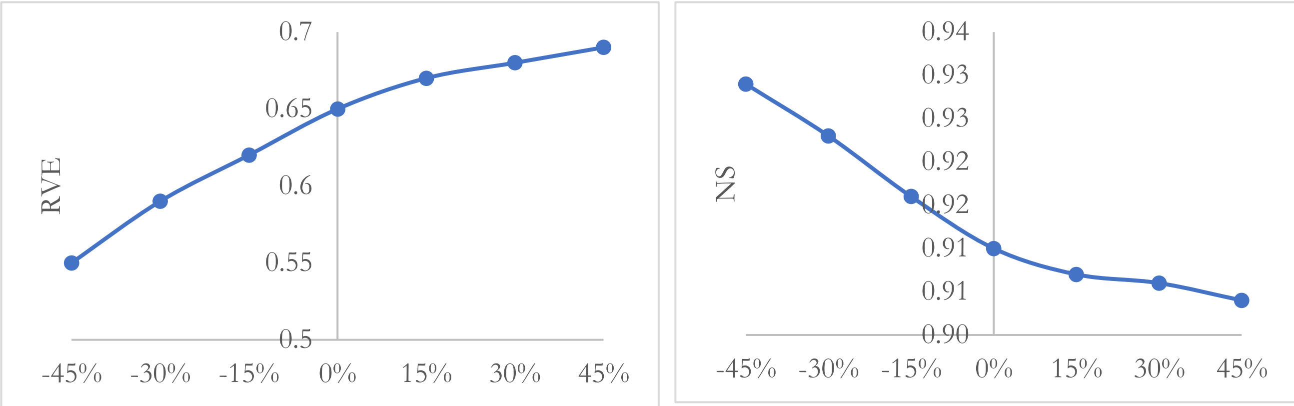

Figure 50. Sensitivity analysis of specific yield [Sy]upon RVE and NS in Sebual

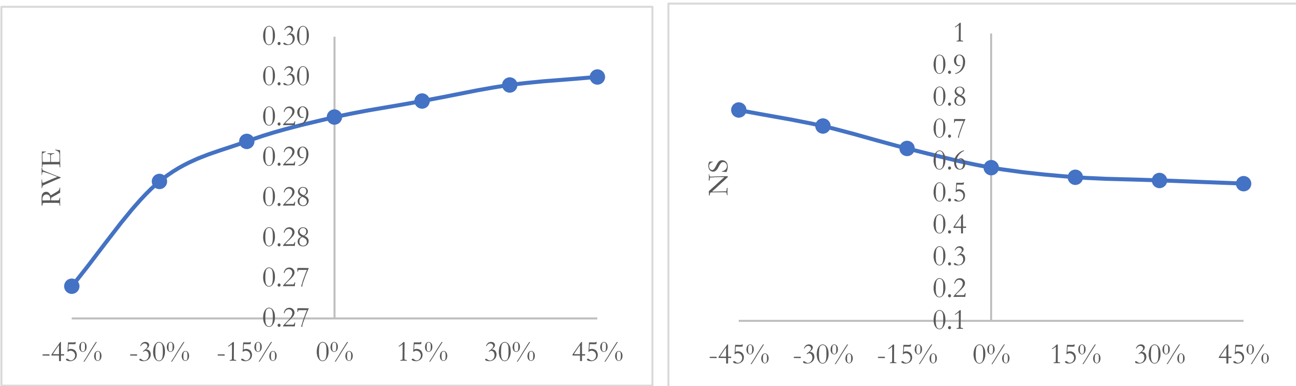

Figure 51. Sensitivity analysis of Specific yield [Sy] upon RVE and NS in Jogading_SC

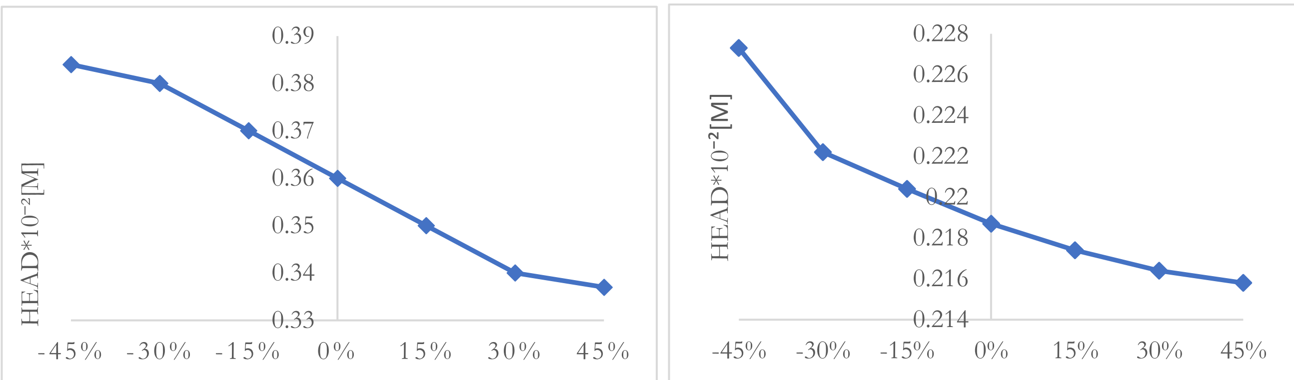

Figure 52. Sensitivity analysis of horizontal hydraulic conductivity [K_h] over the simulated heads in Sebual (left) and Jogading (right)

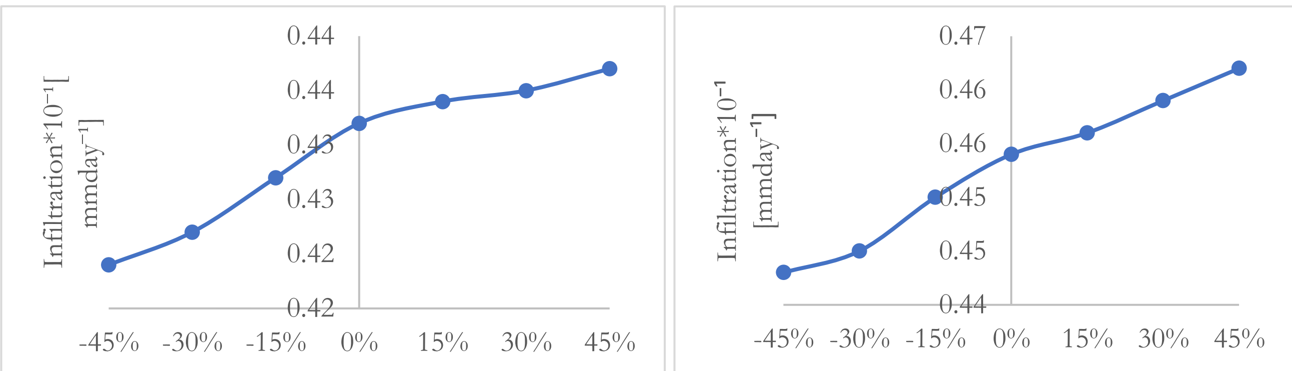

Figure 53. Sensitivity analysis of M_Kvun upon the average of infiltration rate in Sebual (left) and Jogading (right)

4.9. Water Balance

A water budget components for both unsaturated and saturated zones were produced from IHM of Sebual and Jogading. The output files were opened using GW_chart software and then imported to excel spreadsheet software to extract the values. The average of three years water budget in Sebual and Jogading sub catchment presented in Table 15 and 16. Table 13 presented the average of three years unsaturated zone components, the infiltration rate in Sebual was ~173743 m^3day^{-1} while Jogading was slightly lower with ~165742 m^3day^{-1}. Then, the evapotranspiration unsaturated zone [$ETuz$] in Sebual was lower (0.61%) of total outflow compared to Jogading was 0.75% of total outflow.

Table 16 presented the average of three years saturated zone, the percentage of gross recharge (R_g) in Sebual and Jogading were 76.48 % and 87.48 % of the total groundwater budget. In Sebual, stream to groundwater [q_{sg}] and storage [ΔS_{gin}] contributed 15.74% and 7.78%, while in Jogading was 5.84% and 6.67% respectively. The outflow components consist of groundwater to stream [q_{gs}], groundwater evapotranspiration [ET_g], surface leakage [Exf_{gw}] and storage [ΔS_{gout}] which were 90.37%, 2.40%, 0.40% and 6.83 % of the total outflow in Sebual, while in Jogading was 94.74%, 0.53% , 0.07 %, and 4.66 % of the total outflow respectively.

Table 15. Long-term water budget components unsaturated zone for Sebual SC and Jogading_SC; where IN: inflow to Aquifer system, OUT: Outflow from aquifer system

	SEBUAL_SC		JOGADING_SC	
Budget components	IN [m^3day^{-1}]	OUT [m^3day^{-1}]	IN [m^3day^{-1}]	OUT [m^3day^{-1}]
Infiltration	173743		165742	
ETuz		1068		1245
UZF recharge		171557		161024
Storage change		1080		3434
Total	173743	173705	165742	165703
IN-OUT	38		39	
Percent Discrepancy	0%		0%	

Table 16. Long term water budget components saturated for Sebual SC and Jogading_SC; where IN: inflow to Aquifer system, OUT: Outflow from aquifer system

Budget components	SEBUAL_SC		JOGADING_SC	
	IN [m^3day^{-1}]	OUT [m^3day^{-1}]	IN [m^3day^{-1}]	OUT [m^3day^{-1}]
Stream leakage	35299	199535	10752	177547
UZF recharge	171557	0	161025	0
GW ET	0	5296	0	993
Surface leakage	0	873	0	129
Storage	17459	15083	12289	8735
TOTAL	224315	220787	184066	187404
IN-OUT		3520		-3320
Percent Discrepancy		1.60%		-1.70%

As mentioned earlier, the models have been running in transient state condition using IHM MODFLOW-NWT. The model produced cumulative unsaturated and saturated components instead of daily rates which can be opened using GW_chart software. The yearly transient variability of water fluxes were calculated using water balance functions (Equation 3.16 to 3.20). Table 17 and 18 present the yearly average of surface and groundwater fluxes

It can be observed that Rainfall [P], interception [I] and effective infiltration [P_e] in Jogading was lower than Sebual. Jogading performed higher of unsaturated zone evapotranspiration [ET_{uz}] compared to Sebual. The actual infiltration [P_a] in Jogading was higher than Sebual. Also, stream discharges at the outlet [*Qout*] in Sebual defined higher compared to Jogading. R_g and R_n in the models not consider much different but Sebual performed lower of R_g and R_n compared Jogading. Then, stream to groundwater [q_{sg}] higher compared to Jogading. It was around three times higher than Jogading. Meanwhile, groundwater to stream [q_{gs}] was relatively not different between Sebual and Jogading. Groundwater evapotranspiration [ET_g] in Sebual performed higher three times than in Jogading. Also, R_o in Sebual was quite higher compared to Jogading. However, the distribution of R_g and R_n in Jogading was considered higher than Sebual. ET_g in Sebual was more than three times higher than Jogading. Also, surface leakage/groundwater exfiltration [Exf_{gw}] in Sebual was around eight times higher compared to Jogading. However, change storage in groundwater [ΔS_g] and change storage of unsaturated zone [ΔSuz] in Sebual were lower than Jogading.

Table 17. The yearly variability of surface and groundwater fluxes in Sebual sub catchment in three hydrologic year started from 1st October 2009 till 30th September 2012 MODFLOW-NWT simulation period [All units in mm year^{-1}]

Transient model	P	PET	I	P_e	Q_{out}	R_g	R_n	q_{sg}	q_{gs}	ET_g	E_xf_{gw}	ΔS_g	ET_{uz}	ΔS_{uz}	P_a	R_o
1 Oct 2009 to 30 Sept 2010	2887	1843	433	2454	3754	1530	1474	316	1768	48	8	12	6	246	1781	680
1 Oct 2010 to 30 Sept 2011	2345	1774	352	1994	2310	1645	1578	313	1825	58	9	-29	18	-108	1555	448
1 Oct 2011 to 30 Sept 2012	1755	1885	263	1492	2253	1412	1370	315	1740	36	6	81	4	-108	1307	190
Minimum	1755	1774	263	1492	2253	1412	1370	313	1740	36	6	-29	4	-108	1307	190
Maximum	2887	1885	433	2454	3754	1645	1578	316	1825	58	9	81	18	246	1781	680
Average	2329	1834	349	1980	2772	1529	1474	315	1778	47	8	21	9	10	1548	440
Standard deviation	566	56	85	481	851	117	104	1	44	11	2	56	8	204	237	245

Table 18. The yearly variability of surface and groundwater fluxes in Jogading sub catchment in three hydrologic year started from 1st October 2009 till 30th September 2012 MODFLOW-NWT simulation period [All units in mm year^{-1}]

Transient model	P	PET	I	P_e	Q_{out}	R_g	R_n	q_{sg}	q_{gs}	ET_g	E_xf_{gw}	ΔS_g	ET_{uz}	ΔS_{uz}	P_a	R_o
1 Oct 2009 to 30 Sept 2010	2293	1795	344	1949	1513	1606	1620	109	1773	15	1	44	15	274	1895	55
1 Oct 2010 to 30 Sept 2011	2037	1771	306	1732	1324	1682	1696	109	1785	15	1	-19	18	-51	1649	84
1 Oct 2011 to 30 Sept 2012	1711	1887	257	1455	1623	1526	1533	104	1739	8	0	94	5	-120	1410	45
Minimum	1711	1771	257	1455	1324	1526	1533	104	1739	8	0	-19	5	-120	1410	45
Maximum	2293	1887	344	1949	1623	1682	1696	109	1785	15	1	94	18	274	1895	84
Average	2014	1818	302	1712	1487	1605	1616	107	1766	13	1	39	12	34	1651	61
Standard deviation	291	61	44	248	151	78	81	3	24	4	0	57	7	210	242	20

Where P -precipitation, PET – potential evapotranspiration, I- interception, P_e- effective infiltration rate, Q_{out} – streamflow, R_g – gross recharge, R_n – net recharge, q_{sg} – stream to groundwater, q_{gs} – groundwater to stream, ET_{uz} -unsaturated zone evapotranspiration, ET_g – groundwater evapotranspiration, E_xf_{gw}- exfiltration/surface leakage, ΔS_{uz}- change storage in unsaturated zone, ΔS_g- groundwater storage, q_g- lateral groundwater outflow, P_a – actual infiltration rate, and R_o- total runoff of stream.

5. DISCUSSIONS AND CONCLUSIONS

5.1. Discussions

5.1.1. Baseflow Separation [WHAT]

Preliminary catchment assessment was conducted in ten catchments over the Jembrana Region (J.R) using rational and baseflow separation method [WHAT]. Ten catchments of the J.R showed large variability of surface runoff [Qs] and groundwater runoff [Qg] as well (Tables 6 and 7). In J.R, q_s ranges from ~0.02 mmday^{-1} to 2.37 mm day^{-1} while q_g ~0.06 to ~4.2 mm day^{-1}. This variability might occur because each catchment has different distribution of rainfall and also because of different surface topography, thus different slope, lithology, land use and land cover conditions. Rainfall was considered as the only source of groundwater recharge as well as runoff, surface and groundwater. in this region. Hydrograph pattern of stream discharges followed the pattern of rainfall distribution which means that stream discharge was greatly influenced directly by rainfall and indirectly by groundwater runoff (see figure 17 and 20).

Table 6 presents the groundwater fluxes [q_g] in ten catchments over Jembrana region. In general, the eastern part of that region was considered as the wet zone while the western part dry zone. Yeh Satang catchment had the highest of groundwater runoff [q_g] with ~4.2 mm day^{-1} whereas Sangyang Gede had the lowest with ~0.06 mm day^{-1}. However, none of them was selected for IHM simulation and calibration due to lack of monitoring stations around the catchment. Pergung Catchment (P.C) was selected as catchment for IHM simulation due to the relatively good data availability the largest monitoring stations around the Pergung Catchment. The P.C was treated similar way of analysis as the J.R. The P.C consists of four sub-catchments. Two of them, two hydrologically contrasting ones, were selected to be modelled, Sebual and Jogading sub-catchments. From Tables 9 and 10, Sebual had a high surface runoff (~2.42 mm day^{-1}) but low in groundwater runoff (~2.40 mm day^{-1}). Inversely, Jogading had a low surface runoff (~0.82 mm day^{-1}) but high groundwater runoff (2.94 mm day^{-1}). It means that Jogading was a wet zone, whereas Sebual was a dry area. This difference might be because they lay in the transition zone between wet and dry area (Figure 20). Given the values of q_t, q_s, and q_g for Jogading and Sebual, their aquifers were classified as highly permeable (unconfined) layer. This is because a high percentage of total runoff estimated (q_t) was converted to groundwater runoff (q_g).

5.1.2. IHM of Sebual and Jogading

IHM of Sebual and Jogading were generated separately using computer software [MODFLOW-NWT] with UZF1 and SFR2 package. The two models were generated applying four zones (Figure 37) of horizontal hydraulic conductivity [K_h] and then calibrated with stream discharges and controlling the position of water table to be below surface altitude [DEM].

According to the results of stream discharge calibrations, the hydrograph of Sebual calibration matching was good despite an offset, because the simulated temporal pattern was nearly the same as the observed with two spots considered mismatched within the whole simulation period (Figure 30). However, the simulated stream discharge showed not matched well in the lower condition of observed stream discharge. These errors might be due to i) unreliability of data measurement in the field ii) the excess rainfall was stored in the different zones iii) the assigned stream depth, stream width and streambed top elevation in SFR2 package iv) and the size of grid cell in the model (Mehl and Hill 2010).

The difference between simulated and observed steam discharges was assessed using RVE, NS and Y parameters (Table 11). The Sebual model had an RVE of 0.66, an NS of 0.56 and a Y of 34. It was a difficult task to get good calibration of stream discharge in this model because water was excessive in the last stream segment. This condition might be because of the complex stream networks, and they contain an immense amount of water in the channel. Moreover, based on the water balance components, water from aquifer ends up in the streams (Table 14). To cope with this problem, the value of stream depth, specific yield, extinction water content and horizontal hydraulic conductivity (K_h) were adjusted. However, the adjustment was not enough to reach a good value of the three parameters due to the overwhelming amount of water in the last reach of stream networks.

In contrast to Sebual model, Jogading model performed well in the stream discharge calibration. It can be seen from Figure 31 that the hydrograph shapes of simulated and observed model nearly perfectly matched . Then, it was also checked with RVE, NS and Y parameters. In this model, the values RVE, NS, and Y were 0.29, 0.91 and 0.70 respectively. During the calibration of stream discharges, some parameters in UZF and SFR packages such as stream width, extinction water content, saturated water content, specific yield, maximum unsaturated vertical hydraulic conductivity, conductance and horizontal hydraulic conductivity were also adjusted in order to reach convergence model and to give reliable estimation of IHM Sebual and Jogading.

The calibrated heads was assessed spatially using the surface altitude [DEM], and temporally through assigned fictitious piezometers. It was important to crosscheck the simulated heads with surface altitude because in some cases the models can reach good calibration in stream discharges with unrealistic water table above the surface, Therefore, twenty-seven fictitious piezometers were assigned in Sebual and twenty-six in Jogading to record daily simulated heads (Figure 32). The horizontal hydraulic conductivity [K_h] zones and stream depth were required to be adjusted during this calibration. The depth of stream was taken into account during defining the depth of water table. The simulated heads were checked with surface altitude [DEM] and it was found that the groundwater heads were below the surface (Figure 33) although it was difficult to define the reliable estimation of simulated heads in the upstream, mountainous areas due to lack of data of groundwater table in both Sebual and Jogading sub catchments. Sebual heads were generally lower than Jogading heads. It might be because Jogading is located at higher altitude compared to Sebual (Figure 36).

From water balance components (Table 15 and 16), the ET_{uz} value of Sebual was almost the same as Jogading that is ~1.00% of total outflow. The amount of ET_{uz} is influenced by extinction water content value, the lower the extinction water content, the higher ETuz derived from the model is and vice versa. The gross recharge [R_g] in Jogading was higher (87.48% of total budget) than in Sebual (76.48% of total budget). This is because the PET value of Sebual model was higher. Another reason was that R_g distributions in the models were greatly influenced by rainfall distribution where the rainfall of Sebual was lower than of Jogading as shown in Figure 17. The spatial distribution of R_n in Sebual and Jogading as shown in Figure 46 and 47 might be affected by stream segment compositions and topographical condition.

Both Sebual and Jogading showed that much water is transferred by the aquifer into the stream, which were 90.37% and 94.74% of the total outflow respectively. It means that the aquifer received a lot of waters from the total budget. In this models, the values of ET_g and Exfgw were considered low. The ET_g (2.40%) and Exfgw (0.40%) of Sebual were higher compared to Jogading with the ET_g value of 0.53% and the Exf_{gw} value of 0.07% of total outflow. From the models, it was observed that ET_g has negative relationship with K_h. The higher K_h values are assigned in the model, the lower value of ET_g will be obtained and vice versa. Similarly, the higher K_h values are assigned the lower level of water table derived from the model will be.

According to the sensitivity analysis, both Sebual and Jogading were sensitive to the changing parameters of Brooks Corey Epsilon [BCE], maximum unsaturated vertical conductivity [M_K_{vun}], saturated water content [SWC], and extinction depth [EXTDP], and specific yield [S_y]. Then for further study, IHM Sebual and Jogading can be improved by adjusting those parameters to get more reliable estimation. In both Sebual and Jogading, the simulated heads were sensitive to horizontal hydraulic conductivity [K_h] as shown in Figure 54. It was found that the lower value of K_h applied in the zones, implied the higher water table and vice versa. It means that the higher value of K_h is assigned in the zones, the easier water transmition within the zones. Maximum unsaturated zone vertical conductivity [M_K_{vun}] was sensitive to infiltration rate in both Sebual and Jogading sub catchment. The lower value of M_K_{vun} assigned in the model, the lower infiltration rate derived from the models (Figure 53).

5.1.3. Comparison of catchment assessment with IHM Sebual and Jogading

As stated earlier, the hydrology components such as [q_g] and [q_s] of J.R and P.C were estimated using two method namely [WHAT] and IHM MODFLOW-NWT. As shown in Table 13 and 14, IHM MODFLOW-NWT derived q_g and higher than [WHAT] which can be observed. This condition might occur because MODFLOW-NWT was performed in more complex parameters in UZF1 and SFR2 packages and more driving forces. Meanwhile, [WHAT] was used the local minimum with two digital filtering (BFLOW and Eckhardt) to process streamflow data. However, it was interesting because it produced the same trend of percentage q_g and q_s. In [WHAT], the proportion of percentages of q_g to q_s was 49.78% to 50.22% for Sebual and 78.12% to 21.88% in Jogading. In IHM MODFLOW-NWT, 42.11% to 57.89% for Sebual and 88.88% to 11.12% in Jogading. Generally, both [WHAT] and [IHM MODFLOW-NWT] methods were in agreement in terms of estimating q_g and q_s components.

5.1.4. Comparing to other studies

In Bali, the study about groundwater modelling has been conducted by Teketel (2017) and Nielsen and Widjaya (1989). Their study areas are the same, i.e. the southern part of Bali Island. Teketel used IHM MODFLOW-NWT with UZF1 and SFR2 as the actives packages the same as in this study. On the other hand, Nielsen and Widjaya used hydrograph well analysis, annual infiltration and flow net analysis. According to the results of Teketel in transient state, R_g contributes 75% of total groundwater inflow, ΔS_{gin} [21.4%] and q_{sg} (3.3%). Then the outflow components was q_{gs} (30.4%), *Exfgw* (29.4%), ΔS_{gout} (18.94%) , and ET_g (14.1%). In this study, the IHM Sebual and Jogading based on three hydrologic years of transient state simulation. In this way, this study was comparable in terms of transient state condition with the results of Teketel.

The percentage of R_g in Sebual was (76.48) similar to Teketel study (75%) and Jogading was higher (87.48%) of total budget. In Sebual and Jogading , ET_g was (2.4% and 0.53%) and Exf_{gw} (0.40% and 0.07%) lower compared to Teketel results (14.10%). The proportion of groundwater to stream [q_{gs}] in Sebual (90.37%) and Jogading (94.74%) was three times higher than Teketel (30.40%). The clear distinction of this study compared with Teketel results might be because of the difference the land use and land cover percentage, stream segments compositions, interception and infiltration rate, PET and rainfall distribution in this area. The yearly average of PET in this study was (~5 mm day^{-1}) higher than in Teketel model (~3.5 mm day^{-1}). PET estimation of this study was satellite images [MODIS], while Teketel used FAO Penman-Monteith estimation. In this study, spatial interpolation of rainfall using inverse distance weighting [IDW] method while Teketel used Kriging. Also, it might be because the model set up was different, the horizontal hydraulic conductivity zones was quite difference. In this study the model was set up only with four zones, but Teketel's (2017) study consist of seventy two zones. Moreover, the grid cell size of this study was managed with 100m*100m while Teketel was used 500*500m.

5.2. Conclusions

The aim of this study was to generate IHM in the Jembrana Region, the western part of Bali Island. The Jembrana Region with its 10 catchment, was assessed using rational method and baseflow separation [WHAT]. This assessment was also conducted to select two hydrologically contrasting catchments for IHM simulation and calibration. Then, Pergung Catchment was proposed, and its two sub-catchment were selected for IHM simulation and calibration. two sub catchment were selected for IHM simulation and calibration. Sebual and Jogading models were generated in MODFLOW-NWT separately with the coupled UZF1 and SFR2 packages to simulate the flow from unsaturated zone and streamflow. They were simulated and calibrated manually using stream discharge data (1th October 2009 to 30th September 2012), and the heads were calibrated using surface altitude [DEM]. The details of this findings are listed below:

- The catchment assessment was carried out over the Jembrana region which consists of ten catchments. The aim of this assessment was to know the distribution of groundwater runoff [q_g] and then to select the catchment for IHM simulation in this region. The results was that the percentage of groundwater runoff [q_g] of total streamflow was varied across the region. In Melaya, it was 86.54%, Sangyang Gede was 78.63%, Daya Barat was 70.10%, Pergung was 70.60%, Bilok Poh was 62.28%, Yeh Buah was 69.30%, Yeh Embang was 68.10, Yeh Sumbul 77.58%, Yeh Satang was 63.93% and Medewi was 71.28% respectively.

- Pergung Catchment consists of four sub-catchments. They were assessed similar as the J.R. As the results, groundwater runoff [q_g] of Sebual_SC was 49.78%, Jogading was 78.13%, Daya Timur was 68% and Pergung was 76.92% of total estimated flow. The dynamic condition of [q_g] was used as the main reason to select for IHM simulation and calibration in MODFLOW-NWT.

- IHM of Sebual and Jogading were generated using MODFLOW-NWT. They were simulated in three hydrological periods (1st October 2009 till 30th September 2012) and calibrated with stream discharge. Then, the heads calibrated controlling heads to be below the surface altitude. Sebual and Jogading model was generally in good performance, which indicated by the hydrograph patterns of simulated stream and observed discharge. In addition, the volumetric error performance indicated by with Nash-Sutcliffe coefficient efficiency [NS] with 0.56 for Sebual and 0.91 in Jogading. Also, from fictitious piezometers, the simulated heads were below the ground surface. Therefore, based on those parameters the Sebual and Jogading model was performed reasonable well.

- The temporal variability of groundwater fluxes in Sebual can be described separately in wet and dry season. In wet season, R_g ranges from ~5.70 mm day^{-1} (November) to ~4.20 mm day^{-1} (October) with the average of ~4.90 mm day^{-1}, in dry season from ~4.60 mm day^{-1} (April) to ~3.54 mm day^{-1} (September); R_n ranging from ~5.40 mm day^{-1} (November) to ~4.00 mm day^{-1} (October) with the average of ~4.70 mm day^{-1}, in dry season from ~4.45 mm day^{-1} (April) to ~3.40 mm day^{-1} (September) with the average of ~3.90 mm day^{-1}; q_{sg} ranges from~ 0.87 mm day^{-1} (October) to ~0.85 mm day^{-1} (March) with the average of ~0.86 mm day^{-1}, in dry season from~0.86 mm day^{-1} (April) to 0.85 mm day^{-1} (July) with the average of ~0.85 mm day^{-1}; ET_g ranges from ~0.32 mm day^{-1}(November) to ~0.20 mm day^{-1} (March) with the average of ~0.25 mm day^{-1}, in dry season from ~0.22 mm day^{-1} (April) to 0.12 mm day^{-1} (September) with the average of ~0.16 mm day^{-1}. The spatial variability of groundwater fluxes in Sebual are mainly governed by spatial distribution of rainfall and land cover.

- The same condition in Sebual, R_g in Jogading ranges from ~5.20 mm day^{-1} (December) to ~4.25 (October) with the average of ~4.80 mm day^{-1}, in dry season from ~ 4.70 mm day^{-1} (April) to ~4.14 mm day^{-1}

(September) with the average of ~4.41 mm day^{-1}; R_n ranging from ~5.20 mm day^{-1} (December) to ~4.21 mm day^{-1} (October) with the average of ~4.75 mm day^{-1}, in dry season from ~4.65 mm day^{-1} (April) to 4.10 mm day^{-1} (September) with the average of ~4.37 mm day^{-1}; q_{sg} ranging from ~0.30 mm day^{-1} (December) to 0.29 mm day^{-1} (February) with the average of ~0.30 mm day^{-1}, in dry season from ~0.30 mm day^{-1} (April) to 0.29 mm day^{-1} (September) with the average of ~0.30 mm day^{-1}; ET_g ranging from ~0.07 mm day^{-1} (November) to 0.04 mmday^{-1} (March) with the average of ~0.05 mmday^{-1}, in dry season from ~0.04 mm day^{-1} (April) to 0.03 (September) mm day^{-1} with the average of ~0.03 mm day^{-1}. The spatial variability of groundwater fluxes in Jogading are mainly influenced by spatial distribution of rainfall and land cover.

- The three-year average of transient state IHM in Sebual and Jogading can be illustrated in water budget components; the percentage of gross recharge (R_g) in Sebual and Jogading were 76.54 % and 87.50 % of the total groundwater inflow. In Sebual, stream to groundwater [q_{sg}] and storage [ΔS_{gin}] contributed 15.70% and 7.75%, while in Jogading was 5.85% and 6.65% respectively. The outflow components consist of groundwater to stream [q_{gs}], groundwater evapotranspiration [ET_g], surface leakage [Exf_{gw}] and storage [ΔS_{gout}] which were 89.85%, 3.12%, 0.31% and 6.71 % of the total outflow in Sebual, while in Jogading was 94.60%, 0.70% , 0.05 %, and 4.66 % of the total outflow respectively.

- Comparison of baseflow separation of [WHAT] and MODFLOW-NWT was in a good agreement in terms of percentage q_s and q_g of total estimated flow.

5.3. Recommendations

- For further study, the groundwater heads monitoring points such as piezometers or wells should be incorporated into the model to perform more certainty of models. The piezometers should be spatially distributed over the region and also temporally recorded. Thus, the model also can be calibrated with the groundwater heads instead of using stream discharges and topographical surface altitude [DEM].

- Hydrogeology data such as cross section of the region should be obtained because it can be delivered the conceptual model which is considered an important part in groundwater modelling. Moreover, cross section data can be used to determine the number of layer and hydraulic conductivity zones that should be used in the modelling.

- Groundwater abstractions data should be checked and collected in the field and then considered to be in the model. Data location of stream discharges in the area is needed to be validated in the field. In the current condition, the data of stream discharges may not available again in the filed due to inactive or it was moved to another place. Also, hydrology data such as stream depth, stream width, the shape of river should be checked in the field.

- Land use and land cover map were considered an important data in this modelling. It was used for interception and infiltration rate, and extinction depth which are driving forces and important parameters for input data to the model. In this study, a single land use and land cover data were used in two seasons (wet and dry season) for interception. The spatiotemporal data of land use and land cover change need to be considered in the further study. Also, the details of land use and land cover such as crops type, trees type, and plantations type need to be validated in the field.

- In this study, PET MODIS 100 m daily temporal resolution was used as resampled product from PET 1000m with eight days temporal resolution. Therefore, it would be better if there is an satellite images of PET with a higher spatial resolution is required to obtain more reliable estimation.

LIST OF REFERENCES

Akhtar M, Ahmad N, Booij M (2009) Use of regional climate model simulations as input for hydrological models for the Hindukush-Karakorum-Himalaya region. Hydrol Earth Syst Sci 13:1075–1089. doi: 10.5194/hess-13-1075-2009

Ala-aho P, Rossi PM, Isokangas E, Kløve B (2015) Fully integrated surface-subsurface flow modelling of groundwater-lake interaction in an esker aquifer: Model verification with stable isotopes and airborne thermal imaging. Hydrology 522:391–406. doi: 10.1016/j.jhydrol.2014.12.054

Anderson MP, Woessner WW (1992) Applied groundwater modeling: Simulation to flow and advective transport. Academic Press Inc, San Diego, California

Anderson MP, Woessner WW, Hunt RJ (2015) Applied Groundwater Modeling : Simulation of Flow and Advective Transport, Second. Elsevier

Anibas C, Verhoeven R, Meire P, Batelaan O (2009) Transient or steady - state ? Using vertical temperature profiles to quantify groundwater – surface water exchange Transient or steady-state ? Using vertical temperature profiles to quantify groundwater – surface water exchange. doi: 10.1002/hyp.7289

Barnett B, Townley LR, Post V, et al (2012) Australian groundwater modelling guidelines. Canberra

Cole S (2012) A political ecology of water equity and tourism: A Case Study From Bali. Ann Tour Res 39:1221–1241. doi: 10.1016/j.annals.2012.01.003

Corbett ES, Crouse, Robert P (1968) Rainfall interception by annual grass and chaparral . . . losses compared. US For Serv Res Pap PSW. doi: 10.1080/00382167.1962.9629728

D. N. Moriasi, J. G. Arnold, M. W. Van Liew, et al (2007) Model Evaluation Guidelines for Systematic Quantification of Accuracy in Watershed Simulations. Trans ASABE 50:885–900. doi: 10.13031/2013.23153

Doble RC, Crosbie RS (2017) Review : Current and emerging methods for catchment-scale modelling of recharge and evapotranspiration from shallow groundwater. Hydrogeology 3–23. doi: 10.1007/s10040-016-1470-3

Eckhardt K, Fohrer N, Frede HG (2005) Automatic model calibration. Hydrol Process 19:651–658. doi: 10.1002/hyp.5613

El-Zehairy AA, Lubczynski MW, Gurwin J (2017) Interactions of artificial lakes with groundwater applying an integrated MODFLOW solution. Hydrogeol J 109–132. doi: 10.1007/s10040-017-1641-x

Ely D., Kahle SC (2012) Simulation of Groundwater and Surface - Water Resources and Evaluation of Water - Management Alternatives for the Chamokane Creek Basin , Stevens County , Washington Scientific Investigations Report 2012 – 5224. Washington

Fetter CW (2001) Principle of Groundwater Flow, Fourth Edi. Prentice Hall, New Jersey

Francés AP, Lubczynski MW, Roy J, et al (2014) Hydrogeophysics and remote sensing for the design of hydrogeological conceptual models in hard rocks – Sardón catchment (Spain). J Appl Geophys 110:63–81. doi: 10.1016/j.jappgeo.2014.08.015

Ghimire CP, Bruijnzeel LA, Lubczynski MW, Bonell M (2012) Rainfall interception by natural and planted forests in the Middle Mountains of Central Nepal. J Hydrol 475:270–280. doi: 10.1016/j.jhydrol.2012.09.051

Gilfedder M, Rassam DW, Stenson MP, et al (2012) Incorporating land-use changes and surface-groundwater interactions in a simple catchment water yield model. Environ Model Softw 38:62–73. doi: 10.1016/j.envsoft.2012.05.005

Guay C, Nastev M, Paniconi C, Sulis M (2013) Comparison of two modeling approaches for groundwater – surface water interactions. Hydrol Process 27:2258–2270. doi: 10.1002/hyp.9323

Hassan SMT, Lubczynski MW, Niswonger RG, Su Z (2014) Surface–groundwater interactions in hard rocks in Sardon Catchment of western Spain: An integrated modeling approach. J Hydrol 517:390–410. doi: 10.1016/j.jhydrol.2014.05.026

Kayane I, Tanaka T, Shimada J, et al (1993) Investigation of the water cycle using environmental tracers, Bali, Indonesia. Hydrogeol Warm Humid Reg 216:305–316.

Krause S, Bronstert A, Krause S (2007) Groundwater – surface water interactions in a North German lowland floodplain – Implications for the river discharge dynamics and riparian water balance. J Hydrol 347:404–417. doi: 10.1016/j.jhydrol.2007.09.028

Kumar CP, Singh S (2015) Concepts and Modeling of Groundwater System. IJISET -International J Innov Sci Eng Technol 2:262–271.

Lim KJ, Engel BA, Tang Z, Choi J (2005) Automated Web GIS based Hydrographs Analysis Tool, WHAT. J

Am Water Resour Assoc 1397:1407–1416. Retrieved from https://engineering.purdue.edu/mapserve/WHAT/faq/Automated_Web_GIS_based_Hydrograph_Analysis_Tool_WHAT_JAWRA_Dec_2005.pdf

Lubczynski MW, Gurwin J (2005) Integration of various data sources for transient groundwater modeling with spatio-temporally variable fluxes—Sardon study case, Spain. J Hydrol 306:71–96. doi: 10.1016/j.jhydrol.2004.08.038

Lyne, V. D., Hollick, M (1979). Stochastic time-variable rainfall runoff modelling. Hydrology and Water

Resources Symposium , Institution of Engineers Australia, Perth. 89-92.

McDonald M, Harbaugh A (1984) A modular three-dimensional finite-difference ground-water flow model. US Geol Surv Report Fil:539. doi: 10.1016/0022-1694(86)90106-X

McMahon TA, Peel MC, Lowe L, et al (2013) Estimating actual, potential, reference crop and pan evaporation using standard meteorological data: A pragmatic synthesis. Hydrol Earth Syst Sci 17:1331–1363. doi: 10.5194/hess-17-1331-2013

Mehl S, Hill MC (2010) Grid-size dependence of Cauchy boundary conditions used to simulate stream-aquifer interactions. Adv Water Resour 33:430–442. doi: 10.1016/j.advwatres.2010.01.008

Mishra HS, Rathore TR, Tomar VS (1999) Root growth, water potential and yield of irrigated wheat. Irrig Sci 18:117–123. doi: https://doi.org/10.1007/s002710050052

Nash JE, Sutcliffe J V (1970) River Flow Forecasting Through Conceptual Models Part I-a Discussion of Principles*. J Hydrol 10:282–290. doi: 10.1016/0022-1694(70)90255-6

Nielsen GL, Widjaya JM (1989a) Modeling of Ground-Water Recharge in Southern Bali, Indonesia. Ground Water 27:473–480. doi: 10.1111/j.1745-6584.1989.tb01967.x

Nielsen GL, Widjaya JM (1989b) Modeling of Groundwater -Recaharge in Southern Bali, Indonesia. Groundwater 27:473–480. doi: 10.1111/j.1745-6584.1989.tb01967.x

Niswonger RG, Panday S, Ibaraki M (2011) MODFLOW-NWT , A Newton Formulation for MODFLOW-2005.U.S.Geological Survey Techniques and Methods 6-A37, 44 p. Retrieved from https://pubs.usgs.gov/tm/tm6a37/pdf/tm6a37.pdf

Niswonger RG, Prudic DE (2005) Documentation of the Streamflow-Routing (SFR2) Package to Include Unsaturated Flow Beneath Streams — A Modification to SFR1. U.S.Geological Survey Techniques and Methods 6-A13, 48 p. Retrieved from https://md.water.usgs.gov/gw/modflow/MODFLOW_Docs/TM6-A13-SFR2.pdf

Niswonger RG, Prudic DE, Regan SR (2006) Documentation of the Unsaturated-Zone Flow (UZF1) Package for Modeling Unsaturated Flow Between the Land Surface and the Water Table with MODFLOW-2005. U.S.Geological Survey Techniques and Methods 6-A19, 62 p. Retrieved from https://pubs.usgs.gov/tm/2006/tm6a19/pdf/tm6a19.pdf

Purnomo BJ, Pichler T (2015) Geothermal systems on the island of Bali, Indonesia. J Volcanol Geotherm Reserach 304:349–358. doi: 10.1016/j.jvolgeores.2015.09.016

Rai IN, Shoba S, Shchegolkova N, et al (2015) Analysis of the Specifics of Water Resources Management in Regions with Rapidly Growing Population under Different Climate Conditions : Case Study of Bali Island and the Moscow Region 1. Water Resour 42:735–746. doi: 10.1134/S0097807815050127

Rassam D., Pagedam D., Hunter H. (2008) Conceptualisation and application of models for groundwater-surface water interaction and nitrate attenuation potential in riparian zones. Environ Model Softw 23:859–875. doi: 10.1016/j.envsoft.2007.11.003

Searcy JK, Hardison CH (1960) Double-Mass Curves. WaterSupply Pap 1541B 66. doi: http://udspace.udel.edu/handle/19716/1592

Seibert J (1997) Estimation of Parameter Uncertainty in the HBV Model. Nord Hydrol 28:247–262.

Shah N, Nachabe M, Ross M (2007) Extinction depth and evapotranspiration from ground water under selected land covers. Ground Water 45:329–338. doi: 10.1111/j.1745-6584.2007.00302.x

Sophocleous M (2002) Interactions between groundwater and surface water : the state of the science. Hydrogeol J 10:52–67. doi: 10.1007/s10040-001-0170-8

Sophocleous M (2010) Review : Groundwater management practices , challenges , and innovations in the High Plains aquifer , USA-lessons and recommended actions. Hydrogeol J 18:559–575. doi: 10.1007/s10040-009-0540-1

Sophocleous M (2005) Groundwater recharge and sustainability in the High Plains aquifer in Kansas, USA. Hydrogeol J 13:351–365. doi: 10.1007/s10040-004-0385-6

Teketel AT (2017) Integrated Hydrological Modeling of Surface - Groundwater Interactions The case of Denpasar-Tabanan Basin in the Southern Bali Island. University of Twente, Faculty of Geo-Information

and Earth Observation (ITC)
Thompson DB (2006) The Rational Method. Texas. Retrieved from http://drdbthompson.net/writings/rational.pdf
van Dijk AIJ., Bruijnzeel L. (2001) Modelling rainfall interception by vegetation of variable density using an adapted analytical model. Part 1. Model description. J Hydrol 247:230–238. doi: 10.1016/S0022-1694(01)00392-4
Wang YL, Wang X, Zheng QY, et al (2012) A Comparative Study on Hourly Real Evapotranspiration and Potential Evapotranspiration during Different Vegetation Growth Stages in the Zoige Wetland. Procedia Environ Sci 13:1585–1594. doi: 10.1016/j.proenv.2012.01.150
Weldemichael MY (2016) Integrated Numerical Modeling Applying Stratiform Hydrogeological Conceptual Model, Sardon Catchment Study case, Spain. Faculty of Geo-Information Science and Erath Observation (ITC), University of Twente
Winston RB (2009) ModelMuse: A Graphical User Interface for MODFLOW-2005 and PHAST. U.S. Geological Survey Techniques and Methods 6–A29, 52 p. Retrieved from https://pubs.usgs.gov/tm/tm6A29/tm6A29.pdf
Yang X, Xie X, Liu DL, et al (2015) Spatial Interpolation of Daily Rainfall Data for Local Climate Impact Assessment over Greater Sydney Region. Adv Meteorol. doi: 10.1155/2015/563629

APPENDICES

Appendix I: Rain gauges monitoring

No	Rain_gauges	x_utm	y_utm	Elevation [m]	Availability of rainfall data				
					2009	2010	2011	2012	2013
1	Palasari	228977.39	9085505.29	49	v	v	v	v	v
2	Benel Bendungan	235427.25	9084485.53	275	x	v	v	v	v
3	Negara BMKG	237505.24	9077326.73	24	v	v	v	v	v
4	Negara DPU	238541.04	9074059.26	8	v	v	v	v	v
5	Dauh Waru	240756.97	9080812.54	205	v	v	v	v	v
6	Pohsanten	244691.34	9074098.90	18	v	v	v	v	v
7	Tibutanggang	249357.61	9079751.29	198	v	v	v	v	v
8	Pulukan DPU	261847.45	9071167.27	145	v	v	v	v	v

Where, x : no data, and v : data are available.

Appendix II: Discharge gauges monitoring

No	Station	xutm	yutm	Elevation [m]	Availability of data				
					2009	2010	2011	2012	2013
1	Melaya	223330.84	9083989.49	4	v	v	v	v	v
2	Sangyang Gede	225811.56	9081578.97	7	v	v	v	v	v
3	Daya Barat	230258.92	9079076.09	24	v	v	v	v	v
4	Sebual	236709.05	9074880.99	7	v	v	v	v	v
5	Jogading	238567.78	9074823.44	11	v	v	x	v	v
6	Daya Timur 1	242214.66	9074305.81	8	x	x	x	x	x
7	Daya Timur 2	241300.25	9072426.21	5	v	v	v	v	v
8	Pergung	244405.22	9072160.31	6	v	v	v	v	v
9	Biluk Poh	246239.10	9071107.98	2	v	v	v	v	v
10	Yeh Buah	250615.29	9071143.06	2	v	v	v	v	v
11	Yeh Embang	253648.63	9070491.72	2	v	v	v	v	v
12	Yeh Sumbul	256704.23	9069882.51	2	v	v	v	v	v
13	Yeh Satang	258183.27	9069057.41	1	v	v	v	v	v
14	Medewi	258413.19	9068636.58	5	v	v	x	x	x

Where, x : no data, and v : data are available.

Appendix III: Temperature gauges and coefficient of determination

No	Temperature_sation	x_utm	y_utm	elevation [m]	Data availability				
					2009	2010	2011	2012	2013
1	Negara BMKG	237505.2	9077327	24	v	v	v	v	v
2	Negara DPU	238541	9074059	8	v	v	v	v	v

Where, x : no data, and v : data are available.

The computed of coefficient of determination in BMKG and Negara DPU stations

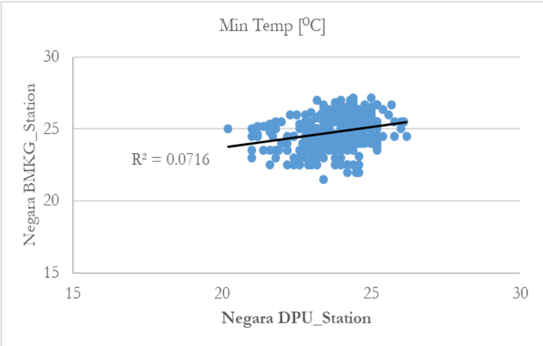

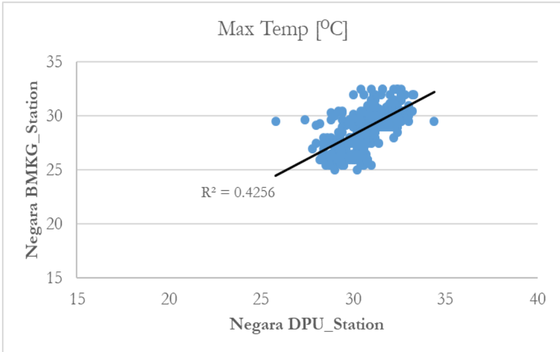

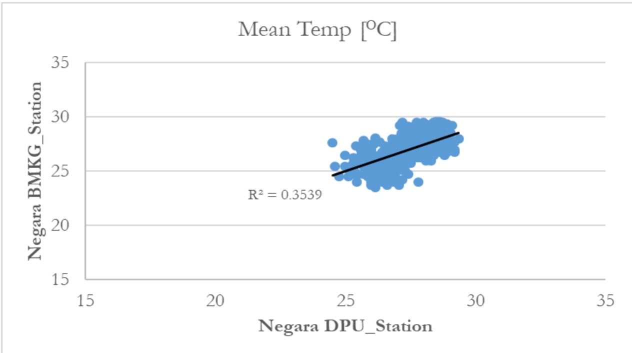

Appendix IV: Double mass curves of precipitation

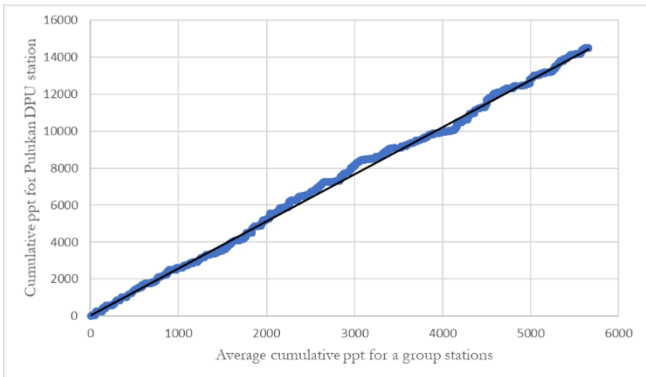

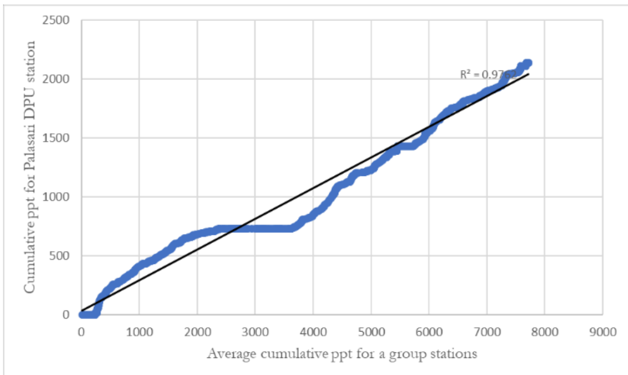

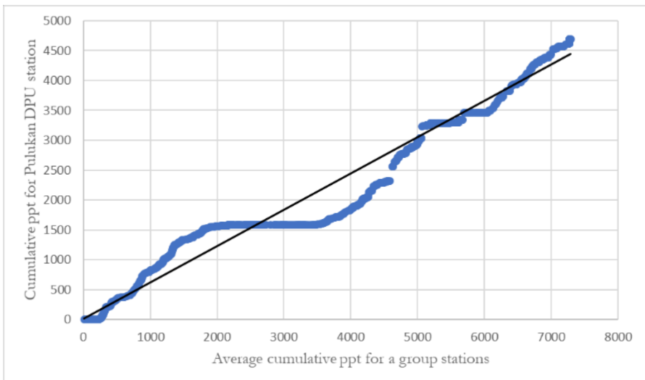

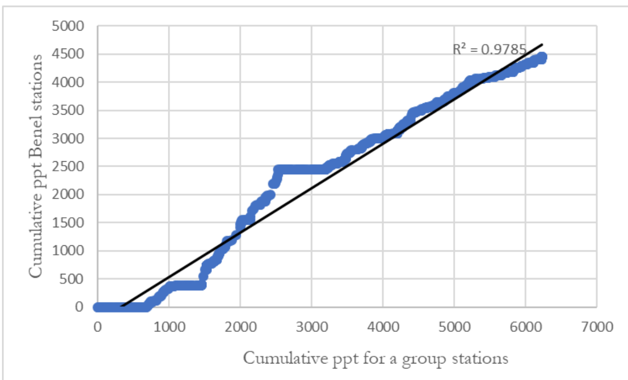

Appendix V: Heads simulated in fictitious piezometer

P3 Sebual

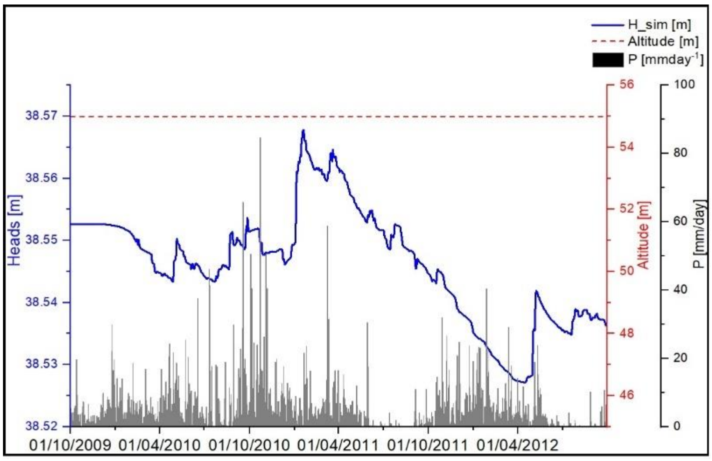

P1 Jogading

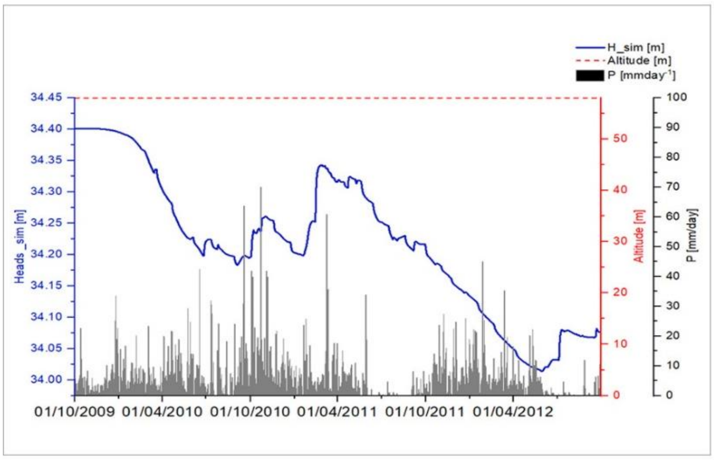

P4 Sebual

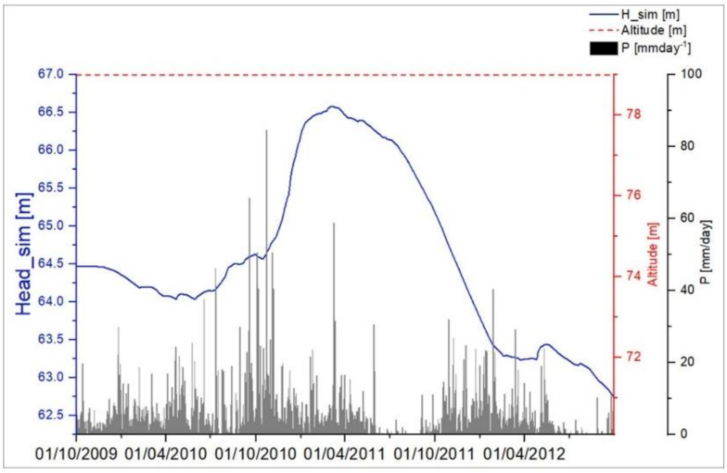

P3 Jogading

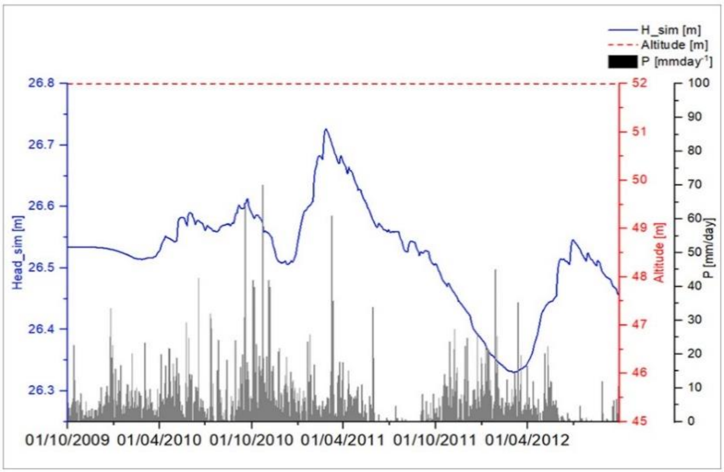

P12 Sebual

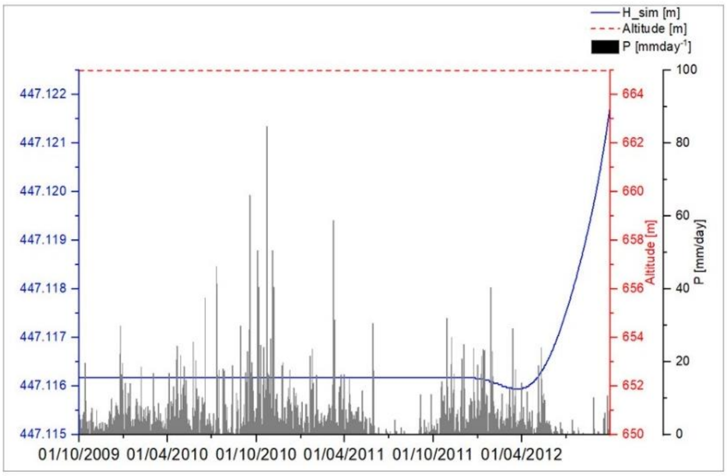

P5 Jogading